

**SMALL MOLECULES AS MODULATORS OF MITOTIC ARREST AND  
SENESCENCE IN CANCER**

by

JENNA LOUISE RIFFELL

B.Sc.H., University of British Columbia, 2006

A THESIS SUBMITTED IN PARTIAL FULFILLMENT OF  
THE REQUIREMENTS FOR THE DEGREE OF

**DOCTOR OF PHILOSOPHY**

in

THE FACULTY OF GRADUATE STUDIES  
(Biochemistry and Molecular Biology)

THE UNIVERSITY OF BRITISH COLUMBIA

(Vancouver)

April 2011

© Jenna Louise Riffell, 2011

## ABSTRACT

Manipulation of the cell cycle is an extensively used and promising strategy for cancer therapy. To identify novel cell cycle modulators, automated fluorescence microscopy assays were designed and used to screen chemical libraries for modulators of mitotic arrest and senescence. 8-azaguanine, IC 261, erysolin and SKF 96365 were identified as chemicals that stimulate senescence, a state of prolonged growth arrest, in a p53-mutated growth arrest-deficient cell line. Microtubule-targeting cancer therapies such as paclitaxel block cell cycle progression at mitosis by prolonged activation of the mitotic checkpoint. Cells arrested in mitosis may remain arrested for extended periods of time, or undergo mitotic slippage through degradation of cyclin B1 in the presence of an active mitotic checkpoint and enter interphase without having separated their chromosomes. Regulation of extended mitotic arrest and mitotic slippage and their contribution to subsequent cell death or survival is incompletely understood. Chlorpromazine and trifluorpromazine were identified as drugs that inhibit mitotic exit through mitotic slippage. Using these drugs to extend mitotic arrest imposed by low concentrations of paclitaxel led to increased cell survival and proliferation after drug removal. SU6656 and geraldol were identified as chemicals that induce mitotic slippage. Cells arrested at mitosis with paclitaxel or vinblastine and induced by these compounds to undergo mitotic slippage underwent several rounds of DNA replication without cell division and exhibited signs of senescence but eventually all died. These results show that reinforcing mitotic arrest with drugs that inhibit mitotic slippage can lead to increased cell survival and proliferation, while inducing mitotic slippage in cells treated with microtubule-targeting drugs seems to invariably lead to protracted cell death. Mitotic

slippage induced by SU6656 or geraldol involved proteasome-dependent degradation of cyclin B1, but also required proteasome- and caspase-3-dependent inactivation of the mitotic checkpoint through degradation of the mitotic checkpoint protein BubR1.

Caspase-3 and p53, both apoptotic effectors, did not affect cell death after exposure to paclitaxel, with or without mitotic slippage induction. The requirement for caspase-3 for chemically induced mitotic slippage reveals a new mechanism for mitotic exit and a link between mitosis and apoptosis that has implications for the outcome of cancer chemotherapy.

## PREFACE

This thesis contains material from previously published works. Some results presented in Chapters 3 and 4 were published with co-authors Carla Zimmerman, Anthony Khong, Dr. Lianne McHardy, and Dr. Michel Roberge (Riffell JL, Zimmerman C, Khong A, McHardy LM, and Roberge M. Effects of chemical manipulation of mitotic arrest and slippage on cancer cell survival and proliferation. *Cell Cycle* 2009; 8: 3029-3042). The data in Figures 3.3 - 3.6, Figure 3.8, Figure 3.10, Figure 4.1 and Figure 4.6 were obtained by Carla Zimmerman in experiments that were designed and analyzed by myself and Dr. Roberge and performed by Carla. The screen presented in Figure 3.9 was designed and analyzed by myself and Dr. Roberge and carried out by Anthony Khong. All other work in these chapters is my own and I wrote the manuscript.

At the time of writing, the majority of the results presented in Chapter 5 were part of a manuscript in press at Molecular Cancer Therapeutics, co-authored with Dr. Reiner Jänicke and Dr. Michel Roberge. The *in vitro* kinase assays in Figure 5.13 were carried out by Signalchem Inc. All other experiments were designed and analyzed by myself and Dr. Roberge and performed by me. Dr. Jänicke contributed the MCF-7pcDNA and MCF-7casp3 cell lines used in Figures 5.7 - 5.9, 5.14, and 5.17 - 5.19. The manuscript was written solely by me.

# TABLE OF CONTENTS

|  |           |
|--|-----------|
| ABSTRACT.....  | ii        |
| PREFACE .....  | iv        |
| TABLE OF CONTENTS .....  | v         |
| LIST OF TABLES.....  | vii       |
| LIST OF FIGURES.....   | viii      |
| LIST OF ABBREVIATIONS .....  | xii       |
| ACKNOWLEDGEMENTS .....   | xv        |
| <b>CHAPTER 1: INTRODUCTION .....</b>   | <b>1</b>  |
| 1.1 USING CHEMICAL BIOLOGY TO DISCOVER BIOLOGICAL MECHANISMS AND NOVEL DRUGS .....   | 1         |
| 1.2 CELL-BASED HIGH-THROUGHPUT SCREENING.....  | 2         |
| 1.3 THE CELL CYCLE.....  | 6         |
| 1.3.1 Mitosis .....  | 8         |
| 1.3.2 Cell cycle regulation.....   | 11        |
| 1.3.2.1 Cell cycle initiation and the G1-S transition.....   | 13        |
| 1.3.2.2 Exit from mitosis and the mitotic checkpoint.....  | 15        |
| 1.3.3 Senescence.....  | 19        |
| 1.4 ANTIMITOTIC CANCER THERAPY .....   | 20        |
| 1.5 APOPTOSIS.....   | 23        |
| 1.6 MITOTIC SLIPPAGE.....  | 25        |
| 1.7 OBJECTIVES .....   | 28        |
| 1.7.1 Question 1: Can we design high-throughput cell-based screens to find chemicals that affect the cell cycle: modulators of mitotic arrest, and stimulators of senescence?..... | 28        |
| 1.7.2 Question 2: What is the outcome of mitotic slippage with respect to cell fate?.....  | 29        |
| 1.7.3 Question 3: What is the molecular mechanism of mitotic slippage? .....   | 29        |
| 1.7.4 Question 4: Is inhibition or induction of mitotic slippage a good strategy for anticancer therapy?.....  | 29        |
| <b>CHAPTER 2: MATERIALS AND METHODS .....</b>  | <b>30</b> |
| 2.1 CELL LINES .....   | 30        |
| 2.2 SCREENING CHEMICALS.....   | 30        |
| 2.3 SCREEN FOR ACTIVATORS OF P21 .....   | 30        |
| 2.4 SCREEN FOR INHIBITORS OF MITOTIC SLIPPAGE .....  | 31        |
| 2.5 SURVIVAL ASSAYS.....   | 32        |
| 2.6 SCREEN FOR INDUCERS OF MITOTIC SLIPPAGE .....  | 32        |
| 2.7 IMMUNOFLUORESCENCE MICROSCOPY .....  | 33        |
| 2.8 FLOW CYTOMETRY .....   | 34        |
| 2.9 SENESCENCE-ASSOCIATED $\beta$ -GALACTOSIDASE STAINING.....   | 34        |
| 2.10 IMMUNOBLOTTING.....   | 35        |
| 2.11 <i>IN VITRO</i> KINASE ASSAYS.....  | 36        |
| <b>CHAPTER 3: HIGH-CONTENT SCREENS FOR CELL CYCLE MODULATORS.....</b>  | <b>37</b> |
| 3.1 SYNOPSIS .....   | 37        |
| 3.2 IDENTIFICATION OF CHEMICAL STIMULATORS OF SENESCENCE .....   | 38        |
| 3.2.1 Screening for p21 promoter activity.....   | 38        |
| 3.2.2 Chemicals that increase p21 promoter activity can induce senescence.....   | 40        |
| 3.3 MITOTIC ARREST AND SLIPPAGE IN THREE CANCER CELL LINES .....   | 44        |
| 3.4 IDENTIFICATION OF CHEMICAL ENFORCERS OF MITOTIC ARREST .....   | 52        |
| 3.4.1 Effect of chlorpromazine and triflupromazine on mitotic slippage.....  | 57        |

|   |            |
|---|------------|
| 3.5 IDENTIFICATION OF CHEMICAL INDUCERS OF MITOTIC SLIPPAGE .....   | 57         |
| <b>CHAPTER 4: EFFECTS OF MITOTIC SLIPPAGE ON CELL SURVIVAL AND<br/>PROLIFERATION.....</b>                             | <b>67</b>  |
| 4.1 SYNOPSIS .....  | 67         |
| 4.2 CHLORPROMAZINE AND TRIFLUPROMAZINE INCREASE SURVIVAL OF PACLITAXEL-TREATED CELLS.....                             | 68         |
| 4.3 CELLS FORCED TO UNDERGO MITOTIC SLIPPAGE BY SU6656 OR GERALDOL EXPERIENCE MYRIAD<br>FATES .....                   | 70         |
| 4.4 CPZ AND TPZ INHIBIT INDUCTION OF MITOTIC SLIPPAGE BY SU6656 AND GERALDOL.....                                     | 78         |
| 4.5 LOSS OF SECURIN INCREASES THE FREQUENCY OF MITOTIC SLIPPAGE .....   | 80         |
| <b>CHAPTER 5: MITOTIC SLIPPAGE VIA PROTEASOME- AND CASPASE-DEPENDENT<br/>MITOTIC CHECKPOINT INACTIVATION .....</b>    | <b>83</b>  |
| 5.1 SYNOPSIS .....  | 83         |
| 5.2 INDUCTION OF MITOTIC SLIPPAGE BY SU6656 AND GERALDOL REQUIRES PROTEASOMAL ACTIVITY<br>84                          |            |
| 5.3 INDUCTION OF MITOTIC SLIPPAGE OCCURS VIA PROTEASOME-DEPENDENT DEGRADATION OF<br>MITOTIC CHECKPOINT PROTEINS ..... | 86         |
| 5.4 SU6656 AND GERALDOL DO NOT INDUCE THE DEGRADATION OF CYCLIN B1, BUBR1 AND Cdc20 IN<br>INTERPHASE CELLS .....      | 89         |
| 5.5 MITOTIC CHECKPOINT INACTIVATION AND SLIPPAGE INDUCTION BY SU6656 AND GERALDOL<br>REQUIRE CASPASE-3 .....          | 91         |
| 5.6 MITOTIC SLIPPAGE CORRELATES TEMPORALLY WITH DEGRADATION OF BUBR1 AND Cdc20.....                                   | 97         |
| 5.7 INHIBITION OF THE AURORA KINASES BY SU6656 AND GERALDOL.....  | 99         |
| 5.8 CASPASE-3 DOES NOT SIGNIFICANTLY IMPACT CELL SURVIVAL AFTER MITOTIC SLIPPAGE.....                                 | 102        |
| 5.9 CASPASE-3 AND P53 ARE NOT ESSENTIAL FOR CELL DEATH SUBSEQUENT TO ANTIMITOTIC<br>TREATMENT .....                   | 106        |
| <b>CHAPTER 6: CONCLUSION .....</b>  | <b>111</b> |
| 6.1 CHEMICAL INDUCERS OF SENESCENCE.....  | 111        |
| 6.1.1 Discussion.....   | 111        |
| 6.1.2 Future perspectives .....   | 112        |
| 6.2 CHEMICAL MODULATORS OF MITOTIC SLIPPAGE.....  | 114        |
| 6.2.1 Discussion.....   | 114        |
| 6.2.2 Future perspectives .....   | 124        |
| <b>BIBLIOGRAPHY .....</b>   | <b>128</b> |

## LIST OF TABLES

|  |     |
|--|-----|
| Table 1.1: Chemical inhibitors of the cell cycle. ....   | 3   |
| Table 3.1: Chemicals that induce transcription of a p21 promoter-regulated reporter<br>protein. .... | 41  |
| Table 3.2: Efficacies of lead p21-activating compounds. ....   | 42  |
| Table 5.1: Geraldol <i>in vitro</i> kinase inhibition. ....  | 103 |

## LIST OF FIGURES

|  |    |
|--|----|
| Figure 1.1: The cell cycle and its regulation by CDK/cyclins.....  | 7  |
| Figure 1.2: Cellular and genetic division during M phase.....  | 9  |
| Figure 1.3: Pathways for cell cycle arrest in response to DNA damage.....  | 12 |
| Figure 1.4: Monitoring of microtubule attachment during mitosis by the mitotic<br>checkpoint.....                      | 16 |
| Figure 1.5: Potential outcomes of cellular exposure to an antimitotic agent.....                                       | 27 |
| Figure 3.1: Screen for senescence-inducing chemicals through p21 promoter activity. ..                                 | 39 |
| Figure 3.2: Induction of senescence-associated $\beta$ -galactosidase activity by p21-activating<br>chemicals.....     | 43 |
| Figure 3.3: Differential induction of mitotic arrest by paclitaxel in three cancer cell lines.<br>.....                | 45 |
| Figure 3.4: Mitotic accumulation in three cancer cell lines during exposure to paclitaxel.<br>.....                    | 47 |
| Figure 3.5: Transient mitotic arrest in MDA-MB-231 and T98G but not MCF-7mp53<br>cells due to mitotic slippage.....    | 49 |
| Figure 3.6: Mitotic arrest and slippage during exposure of MCF-7mp53, MDA-MB-231<br>and T98G cells to paclitaxel. .... | 51 |
| Figure 3.7: Screen for chemical reinforcers of mitotic arrest. ....  | 53 |
| Figure 3.8: Results of the screen for chemical enforcers of mitotic arrest. ....                                       | 55 |
| Figure 3.9: Structures of the chemical reinforcers of mitotic arrest chlorpromazine and<br>triflupromazine.....        | 56 |

|  |    |
|--|----|
| Figure 3.10: Induction of mitotic arrest by combinations of chlorpromazine and paclitaxel or triflupromazine and paclitaxel. ....              | 58 |
| Figure 3.11: Screen for inducers of mitotic slippage. ....   | 59 |
| Figure 3.12: Results of the screen for inducers of mitotic slippage. ....  | 61 |
| Figure 3.13: Nuclear morphology of cells induced to undergo mitotic slippage by exposure to paclitaxel and SU6656 or geraldol. ....            | 62 |
| Figure 3.14: Structures of SU6656 and geraldol. ....   | 64 |
| Figure 3.15: Disappearance of mitotic histone H3 Ser10 phosphorylation in cells treated with SU6656 or geraldol. ....                          | 65 |
| Figure 3.16: Induction of mitotic slippage after mitotic arrest induced by paclitaxel, vinblastine or <i>S</i> -trityl-L-cysteine (STLC). .... | 66 |
| Figure 4.1: Increase in cell survival caused by combinations of chlorpromazine and paclitaxel or triflupromazine and paclitaxel. ....          | 69 |
| Figure 4.2: Cell death after exposure to chemical stimulators of mitotic slippage. ....  | 71 |
| Figure 4.3: Endoreduplication after mitotic slippage. ....   | 72 |
| Figure 4.4: Formation of giant multinucleated cells after mitotic slippage. ....   | 74 |
| Figure 4.5: Senescence induction by chemical stimulators of mitotic slippage. ....   | 75 |
| Figure 4.6: Decrease in cell viability caused by combinations of SU6656 and paclitaxel or geraldol and paclitaxel. ....                        | 77 |
| Figure 4.7: Antagonistic activity of chemical inhibitors and stimulators of mitotic slippage. ....   | 79 |
| Figure 4.8: An increase in the frequency of mitotic slippage due to loss of securin. ....  | 81 |
| Figure 4.9: Death of cells lacking securin after mitotic slippage. ....  | 82 |

|   |     |
|---|-----|
| Figure 5.1: Proteasome-dependent mitotic slippage induction by SU6656 and geraldol.   | 85  |
| Figure 5.2: Mitotic slippage induction through proteasome-dependent degradation of mitotic checkpoint proteins.   | 87  |
| Figure 5.3: Mitotic checkpoint degradation during mitotic exit.   | 88  |
| Figure 5.4: Degradation of mitotic checkpoint proteins in response to SU6656 or geraldol in cycling cells.  | 90  |
| Figure 5.5: Caspase-dependent mitotic slippage induction by SU6656 and geraldol.  | 92  |
| Figure 5.6: Caspase-dependent mitotic checkpoint protein degradation induced by SU6656 and geraldol.  | 93  |
| Figure 5.7: Requirement for caspase-3 for mitotic slippage induction by SU6656 and geraldol.  | 95  |
| Figure 5.8: Requirement for caspase-3 for mitotic checkpoint inactivation by SU6656 and geraldol.   | 96  |
| Figure 5.9: Caspase-3-independence of spontaneous mitotic slippage.   | 98  |
| Figure 5.10: Timeline of mitotic slippage stimulation by geraldol.  | 100 |
| Figure 5.11: Timeline of mitotic checkpoint inactivation by SU6656 and geraldol.  | 101 |
| Figure 5.12: Inhibition of Aurora A and Aurora B by SU6656 and geraldol.  | 104 |
| Figure 5.13: Caspase-independent induction of mitotic slippage by ZM447439.   | 105 |
| Figure 5.14: Cell death after mitotic slippage with or without caspase-3 activity.  | 107 |
| Figure 5.15: Cell death after exposure to combinations of paclitaxel and SU6656 or paclitaxel and geraldol with or without caspase-3 or p53 activity.                 | 108 |
| Figure 5.16: Decrease in cell viability after exposure to combinations of paclitaxel and SU6656 or paclitaxel and geraldol with or without caspase-3 or p53 activity. | 110 |

Figure 6.1: Model for spontaneous and induced mitotic slippage..... 122

## LIST OF ABBREVIATIONS

|                  |   |
|------------------|---|
| APAF-1           | apoptotic protease activating factor 1  |
| APC/C            | anaphase-promoting complex/cyclosome    |
| ATM              | ataxia telangiectasia mutated           |
| ATP              | adenosine triphosphate                  |
| ATR              | ataxia telangiectasia and rad-3-related |
| Bak              | Bcl-2 homologous antagonist/killer      |
| Bax              | Bcl-2 associated X protein              |
| Bcl-2            | B-cell lymphoma 2                       |
| BH3              | Bcl-2 homology domain 3                 |
| Bid              | BH3 interacting domain death agonist    |
| Bub              | budding uninhibited by benzimidazole    |
| BubR1            | Bub1-related protein 1                  |
| CDC              | cell division cycle                     |
| CAK              | CDK-activating kinase                   |
| CDK              | cyclin-dependent kinase                 |
| CENP             | centromere protein                      |
| CPZ              | chlorpromazine                          |
| DMEM             | Dulbecco's modified Eagle medium        |
| DMSO             | dimethyl sulphoxide                     |
| EC <sub>50</sub> | 50% effective concentration             |
| EDTA             | ethylenediaminetetraacetic acid         |
| EGTA             | ethyleneglycoltetraacetic acid          |

|         |  |
|---------|--|
| g       | gravity  |
| G1      | gap 1  |
| G2      | gap 2  |
| H3P     | phospho-histone H3   |
| HCS     | high-content screening                                       |
| HDAC    | histone deacetylase complex                                  |
| HEPES   | 4-(2-hydroxyethyl)-1-piperazineethanesulphonic acid          |
| KSP     | kinesin spindle protein                                      |
| M       | mitosis  |
| M phase | mitosis and cytokinesis                                      |
| Mad     | mitotic arrest dependent                                     |
| MAP     | microtubule-associated protein                               |
| MCC     | mitotic checkpoint complex                                   |
| Mcl-1   | myeloid cell leukemia sequence 1                             |
| Mcm     | mini-chromosome maintenance                                  |
| Mps     | monopolar spindle  |
| MTT     | 3-(4,5-dimethylthiazol-2-yl)-2,5-diphenyltetrazolium bromide |
| PARP    | poly(ADP-ribose) polymerase                                  |
| PBS     | phosphate-buffered saline                                    |
| PKC     | protein kinase C   |
| Plk1    | polo-like kinase 1   |
| Rb      | retinoblastoma protein                                       |
| RNAi    | RNA interference   |

|               |  |
|---------------|--|
| RPMI          | Roswell Park Memorial Institute medium               |
| S             | synthesis phase; DNA replication                     |
| SAB           | serum azide buffer                                   |
| STLC          | <i>S</i> -trityl-L-cysteine                          |
| TBS           | Tris-buffered saline                                 |
| TNF- $\alpha$ | tumour necrosis factor $\alpha$                      |
| TPZ           | triflupromazine                                      |
| Tris          | tris(hydroxymethyl)aminomethane                      |
| Tw-SAB        | Tween-serum azide buffer                             |
| VB            | vinblastine  |
| X-gal         | 5-bromo-4-chloro-3-indolyl-beta-D-galacto-pyranoside |
| XIAP          | X-linked inhibitor of apoptosis protein              |

## ACKNOWLEDGEMENTS

First and foremost, I would like to acknowledge the invaluable guidance and mentorship of my supervisor, Dr. Michel Roberge. Past and present members of the Roberge lab provided helpful conversations and support: Elizabeth Donohue, Bruno Fonseca, Aruna Balgi, Karen Lam, Carla Zimmerman, Lianne McHardy, Pamela Austin Dean and Danielle Kemmer. My supervisory committee, Dr. George Mackie and Dr. Phil Hieter, provided helpful discussions and support. I would also like to thank the various undergraduate students I have worked with for allowing me to practice my supervisory skills on them.

I would like to acknowledge my family for their belief and pride in me. This thesis would have been a master's thesis without the support, suggestions, and commiseration at Mahony's of my fellow scientists, particularly Elizabeth Donohue, Kristina McBurney, and Jan Hankins. In an even direr situation, this thesis would probably not have been written at all without the love and support of my husband Erik.

# CHAPTER 1: INTRODUCTION

## 1.1 Using chemical biology to discover biological mechanisms and novel drugs

Chemical biology, defined as the use of chemicals to understand “the function of genes and proteins and their role in physiology and pathology” (1), has provided a new method for elucidating biological processes and for drug discovery. Chemicals can be used *in vitro* or *in vivo* to probe a particular protein or pathway and assess the function of that protein or pathway. If the pathway is associated with a disease phenotype, chemical probes can both validate ‘druggable’ therapeutic targets and provide lead compounds for drug discovery.

There are numerous advantages to taking a chemical biology approach to understanding a particular pathway: chemicals act rapidly and often reversibly within the cell; they can be used for large-scale biochemical experiments in many cell types or even in model organisms; and they can be combined with RNAi or other chemicals for multiple effects (2).

Chemical biology can provide advantages over RNAi techniques as well as a complementary approach. Unlike RNAi, the use of chemicals can be precisely timed, particularly important for cell cycle studies, and can allow inhibition of specific functions of certain proteins while not overtly interfering with others (such as inhibition of kinase activity while allowing the kinase to act as a scaffold for assembly of a protein complex). Unlike chemical biology, RNAi techniques are not possible in all cell types or organisms and cannot easily be scaled up for large-scale experiments. RNAi, however, is less susceptible to off-target effects than chemicals are, and thus can provide concrete

evidence of the involvement of a particular protein in the biological process of interest.

Taken together, the two approaches can produce comprehensive information.

Chemical biology has been used extensively to better understand pathways associated with cancer and with the cell cycle. Table 1.1 outlines several categories of molecules used to inhibit the cell cycle. All of these compounds have been used as biological tools and some have been developed as therapeutics. As an example of the role chemicals can play in understanding biology, and how chemical probes can become novel therapeutics, specific inhibitors of the mitotic kinase Plk1 have been used to elucidate Plk1 function in late mitosis. Plk1 was found to trigger cytokinesis by activation of Rho GTPase through recruitment of the exchange factor Ect2 to the mitotic spindle, creating the contractile actin-myosin ring at the cleavage furrow (3-6). RNAi or genetic techniques could not have revealed this function of Plk1 due to the fact that knockout of Plk1 arrests cells at prometaphase. Plk1 inhibitors have now progressed into clinical trials for use in solid tumours: BI2536 is currently undergoing phase I and II clinical trials for use in non-small cell lung cancer, head and neck cancer, breast cancer, ovarian cancer, soft tissue sarcoma and melanoma (7-9). This example, one of many, demonstrates the power of chemical biology in studies of the cell cycle and cancer.

## **1.2 Cell-based high-throughput screening**

High-throughput screening for chemical probes and drug leads may be carried out through biochemical screening, where the action of screening compounds on the activity of a purified protein or enzyme is measured *in vitro*, or through cell-based assays, where the action of screening compounds on a cellular phenotype is measured. In cell-based

| <b>Type of inhibitor</b>  | <b>Phase of cell cycle arrest</b> | <b>Examples</b>  |
|---------------------------|-----------------------------------|--|
| CDK inhibitor             | Various                           | roscovitine<br>quercetin<br>flavopiridol<br>staurosporine/UCN-01   |
| PKC inhibitor             | Various                           | staurosporine/UCN-01   |
| Tyrosine kinase inhibitor | Various                           | lavendustin A<br>radicicol   |
| Proteasome inhibitor      |                                   | lactacystin<br>PS-341<br>epoxomycin<br>aclacinomycin A   |
| HDAC inhibitor            | Various                           | trapoxin<br>trichostatin A   |
| Cytoskeletal inhibitor    | Mitosis                           | paclitaxel<br>colchicine<br>vinblastine<br>latrunculin A/B<br>jasplakinolide<br>monastrol<br><i>S</i> -trityl-L-cysteine |
| ATPase pump inhibitor     | G1                                | apoptolidin<br>oligomycin<br>bafilomycin   |

**Table 1.1: Chemical inhibitors of the cell cycle.**

(adapted from (10))

screens, the phenotype measured may vary greatly but is often increased or decreased fluorescence emitted by a tagged protein, localization of a fluorescent protein, or co-localization of two fluorescent proteins.

High-throughput screening is defined as the testing of 10,000 to 100,000 compounds per day, usually accomplished using mechanization (11). While biochemical screens have been more common for high-throughput screening in the past, the advent of technology for acquiring and analyzing the large amounts of data collected in cell-based screens has increased their feasibility. As of 2006, approximately half of all high-throughput screens were cell-based (12). Biochemical screens offer the advantages of a direct, specific approach and little variability, but cell-based screens allow screening for effects on an entire pathway or an unknown target. In addition, the chemicals identified in cell-based screens are cell-permeable, and have the desired effect in the cell, while chemicals identified in a biochemical screen may be membrane-impermeable or have off-target effects *in vivo* (13, 14). If a compound is acutely toxic to cells and causes a reduction in cell numbers or condensed DNA indicative of apoptosis, it may be eliminated prior to secondary assays if toxicity was not the aim of the screen, streamlining the screening process.

Cell-based assays where more than one measurement is taken per well are defined as high-content screens (HCS) (13); HCS uses image processing algorithms to analyze images taken by an automated fluorescence microscope (15). High-content screening can be particularly useful when little is known about the target protein or when the pathway of interest is dependent on biological context (16), but diverse chemical libraries with good bioavailability are required (16, 17). Subtle changes within the cell, such as

micronucleation, re-localization of a protein, or dendritic spine growth, can be measured using high-content screening, and it can also identify effects on sub-populations of cells within a well (13, 18). The images generated can be used to measure multiple phenotypes, as cells can be labelled with more than one fluorophore. This advantage can allow estimation of the toxicity of a compound and easy secondary screening (e.g. for cell cycle arrest) (15, 18). As such, HCS assays are now used for many applications, including identification of probes for pathways with significance in cancer that were previously difficult to target.

Design and implementation of a successful cell-based screen involves four steps (13, 14): experimental design, assay development, screen execution, and target identification. Experimental design involves selecting the protein or pathway for which the screen will identify probes and designing an assay to measure the intended effect in cells. During assay development, that assay is modified so that it can be used in high-throughput format and validated for sensitivity and robustness. Cell-based screens can be carried out in 96-, 384- or even 1536-well format, but 384-well format is currently standard. The screen is then executed and active compounds are confirmed by a secondary assay. Finally, when the screen is for chemical probes of a pathway, the targets of active compounds must be identified. This last step can pose some difficulty, as there is no systematic approach to finding the target of a compound. If the compound retains activity after chemical modification, then affinity-based approaches, involving conjugation of a compound to beads for a pulldown of the target protein, or chemistry-based approaches, involving addition of a chemically reactive group to an active compound and a subsequent intracellular chemical reaction that allows isolation of the active compound

and its target, may be used (19). However, these approaches are often not possible due to loss of activity when a compound is modified, and other systematic approaches to target identification have yet to be developed.

Chemical genomics combines chemical biology with traditional genetic approaches by using chemicals, rather than mutations, that perturb a pathway or protein of interest to understand biological functions of that pathway or protein. Forward chemical genetics involves high-throughput or high-content screening for chemicals that induce a desired phenotype and identification of the chemical target, allowing observation of the *in vivo* activities of novel targets, while reverse chemical genetics involves the use of a target-specific chemical to study a particular protein. This approach has proved to be powerful in profiling cancer cell biology (20), and, as mentioned in Section 1.1, chemical probes identified using chemical genomics can often be useful lead compounds in the development of specific cancer therapeutics.

### **1.3 The cell cycle**

The cell cycle comprises four phases, represented in Figure 1.1. Gap 1 (G1) is a growth phase. DNA replication takes place during DNA synthesis (S) phase, and cell growth continues during gap 2 (G2) following DNA replication. During mitosis (M) (Section 1.3.1), the cell segregates its chromosomes and cytoplasm equally between two daughter cells. Cytokinesis, when the cytoplasm separates to form two daughter cells, accompanies telophase and is often defined as a separate process from mitosis. M phase comprises both mitosis and cytokinesis.

Completion of the cell cycle can take anywhere from a number of hours for rapidly

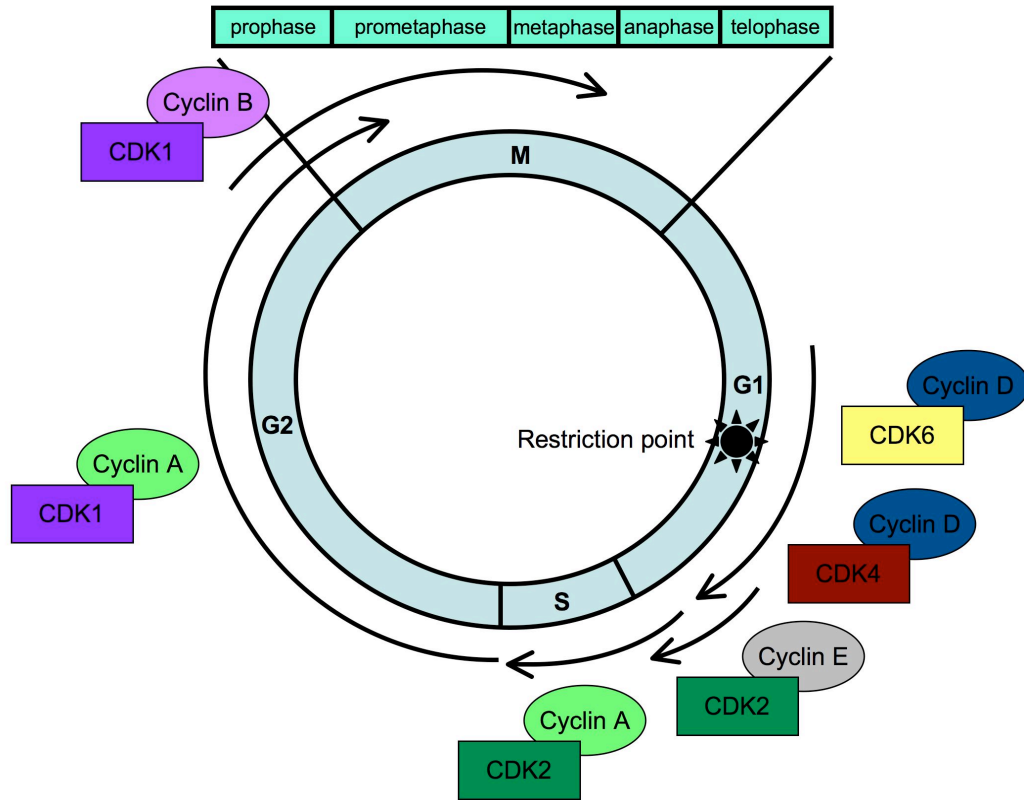


**Figure 1.1: The cell cycle and its regulation by CDK/cyclins.**

proliferating cells, to years for nonproliferating cells. Indeed, G1 may last indefinitely in the absence of stimuli for cell division, in which case it is termed G<sub>0</sub>.

### **1.3.1 Mitosis**

Mitosis is characterized by the equal segregation of replicated chromosomes to two daughter nuclei via function of the bipolar mitotic spindle. Five phases comprise mitosis (Figure 1.2): prophase, prometaphase, metaphase, anaphase and telophase. Prophase is initiated by activation of CDK1/CDC2, a cyclin-dependent kinase whose activity is crucial for the G<sub>2</sub>/M transition and during mitosis (21, 22). CDK1 activation requires accumulation of cyclin B1 (23), which takes place throughout G<sub>2</sub> phase (24), phosphorylation of the CDK1 catalytic subunit at activating sites (25), and dephosphorylation of the CDK1 catalytic subunit at an inhibitory site (Tyr15) by CDC25 phosphatases (26, 27), localizing it to the nucleus (28) and stimulating phosphorylation of numerous targets that control chromosome division. Chromosomes undergo extensive condensation and the mitotic spindle begins to form. When CDK1 phosphorylates nuclear lamins, the nuclear envelope breaks down and prometaphase begins (29); the condensed sister chromatids begin their microtubule-directed migration to the midbody of the cell, or the metaphase plate. Microtubules interact with kinetochores, large protein complexes located at the centromere of each sister chromatid. When free, kinetochores generate a ‘wait-anaphase’ signal through the mitotic checkpoint (30) (reviewed in Section 1.3.2.2) that maintains high CDK1/cyclin B1 activity while chromatids align and attach to microtubules emanating from both spindle poles. At metaphase, when chromosomes are all aligned and bioriented (30, 31), cyclin B1 and securin, a positive regulator of sister

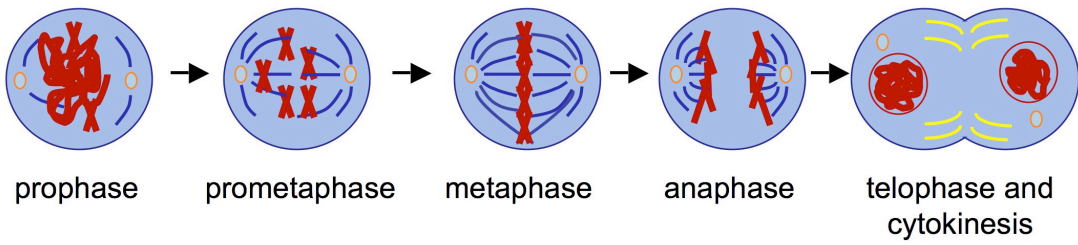


**Figure 1.2: Cellular and genetic division during M phase.**

chromatid attachment (32), are ubiquitylated by APC/C<sup>Cdc20</sup> and degraded by the proteasome (33, 34). The resulting CDK1 inactivation (35) signals initiation of anaphase and exit from mitosis. Securin degradation frees separase to cleave the cohesin complexes that attach sister chromatids (36), and the chromatids then separate and migrate to spindle poles through depolymerization of the microtubules of the mitotic spindle (37, 38). During telophase, the chromosomes decondense as two nuclear envelopes reform around the genome of each daughter cell, completing mitosis. Cytokinesis occurs concomitantly with telophase as a contractile actinomyosin ring forms at the cell midbody and cleaves the cytoplasm, forming two complete cells.

A bipolar mitotic spindle is central to the process of cell division. It is nucleated by two centrosomes that segregate to different regions of the cell during prophase and constitute the poles of the spindle (39, 40). The mitotic spindle itself is composed of microtubules, protofilaments of  $\alpha$ - and  $\beta$ -tubulin that form a polymeric tube. Microtubules can be described as being 'dynamically unstable', as they rapidly cycle between phases of GTP-dependent growth and phases of shrinkage. Chromosome attachment to spindle microtubules and chromosome congression to the metaphase plate is dependent on the dynamic instability of microtubules. The 'search-and-capture' model (41) of chromosome attachment and alignment describes random polymerization and depolymerization of microtubules through the cytoplasm until an interaction with a chromosome kinetochore is formed. Microtubule growth and shrinkage stochastically continues until a bipolar spindle is formed, with all sister chromatids aligned and bioriented along the metaphase plate. When anaphase is initiated, mass microtubule depolymerization as well as centrosome migration draw the separated sister chromatids to

the spindle poles and to the separating daughter cells (37). This dynamic behaviour of microtubules allows them to be targeted by antimitotic cancer therapies (Section 1.4) that inhibit microtubule polymerization or depolymerization and thus halt mitosis.

### **1.3.2 Cell cycle regulation**

To ensure genomic stability, the cell cycle must be tightly regulated to prevent replication of damaged DNA and division of cells with damaged DNA or improperly aligned chromosomes. Regulation is carried out through a complex system involving activation and inactivation of cyclin-dependent kinases (CDKs) at different phases of the cell cycle. CDKs drive every step of the cell cycle, and control of CDK activities determines progression through the cycle. Regulation of CDKs is carried out in several ways (42): first, through the expression of cyclins, cofactors required for CDK activity that direct them to their kinase substrates; second, through inhibitory phosphorylations by members of the Wee1 kinase family, which can be removed by members of the Cdc25 phosphatase family; third, through activating phosphorylations by CDK-activating kinases (CAKs); and fourth, through the binding of CDK inhibitors such as p21, p27 and p16.

Cell cycle checkpoints chiefly function to control cell division in response to insufficient growth or threats to the integrity of the genome, such as DNA damage or chromosome misalignment. Any errors in DNA replication or cell division have the potential to introduce genetic abnormalities into daughter cells that may prove problematic and even fatal. Therefore, if the genome is damaged at any stage of the cell cycle, checkpoint mechanisms delay cell cycle progression (Figure 1.3). If the damage occurs during G1, DNA replication is prevented, while if the damage occurs during G2,

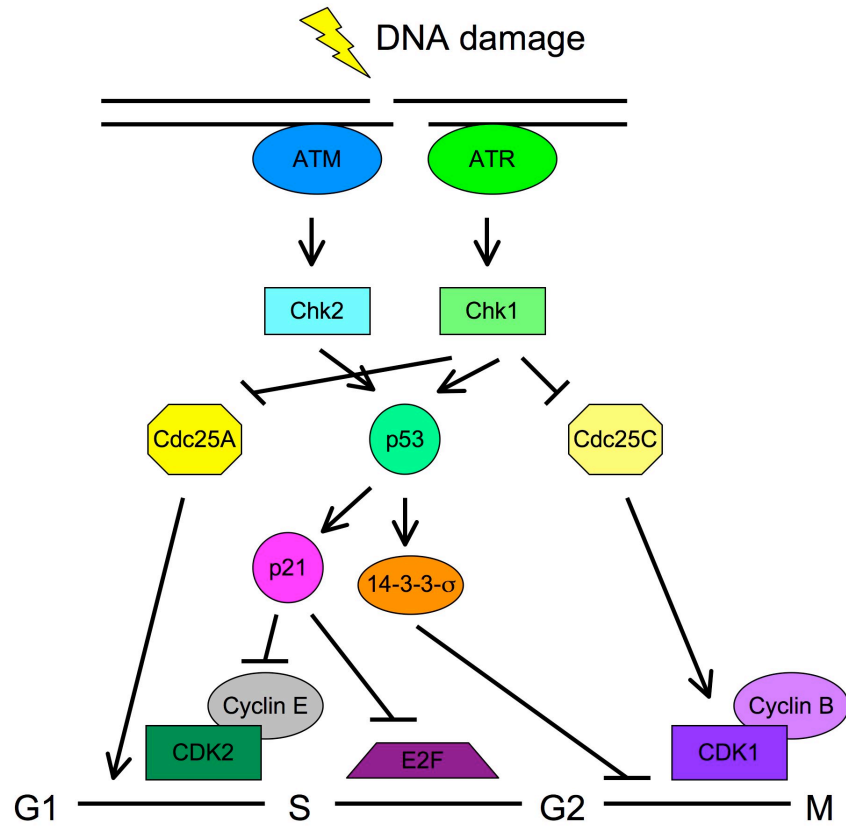


Figure 1.3: Pathways for cell cycle arrest in response to DNA damage.

the cell cycle is arrested while repair by homologous recombination takes place. Briefly, when DNA is damaged, ATM or ATR kinases localize to sites of DNA damage (43, 44) and activate CHK1 and CHK2 kinases (45, 46), which in turn phosphorylate and stabilize p53 and phosphorylate and inactivate members of the CDC25 family (47, 48). p53 induces cell cycle arrest through activation of p21, a CDK inhibitor that can arrest the cell cycle either independently of p53 or as part of the p53-dependent DNA damage response (49-51), and activation of 14-3-3- $\sigma$ , which plays a role in long-term G2 arrest (52). p21 can also inactivate the replication factor E2F, preventing cell cycle progression through S phase (53). Inhibitory phosphorylation of the CDC25 family proteins during G1 leads to ubiquitination and degradation of CDC25A (48, 54), delaying the G1-S transition, while inhibitory phosphorylation during G2 prevents CDC25C phosphatase activity on CDK1/cyclin B1, delaying entry into mitosis (55, 56) (Figure 1.3).

### **1.3.2.1 Cell cycle initiation and the G1-S transition**

When cell growth during G1 has been sufficiently robust (57), mitogenic signalling stimulates cyclin transcription and licensing of replication origins. Replication origins are primed during G1 phase by binding of Mcm2-7, part of the pre-replicative complex that facilitates formation of replication forks during S phase (58). When cyclin D1 is expressed in mid-G1, it associates with CDK4 and CDK6 and facilitates their translocation into the nucleus, where they phosphorylate proteins of the Rb family: pRb, p107 and p130 (59-61). These proteins activate the E2F transcription factors (62-64), which induce expression of proteins required for G1 and S phases. The CDK inhibitors p21 and p27 are also expressed at this time (65, 66); they inhibit CDK2/cyclin E1.

CDK2/cyclin E1 also regulates its own activity by phosphorylation of p27 and cyclin E1, both of which lead to its ubiquitination and proteasome-dependent degradation (67, 68). Additionally, the INK4 family of CDK inhibitors (p15, p16, p18 and p19) inhibits CDK4 (69, 70). When CDK2/cyclin E1 is activated, S phase is initiated through additional phosphorylation of pRb by CDK2/cyclin E1 (71, 72).

At the G1-S transition, the CDKs phosphorylate licensed replication origins to allow DNA replication to begin (73, 74). Cyclin A is also expressed at this time. CDK2/cyclin A activity is required for DNA replication and also increases transcription of histones and other proteins required for S phase (75, 76).

During this process, the cell must pass the restriction point, where cell cycle progression becomes independent of extracellular signals (77, 78), although it can still be delayed or prevented in the case of genomic damage. The restriction point represents the time when the cell commits to division, and thus this point is especially vulnerable to deregulation in cancer (79, 80). The majority of tumours have defects in the pRb pathway, through many mechanisms, including but not limited to mutation of pRb, CDK4 or CDK6, overexpression of CDK4, CDK6, CDK2, cyclin D1, cyclin E1, or CDC25 A/B, or oncogenic signalling (81-83). Activation of Ras, for instance, increases levels of cyclin D1, CDK4 and CDK6 and leads to p27 degradation, resulting in an increase in CDK2 activity and pRb phosphorylation (81, 82). Deregulation of cell cycle entry through one of these mechanisms appears to give cells a direct growth advantage and contribute to tumourigenesis.

### 1.3.2.2 Exit from mitosis and the mitotic checkpoint

During mitosis, genetic integrity is maintained by ensuring that all chromosomes are attached to microtubules emanating from both poles of the mitotic spindle before segregation of sister chromatids begins (31, 84). This process is monitored by the mitotic checkpoint, which prevents initiation of anaphase until every kinetochore is attached and tension between kinetochores of paired sister chromatids is sufficient, ensuring biorientation (85, 86). To prevent aneuploidy and ensuing genetic defects leading to cell death or tumourigenesis (87, 88), the mitotic checkpoint must be sufficiently sensitive to delay chromosome separation when even one kinetochore is unattached. Exposure to drugs that interfere with microtubule dynamics, such as the taxanes (85, 89) and the *Vinca* alkaloids (90, 91) (reviewed in Section 1.4), similarly activates the mitotic checkpoint and arrests cells at mitosis, effectively preventing further proliferation.

The mitotic checkpoint, graphically represented in Figure 1.4, acts through inhibition of the anaphase-promoting complex/cyclosome (APC/C) (92, 93). APC/C is the E3 ubiquitin ligase (94, 95) that, when activated by cofactors Cdc20 or Cdh1 (96) at the metaphase – anaphase transition, polyubiquitinates the CDK1 cofactor cyclin B1 (94) and the separase regulator securin (32), among other substrates (97-99), targeting them for degradation by the proteasome. This results in CDK1 inactivation, separation of sister chromatids, and exit from mitosis. Unattached kinetochores generate a diffusible signal, the ‘mitotic checkpoint complex’ (MCC), comprised of BubR1, Bub3, and Cdc20 (100-102). The MCC binds to and inhibits APC/C to prevent premature degradation of cyclin B1 and securin.

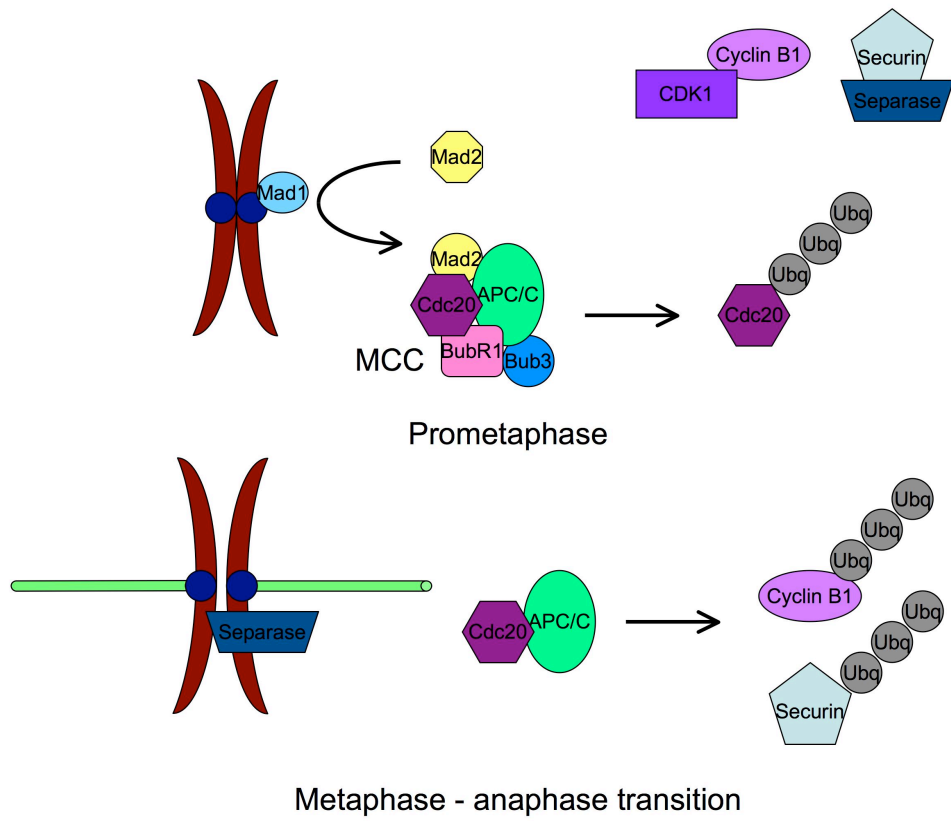


**Figure 1.4: Monitoring of microtubule attachment during mitosis by the mitotic checkpoint.**

The MCC is assembled at kinetochores by Mad1, which is thought to catalyze a conformational change in free Mad2 that allows it to bind Cdc20 (103, 104). Mad2 then catalyzes the binding of Cdc20 to BubR1 and subsequent formation of the MCC (105-107). Cdc20 is an activating cofactor of APC/C during mitosis (92, 96); an active spindle assembly checkpoint inhibits APC/C through APC/C-dependent polyubiquitylation of Cdc20 and subsequent degradation by the proteasome (107, 108). Acetylated BubR1 binds to and inhibits both Cdc20 (101) and APC/C itself (109), acting as a pseudosubstrate inhibitor. When the mitotic checkpoint is satisfied, BubR1 is deacetylated, ubiquitylated by APC/C<sup>Cdc20</sup>, and degraded by the 26S proteasome (110) (Figure 1.4). The role of Bub3 in the MCC is unclear, although in fission yeast it appears to be involved in MCC localization (111). Other components of the mitotic checkpoint include the kinases Bub1, Mps1, and Aurora A and B (86).

Besides activation in response to unattached kinetochores, the mitotic checkpoint must also be able to arrest cell division in response to improper microtubule-kinetochore interactions such as syntelic (kinetochores attached to microtubules emanating from the same spindle pole) and merotelic (one kinetochore attached to microtubules emanating from both spindle poles) attachments. While merotelic attachments do not activate the mitotic checkpoint, Aurora B is crucial for sensing both types of faulty interaction and correcting them through phosphorylation of several substrates that induce microtubule depolymerization at faulty connections (112-115). Additionally, Aurora B is a member of the chromosomal passenger complex, also composed of borealin, survivin and INCENP, which functions in chromosome congression, the process of aligning chromosomes at the

midpoint of the mitotic spindle (116). The related kinase Aurora A regulates centrosome maturation and mitotic spindle assembly (117).

During mitosis, cytokinesis failure or mitotic slippage (reviewed in Section 1.6) can give rise to tetraploid cells. Aneuploidy and tetraploidy have been observed in human cancer (118, 119), and can indeed drive tumour formation (120). Polyploidy can generate aneuploidy through aberrant multipolar divisions resulting from an increased number of centrosomes (120, 121). Overexpression of Aurora A has been observed in tumours (122) and generates tetraploid cells through cytokinesis failure (122, 123).

For many years, the observation of extensive polyploidy and aneuploidy in cancer led to the conclusion that cancer cells had some defect in the mitotic checkpoint that facilitated abnormal cell divisions and the transformation of normal cells into cancer cells. Indeed, mutation in or deletion of one allele of BubR1 has been observed in some types of cancer (124). BubR1 loss is sufficient to compromise the mitotic checkpoint (109, 125, 126) and results in aneuploidy (124). Studies in mouse models have revealed that loss of one allele of many other genes involved in the mitotic checkpoint, including Mad1, Mad2, Bub1, Bub3, and CENP-E, results in aneuploidy and increased tumour formation (127). However, overexpression of mitotic checkpoint components is more commonly observed in human cancer (128), indicating that increased mitotic checkpoint robustness may make a greater contribution to tumourigenesis than loss of mitotic checkpoint functionality. Most notably, Mad2 is overexpressed as a result of loss of p53 or pRb (83), the most prevalent mutations in tumours, and Mad2 overexpression results in chromosome instability and aneuploidy that is sufficient for tumourigenesis (129). Overexpression of Cdc20 also leads to aneuploidy (130). How aneuploidy contributes to

tumorigenesis is not clear, although it has been postulated that it may allow cells to accumulate mutations that increase cell transformation and survival (127, 131).

### **1.3.3 Senescence**

Senescence, a state of permanent growth arrest, functions to protect cells from the effects of DNA replication and cell division in the presence of irreparable DNA damage. Senescence is thought to occur as a result of non-repairable DNA damage, either when telomeres shorten below a critical length and single-stranded DNA is exposed, or when oncogene overexpression causes hyper-replication leading to DNA breaks (132). In the former scenario, after many cell divisions, telomeric DNA at the ends of chromosomes becomes too short to bind the proteins with which it normally forms a complex, as there is no cellular machinery to replicate DNA at the ends of chromosomes (133-136). The exposed single-stranded DNA triggers the p53-dependent DNA damage response, characterized by the formation of  $\gamma$ H2AX foci that assemble and activate DNA damage response kinases (137-139). In the latter scenario, oncogene expression causes sufficiently high rates of DNA replication that replication forks stall, DNA breaks, and the same DNA damage response is generated (140). The pathway leading to cell cycle arrest is reviewed in Section 1.3.2. When the damage cannot be repaired, the cell cycle is permanently arrested and senescence is initiated. Senescence is characterized by irreversible growth arrest (141), morphological changes including enlargement and flattening of cells in culture (142), and  $\beta$ -galactosidase activity at pH 6 (senescence-associated  $\beta$ -galactosidase) (143).

Since senescence halts division of oncogene-expressing cells, senescence may act as a tumour suppressor, providing a barrier that normal cells must overcome to become cancerous (144). Indeed, senescent cells are observed early in tumourigenesis (145, 146). However, senescence can be bypassed when further mutations accumulate (147). When p53 is mutated, as in most human cancers, the DNA damage response is compromised and the cell can escape senescence, re-enter the cell cycle and become immortal and cancerous (137, 148).

#### **1.4 Antimitotic cancer therapy**

Many approaches to cancer therapy utilise antimitotic drugs, with the rationale that cancer is a disease of uncontrolled cell proliferation. All currently approved antimitotic agents block cells in mitosis by targeting microtubule dynamics (149), which affect assembly and function of the mitotic spindle and trigger activation of the mitotic checkpoint (reviewed in Section 1.3.2.2).

There are two primary classes of antimitotic agents: the taxanes and the *Vinca* alkaloids. The taxanes, which include paclitaxel (Taxol) and docetaxel (Taxotere), bind to  $\beta$ -tubulin in polymerized microtubules and cause a conformational change that increases the strength of tubulin interactions (150-152). As such, the mitotic spindle cannot contract and exert the tension on kinetochores that is required to satisfy the mitotic checkpoint (91, 153). Conversely, the *Vinca* alkaloids, which include vinblastine and vinorelbine, bind to  $\beta$ -tubulin at the plus ends of microtubules and induce microtubule depolymerization (154), preventing formation of the mitotic spindle (90). The taxanes are approved for use in breast, ovarian, prostate, gastric and head and neck cancers and in

non-small cell lung cancer (155), while the *Vinca* alkaloids are mostly used in haematological cancers (149).

However, since these antimetabolic agents affect microtubules required for essential processes in all cells, side effects are common in antimetabolic therapy and include myelosuppression and peripheral neuropathy (149), which can cause permanent damage (156). Additionally, paclitaxel is poorly soluble and must be formulated for administration with a solvent such as polyoxyethylated castor oil (Cremophor EL) or polysorbate, which can lead to other adverse reactions (157). Drug resistance is also common (158). Mechanisms of resistance include expression of the P-glycoprotein efflux pump, a product of the multidrug resistance gene (159), mutations in  $\beta$ -tubulin that affect the drug binding site (160), and expression of alternate tubulin isotypes such as  $\beta$ III-tubulin (161, 162). Less commonly, expression of the proteins stathmin (163), which destabilizes microtubules, MAP4 (164), which promotes microtubule polymerization,  $\gamma$ -actin (165), or tau (166, 167) can contribute to drug resistance.

To eliminate the problems of toxicity and resistance, new classes of antimetabolic agents are being developed. The most prominent of these agents are those directed against kinesin spindle protein (KSP)/Eg5, a microtubule-based motor protein involved in the sliding of microtubules that is required for the establishment of a bipolar mitotic spindle (168, 169). KSP inhibition results in mitotic arrest with a monopolar mitotic spindle (170) and apoptosis through activation of the proapoptotic protein Bax, leading to mitochondrial membrane permeabilization and caspase activation (Section 1.5) (171, 172). Examples of KSP inhibitors include monastrol (170), *S*-trityl-L-cysteine (173), and ispenisib (174). The primary advantage of KSP inhibitors for cancer treatment is that

there is little or no expression of KSP in non-proliferating cells, reducing side effects particularly in neural cells, although myelosuppression is still observed (175). However, clinical response to these agents has been limited, so far preventing inclusion of KSP inhibitors in cancer treatments (175). Spindle formation is also affected by inhibitors of the Aurora kinases (VX-680, AZD1152), Polo-like kinases (BI2536, ON01910) and the CENP-E motor protein (GSK-923295). Some of these agents are currently undergoing clinical trials (176).

Several questions remain unanswered: how and when do cancer cells treated with an antimetabolic agent die? What is the mechanism of cell death, and how does it relate to the genetic background of the cancer? Cells have been observed to die during the perturbed mitosis (177), after mitotic slippage (reviewed in Section 1.6) (153) or after an abnormal cell division (178), and may die through caspase-independent cell death (179), through autophagy (180-183) or through apoptosis (184), which seems to be connected to mitotic progression (see Section 1.5). There are extensive differences in response to antimetabolic agents between cell lines and between populations within the same cell line (185), and response does not seem to depend on length of mitotic arrest (185), mitotic exit (171), or the presence of microtubules (186). Response does seem to depend on the concentration of the antimetabolic agent in the cell (185, 186), the levels and activity of apoptotic proteins (187, 188), and whether or not mitotic slippage occurs (171, 185) (reviewed in Section 1.6). The complexity of the outcome of treatment with an antimetabolic agent is also reflected in the clinic (189), especially since tumours are exposed to antimetabolic drugs transiently and at variable concentrations. As such, development of strategies for overcoming side effects of and resistance to antimetabolic agents and identification of

factors that affect cell death after treatment with antimetabolic agents is clearly of paramount importance.

## **1.5 Apoptosis**

Apoptosis, or programmed Type I cell death, is probably the most common mode of cell death, although there are other cell death mechanisms such as autophagic cell death, necrosis, and PARP-1 mediated cell death. Apoptosis plays a significant role in cell death during normal human development and in maintenance of homeostasis (190), especially in the immune system, and is characterized phenotypically by DNA fragmentation (resulting in cells with sub-G1 DNA content), membrane blebbing, and formation of apoptotic bodies (191). Improperly regulated apoptosis, either too much or too little cell death, is involved in cancer, autoimmune diseases, and tissue injury and decline in a variety of disorders (190).

There are two well-established pathways leading to apoptosis. Of most importance in cancer is the intrinsic pathway, in which apoptosis is induced in response to intracellular stresses such as irreparable DNA damage or mitochondrial damage. First, the pro-apoptotic BH3-domain-only proteins are upregulated by a variety of mechanisms including transcription, cleavage of zymogens, phosphorylation, myristolation and ubiquitination (192-196) and bind and inhibit the anti-apoptotic Bcl-2 family proteins Bcl-2, Bcl-x<sub>L</sub> and Mcl-1 (197). These proteins reside in the outer mitochondrial membrane and protect it from damage by the pro-apoptotic Bcl-2 family proteins Bax and Bak (197, 198). When the anti-apoptotic Bcl-2 proteins are inhibited, Bax and Bak form a channel in the outer mitochondrial membrane that allows the release of

cytochrome c from mitochondria (199). In the cytosol, cytochrome c induces formation of the apoptosome, a complex containing APAF-1 and caspase-9 that activates caspase-9 (200, 201). Caspase-9 then cleaves and activates the effector caspases, caspases-3, -6 and -7 (202). Caspases are a family of cysteine proteases that carry out the downstream steps of apoptosis, leading to the morphological changes associated with this form of cell death (203-205). They can also stimulate pro-apoptotic activity of normally anti-apoptotic Bcl-2 family proteins through cleavage (206).

The extrinsic apoptotic pathway also leads to the activation of effector caspases. However, it is initiated by extracellular signals when pro-apoptotic or pro-inflammatory cytokines such as the Fas ligand or TNF- $\alpha$  bind to transmembrane death receptors (207). These death receptors catalyze the formation of intracellular death-induced signalling complexes that activate the upstream caspases-8 and -10 (208), which cleave and activate caspases-3 and -7 (209). This extracellular death signal can be amplified through caspase-8 cleavage and activation of Bid, a BH3-only pro-apoptotic protein that causes mitochondrial damage and intrinsic apoptotic signalling (210).

In response to DNA damage, p53 exerts its effects on apoptosis through activation of caspase-2 (211) and subsequent formation of an active Bax/Bak pore in the outer mitochondrial membrane (212), leading to mitochondrial damage, cytochrome c release and downstream intrinsic apoptotic signalling.

During mitosis, caspase activity is tightly regulated and must be restrained during mitotic stress to prevent extensive cell death, most notably through survivin, which inhibits caspase activation during mitotic arrest and functions as part of the mitotic checkpoint machinery (213-215). Cell death in mitosis occurs through apoptosis, as it is

caspase-dependent (185, 186, 216). Loss of expression of X-linked inhibitor of apoptosis protein (XIAP) is thought to increase cancer cell survival in response to antimetabolic agents (188, 216). Besides their well-characterized apoptotic functions, caspase-3 and caspase-7 have both recently been observed to play a role, yet to be defined, in mitotic progression (217, 218). Caspase inhibition has been observed to prolong mitotic arrest and prevent exit from mitosis (149), perhaps due to increased CDK1 activity when inhibition of caspase-9 prevents its inactivating phosphorylation of CDK1 (184).

## **1.6 Mitotic slippage**

Mitotic checkpoint activation during an unperturbed mitosis provides sufficient time for microtubule attachment, preventing aneuploidy (88, 219) and increasing cell survival (220, 221). However, long-term activation of the mitotic checkpoint during exposure to antimetabolic agents can be problematic because chromosome condensation hinders RNA transcription (222, 223). With time, an imbalance between new protein production and protein degradation may cause the levels of proteins essential to maintain mitotic arrest to fall, triggering mitotic slippage. Also termed mitotic checkpoint adaptation, mitotic slippage occurs when cells exit mitosis without chromosome segregation or cell division (219, 224, 225). Slippage results from slow ubiquitination of cyclin B1 by APC/C<sup>Cdc20</sup> and subsequent proteasome-dependent degradation in the presence of an active mitotic checkpoint (226, 227). Cells that have undergone mitotic slippage enter a G1-like state with decondensed chromosomes that form multiple micronuclei (225), allowing resumption of transcription and other cellular processes. The development of polyploidy has been identified as a potential step towards tumorigenesis (87, 120, 228) (reviewed in

Section 1.3.2.2), although it is not clear whether these cells can stably proliferate at higher ploidy levels. Whether mitotic slippage constitutes a cell survival strategy or a cell death mechanism remains unclear, as mitotic slippage has been connected to a higher frequency of cancer cell death in response to antimetabolic agents (149, 185) but prevention of mitotic slippage by Cdc20 knockdown results in cell death (229). The variable responses of cells to an antimetabolic agent are represented schematically in Figure 1.5. Regardless of the role mitotic slippage plays in cancer cell death during antimetabolic therapy, there is considerable interest in factors that govern this process (149).

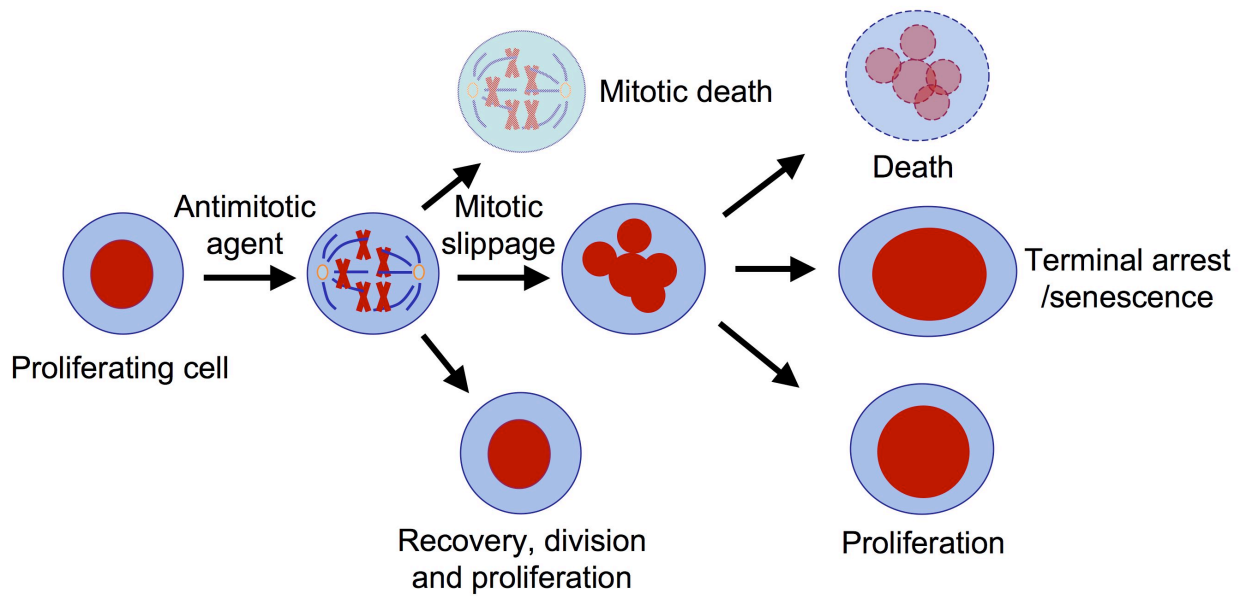


**Figure 1.5: Potential outcomes of cellular exposure to an antimetabolic agent.**

## 1.7 Objectives

### 1.7.1 Question 1: Can we design high-throughput cell-based screens to find chemicals that affect the cell cycle: modulators of mitotic arrest, and stimulators of senescence?

At the time of beginning this thesis, the only method for studying mitotic slippage was video microscopy. Cells in culture would be exposed to an antimetabolic agent and mitotic slippage would be monitored, usually with a fluorescent marker for chromatin. This process involves treatment with antimetabolic agents for 24-48 hours, a prolonged period of time that increases the likelihood of cell death and is unlikely to be physiologically relevant, thus making it difficult to draw conclusions about the outcome of mitotic slippage. The only known chemical modulators of mitotic slippage were CDK1 inhibitors (230, 231) such as roscovitine, which suffer from lack of specificity (232), and Aurora B inhibitors such as ZM447439 (233). Likewise, the only chemicals known to drive cells into senescence were HDAC inhibitors such as trichostatin A (234, 235), which have myriad effects on cells (236). There was a clear requirement for chemicals that specifically modulate the cell cycle in these ways.

Therefore, I aimed to design and execute high-throughput cell-based screens to identify chemical inducers of senescence, chemical inhibitors of mitotic slippage, and chemical inducers of mitotic slippage.

### **1.7.2 Question 2: What is the outcome of mitotic slippage with respect to cell fate?**

I used the chemical inhibitors and inducers of mitotic slippage identified as the outcomes of Question 1 to determine whether, as shown in Figure 1.5, mitotic slippage leads to cell survival and continued proliferation, cell cycle arrest, or cell death.

### **1.7.3 Question 3: What is the molecular mechanism of mitotic slippage?**

Using the chemical inducers of mitotic slippage identified in Question 1, I probed the mechanism of mitotic slippage to discover factors that influence whether cancer cells are likely to undergo mitotic slippage.

### **1.7.4 Question 4: Is inhibition or induction of mitotic slippage a good strategy for anticancer therapy?**

Using the knowledge gained from Question 2 and Question 3, I evaluated the potential impact of mitotic slippage during cancer therapy with an antimetabolic agent and whether cancer therapies combining antimetabolic agents and inhibitors or inducers of mitotic slippage could be useful in the clinic.

## **CHAPTER 2: MATERIALS AND METHODS**

### **2.1 Cell lines**

T98G human glioblastoma cells obtained from the American Type Culture Collection were maintained in DMEM (Sigma). T98G WAF1 cells (a gift from Dr. John Th'ng, Lakehead University) were cultured in DMEM supplemented with 400 µg/mL G418 (Invitrogen). The breast cancer cell lines MCF-7pcDNA and MCF-7casp3 (a gift from Dr. Reiner Jänicke, University of Düsseldorf) were maintained in RPMI (Sigma) supplemented with 10 mM HEPES, pH 7.4, (Gibco) and 400 µg/mL G418 (Invitrogen). MCF-7mp53, MDA-MB-231 (human breast cancer) and HCT116 wild-type, p53<sup>-/-</sup> and securin<sup>-/-</sup> (human colon cancer, a gift from Dr. Phil Hieter) cell lines were cultured in RPMI (Sigma) supplemented with 10 mM HEPES (Gibco). All cell culture media were supplemented with 10% fetal bovine serum (Gibco), 100 units/mL penicillin and 100 µg/mL streptomycin.

### **2.2 Screening chemicals**

All screening chemicals came from a collection of 31,600 known drugs and pharmacologically active agents that is part of the Canadian Chemical Biology Network screening node housed in the Roberge laboratory. A searchable database is available in the laboratory.

### **2.3 Screen for activators of p21**

T98G WAF1 cells seeded in 96-well plates (PerkinElmer Viewplate) were exposed to screening chemicals at concentrations of approximately 15 µM for 48 h at 37°C. The cells

were then fixed in 3% paraformaldehyde (Fisher) in PBS (10 mM Na<sub>2</sub>HPO<sub>4</sub>/1.75 mM KH<sub>2</sub>PO<sub>4</sub>, pH 7.4, 140 mM NaCl (Fisher), 3 mM KCl (Fisher)) for 15 min at room temperature and the nuclei were stained with 500 ng/mL Hoechst 33342 (Invitrogen) in PBS for 10 min at room temperature. The plates were imaged and analyzed using a Cellomics VTI high content screening instrument using the Hoechst (excitation 365 nm, emission 515 nm) and red (excitation 549 nm, emission 600 nm) channels. The average red fluorescence per cell corresponds to the level of p21 promoter activity within the cell.

#### **2.4 Screen for inhibitors of mitotic slippage**

MDA-MB-231 cells were seeded in 96-well plates (PerkinElmer Viewplate) and treated with 20-50 nM paclitaxel for 4 h at 37°C. The compounds to be screened were then added at concentrations of approximately 15 µM and the cells were incubated for a further 20 h. The plates were centrifuged at 50 x g for 2 min and then fixed and permeabilized with 3.7% formaldehyde (Fisher) and 0.1% Triton X-100 (LabChem Inc.) in TBS for 15 min. Cells were blocked in 1% bovine serum albumin (Sigma) in TBS for 30 min at room temperature and incubated with 1:50 TG3, an antibody obtained from tissue culture supernatants (a gift from Peter Davies, Albert Einstein College of Medicine) that recognizes mitotically phosphorylated nucleolin (237). After 1 h, the cells were washed in TBS and incubated with 13.3 µg/mL goat anti-mouse AlexaFluor 568 (Invitrogen) for 1 h at room temperature. Nuclei were stained with 500 ng/mL Hoechst 33342 (Invitrogen) for 10 min and the plates were analyzed using a Cellomics ArrayScan VTI. Cells were identified by their nuclear staining and the number of cells in each field

with the strong TG3 staining indicative of a mitotic cell was quantified in the second red channel, allowing calculation of the percentage of cells in mitosis.

## **2.5 Survival assays**

MCF-7mp53, MDA-MB-231 or T98G cells were seeded in 96-well plates (Falcon) and treated with 0, 3 or 5  $\mu$ M paclitaxel for 4 h at 37°C. 1-20  $\mu$ M chlorpromazine, triflupromazine, SU6656 or geraldol was added for a further 44 h. The chemicals were then washed away and the cells were incubated in drug-free medium for 2-4 days until the control untreated cells reached confluency. 2.5 h before the end of the incubation period, 25  $\mu$ L of 5 mg/mL 3-(4,5-dimethylthiazol-2-yl)-2,5-diphenyltetrazolium bromide (MTT) (Sigma) in PBS was added to each well. Finally, 100  $\mu$ L of extraction buffer (20% w/v SDS (Fisher), 2.5% acetic acid (Fisher), 2.5% 1M hydrochloric acid (Sigma), 50% N,N-dimethyl formamide (EMD)) was added to each well and the plate was incubated overnight at 37°C. The absorbance at 570 nm, which corresponds to the metabolic activity of the cells, was measured on a Dynex Technologies Opsys MR plate reader, corrected for absorbance of the cell culture medium, and compared to the absorbance of cells treated with paclitaxel alone.

## **2.6 Screen for inducers of mitotic slippage**

T98G cells at approximately 75% confluency were treated with 0.33  $\mu$ M nocodazole or 30 nM paclitaxel for 20 h at 37 °C. Mitotic cells were then isolated by shake-off, counted using a hemacytometer, transferred to 96-well plates (PerkinElmer Viewplate) at 5,000 cells per well and treated with screening chemicals at approximate concentrations

of 15  $\mu\text{M}$ . After incubation for 4 h at 37°C, the medium and unattached cells were aspirated and the attached cells were fixed with 3% paraformaldehyde (EMD) in PBS for 15 min at room temperature. The cells were then stained with 500 ng/mL Hoechst 33342 (Invitrogen) for 10 min at room temperature and counted using a Cellomics ArrayScan VTI. The instrument was programmed to detect and count the Hoechst-stained nuclei in 5 fields per well, and the Valid Object Count parameter was used to quantify the number of slipped cells per well.

## **2.7 Immunofluorescence microscopy**

T98G cells were treated with 30 nM paclitaxel for 20 h at 37°C. Mitotic cells were shaken off, seeded on glass coverslips in 12-well plates, and treated with 0.1% DMSO or 5  $\mu\text{M}$  SU6656 or geraldol for 4 h at 37°C. The following steps took place at room temperature: after centrifugation at 50 x g for 5 min, the cells were fixed in 3.7% formaldehyde (Fisher Scientific) in PBS for 20 min, permeabilized in 0.1% Triton X-100 (LabChem Inc.) in PBS for 5 min, and blocked in 2% bovine serum albumin (Sigma)/10% fetal bovine serum (Gibco) in PBS for 30 min at room temperature. The coverslips were incubated with primary antibody in PBS for 1 hour, washed in PBS, and incubated with secondary antibody in PBS for 1 h. Finally, the cells were stained with 500 ng/mL Hoechst 33342 (Invitrogen) for 5 min, mounted on slides and sealed. The primary antibodies were mouse  $\beta$ -tubulin (1:40; Developmental Studies Hybridoma Bank, University of Iowa), and mouse phospho-histone H3 (1:400). The secondary antibody used was goat anti-mouse AlexaFluor 568 (13.3  $\mu\text{g}/\text{mL}$ ; Invitrogen).

## 2.8 Flow cytometry

75% confluent T98G cells were treated with 30 nM paclitaxel, 30 nM vinblastine or 1  $\mu$ M *S*-trityl-L-cysteine for 20 h at 37°C. Mitotic cells were then harvested by shake-off, seeded in 10-cm dishes, and treated with 0.1% DMSO, 5  $\mu$ M SU6656, or 5  $\mu$ M geraldol in the continued presence of paclitaxel for 4 h at 37°C. The drugs were then washed away and the cells were allowed to grow in fresh culture medium. Mitotic cells, cells exposed to a slippage inducer for 4 h, or cells induced to slip and incubated in fresh culture medium for different times were trypsinized and centrifuged for 7 min at 400 x g and 4°C. They were then washed twice in SAB (1% fetal bovine serum (Gibco)/0.1% azide (Sigma) in PBS) and fixed in 10 volumes 70% ethanol at 4°C. Following overnight fixation, cells were washed twice in Tw-SAB (0.5% Tween-20 (MP Biomedicals) in SAB), permeabilized in Tw-SAB for 30 min on ice, and centrifuged as before. The cells were resuspended in 1.12% sodium citrate (EMD), pH 8.4, supplemented with 100  $\mu$ g/mL RNase A (Qiagen) and incubated for 30 min at 37°C. They were then stained with propidium iodide (Calbiochem) for 20 min at 37°C and analyzed for cell cycle profile using a BD LSRII flow cytometer.

## 2.9 Senescence-associated $\beta$ -galactosidase staining

75% confluent T98G cells were treated with 30 nM paclitaxel, 30 nM vinblastine or 1  $\mu$ M *S*-trityl-L-cysteine for 20 h at 37°C. The mitotic cells were shaken off, transferred to 6-well plates (Falcon) and treated with 0.1% DMSO, 5  $\mu$ M SU6656 or 5  $\mu$ M geraldol for 4 h at 37°C, at which time the drug-containing medium was replaced with fresh DMEM and the cells were allowed to grow at 37°C for 8 days. The cells were then washed thrice

in PBS and fixed in 3% formaldehyde (Fisher) in PBS for 3 min at room temperature. They were washed again 3x in PBS and stained overnight at 37°C in X-gal staining solution (40 mM citric acid (Fisher)/40 mM dibasic sodium phosphate (Merck), 150 mM NaCl (Fisher) and 2 mM MgCl<sub>2</sub> (Fisher)) with freshly added 5 mM K<sub>3</sub>Fe(CN)<sub>6</sub> (Sigma), 5 mM K<sub>4</sub>Fe(CN)<sub>6</sub> (Sigma) and 1 mg/mL X-gal (Roche). Three fields were counted under a phase contrast/bright field microscope and the percentage of senescent cells was averaged over the three fields.

## **2.10 Immunoblotting**

Cells were washed in PBS and lysed for 5 min on ice in lysis buffer containing 20 mM Tris-HCl (Fisher), pH 7.5, 150 mM NaCl (Fisher), 1 mM EDTA (Sigma), 1 mM EGTA (Sigma), 1% Triton X-100 (LabChem Inc.), 2.5 mM sodium pyrophosphate (Fisher), 1 mM β-glycerolphosphate (Sigma), 1 mM sodium orthovanadate (Sigma) and 1x protease inhibitor cocktail (Roche). Lysates were spun at 15,000 x g for 15 min and supernatants were removed and assayed for protein concentration using the Bradford assay (Sigma). Protein concentration was equalized and samples were diluted in 50 mM Tris-HCl (Fisher), pH 6.8, 2% SDS (Fisher), 0.1% bromophenol blue (Sigma) and 10% glycerol (Fisher). Samples were separated on a 12% acrylamide (Bio-Rad) gel, and stained with Coomassie Brilliant Blue to verify equal protein loading or transferred to a PVDF membrane (Millipore Immobilon-P). The membrane was blocked in 5% milk (Nestle) in TBS containing 0.1% Tween-20 (MP Biomedicals) (TBS-T) for 30 min and incubated overnight at 4°C with primary antibody in 5% milk in TBS. Membranes were then washed 2 x 10 min in TBS-T, incubated at room temperature with secondary

antibody in 5% milk for 1 h, washed 3 x 10 min. in TBS-T and imaged by chemiluminescence (Millipore Immobilon Western). Antibodies used were mouse  $\alpha$ -cyclin B1 (1:100, BD Pharmingen 554178), mouse  $\alpha$ -BubR1 (1:100, BD Transduction 612502), mouse  $\alpha$ -Mad2 (1:500, Santa Cruz sc-47747), mouse  $\alpha$ -p55CDC/Cdc20 (1:100, Santa Cruz sc-13162), mouse  $\alpha$ -Mps1 (1:500, Abcam ab11108), rabbit  $\alpha$ - $\beta$ -tubulin (1:5000, Santa Cruz sc-9104), goat  $\alpha$ -mouse HRP (1:10,000, Thermo Scientific 31430), and goat  $\alpha$ -rabbit peroxidase conjugate (1:10,000, Mandel Scientific KP-074-1506).

### **2.11 *In vitro* kinase assays**

SU6656 or geraldol were incubated for 20-30 minutes at room temperature with 20-40 nM active kinase, 0.2 mg/mL myelin basic protein (Aurora kinases) or 0.4 mg/mL synthetic Src substrate (KVEKIGEGTYGVVYK) and 50  $\mu$ M  $^{33}$ P-ATP in kinase assay buffer containing 25 mM MOPS, pH 7.2, 12.5 mM  $\beta$ -glycerol-phosphate, 25 mM  $MgCl_2$ , 5 mM EGTA, 2 mM EDTA and 0.25 mM DTT (Aurora kinases) or 25 mM MOPS, pH 7.2, 12.5 mM  $\beta$ -glycerol-phosphate, 20 mM  $MgCl_2$ , 25 mM  $MnCl_2$ , 5 mM EGTA, 2 mM EDTA and 0.25 mM DTT (Src). 10  $\mu$ L of this reaction mixture was then spotted on a phosphocellulose Multiscreen plate, washed 3 x 15 min. in 1% phosphoric acid. Scintillation fluid was added and the radioactivity on the plate was counted using a Trilux scintillation counter against a control incubated without substrate.

# CHAPTER 3: HIGH-CONTENT SCREENS FOR CELL CYCLE MODULATORS

## 3.1 Synopsis

High-content screens for cell cycle modulation via stimulation of senescence, strengthening of mitotic arrest and induction of mitotic slippage are reported in this chapter.

3800 pure chemicals were screened for stimulation of p21 promoter activity in the absence of p53. Thirty-eight active chemicals were identified, 8 of which were known antimitotic agents and 5 of which were known DNA topoisomerase inhibitors. Seven compounds with unknown mechanisms were chosen for further study, of which 8-azaguanine, erysolin, IC 261 and SKF 96365 were observed to induce senescence, measured by senescence-associated  $\beta$ -galactosidase activity, in T98G cells.

Two observations prompted screens for chemicals that inhibit or induce mitotic slippage. First, cancer cell lines exhibit varying responses to paclitaxel exposure. Second, cell lines that cannot maintain mitotic arrest in the presence of an unsatisfied mitotic checkpoint exit mitosis through mitotic slippage. Of the 3600 compounds screened for strengthening of mitotic arrest in MDA-MB-231 cells, 7 did so through their known antimitotic activities. Two of these chemicals, the antipsychotic drugs chlorpromazine and triflupromazine, reinforced paclitaxel-induced mitotic arrest at low micromolar concentrations and induced mitotic arrest at high concentrations. Screening of 4800 chemicals for induction of mitotic slippage in T98G cells identified 4 chemicals, two of

which had known activities that could stimulate mitotic slippage and were not examined further. The two compounds selected for further study, SU6656 and geraldol, induced cell attachment and loss of mitotic histone phosphorylation in T98G cells arrested in mitosis by antimitotic agents that act by various mechanisms.

## **3.2 Identification of chemical stimulators of senescence**

### **3.2.1 Screening for p21 promoter activity**

To determine whether small molecules can be used to force a cancer cell to become senescent in the absence of p53, which is normally involved in growth arrest and senescence (Section 1.3.3), I designed and carried out a screen for compounds that could activate senescence through upregulation of the CDK inhibitor p21, an important modulator of cell cycle arrest and senescence. p21 is activated by p53 in response to DNA damage (see Section 1.3.2), and p53 is commonly mutated in cancer, allowing bypass of damage-induced growth arrest (see Section 1.3.3). I screened for chemicals that increased p21 promoter activity in the p53-negative T98G glioblastoma cell line and determined whether compounds that increased p21 promoter activity induced senescence, utilising a cell-based system that allows measurement of the levels of a fluorescent reporter protein whose transcription is under the control of the p21 promoter region. Active compounds would upregulate p21, resulting in increased intracellular fluorescence (Figure 3.1). Briefly, T98G WAF1 cells were seeded in 96-well plates and exposed to screening chemicals for 48 h before fixing and nuclear staining. Intracellular fluorescence was quantified by automated fluorescence microscopy and an active compound was defined as one that induced fluorescence ten-fold over background fluorescence levels.

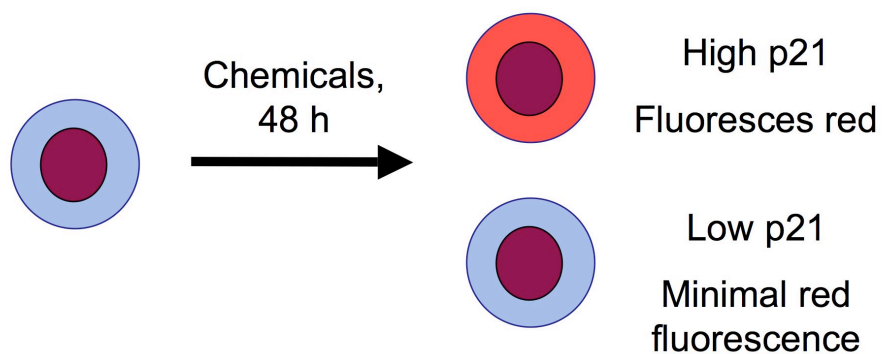


**Figure 3.1: Screen for senescence-inducing chemicals through p21 promoter activity.**

T98G WAF1 cells containing a fluorescent reporter protein under control of the p21 promoter were exposed to screening chemicals in 96-well plates for 48 h, fixed, stained with Hoechst 33342 to label nuclei, and cell number and reporter protein fluorescence were quantified by automated microscopy (see Section 2.3).

Quantification of cells allowed identification and elimination of toxic compounds that decreased cell number by 50% or more. Screening of 3800 compounds from the Canadian Chemical Biology Network collection of pure chemicals revealed 38 active compounds, listed in Table 3.1. A number of these compounds fell into two broad categories: inhibitors of microtubule polymerization and inhibitors of DNA topoisomerases (Table 3.1).

From this array of chemicals, I selected for further study seven whose biological functions, if known, were not obviously connected to senescence: 8-azaguanine, parbendazole, dihydroouabain, ceftibuten, erysolin, IC 261 and SKF 96365. Concentration curves for these compounds revealed that they were effective in increasing p21 promoter activity at low micromolar concentrations (Table 3.2).

### **3.2.2 Chemicals that increase p21 promoter activity can induce senescence**

To ascertain whether exposure to compounds that increased intracellular p21 levels also induced senescence, the activity of the main marker of senescence, senescence-associated  $\beta$ -galactosidase, was measured in T98G cells exposed to p21-increasing chemicals. The cells were exposed to chemicals at active concentrations for 48 h before the drugs were washed away and the cells were allowed to grow in fresh cell culture media for a further 3 d before overnight X-gal staining. The proportion of cells that were positive for  $\beta$ -galactosidase activity at pH 6.0 was determined in three fields of view or 500 cells, and the results are expressed in Figure 3.2. Cells exposed to parbendazole, dihydroouabain or ceftibuten re-entered the cell cycle when the drugs were washed away and no senescent cells were observed. Approximately 60% of cells exposed to sodium

| <b>Compound</b>               | <b>Inhibitor of microtubule polymerization</b> | <b>Inhibitor of DNA topoisomerases</b> |
|-------------------------------|--|--|
| <b>8-azaguanine</b>           |  |  |
| Nortriptyline                 |  |  |
| Ethinyl estradiol             |  |  |
| Thimerosal                    |  |  |
| 4'-demethylepipodophyllotoxin | √  |  |
| Picropodophyllotoxin          | √  |  |
| Picropodophyllotoxin acetate  | √  |  |
| Podophyllotoxin acetate       | √  |  |
| N-formyldeacetylcholine       | √  |  |
| <b>Parbendazole</b>           |  |  |
| β-lapachone                   |  |  |
| <b>Dihydroouabain</b>         |  |  |
| Camptothecin                  |  | √                                      |
| Idarubicin                    |  | √                                      |
| <b>IC 261</b>                 |  |  |
| <b>SKF 96365</b>              |  |  |
| Brefeldin A                   |  |  |
| Crinamine                     |  |  |
| Murolladi-3-one               |  |  |
| Gentian violet                |  |  |
| Cymarin                       |  |  |
| Vinblastine                   | √  |  |
| Vinorelbine                   | √  |  |
| Vincristine                   | √  |  |
| Tetrachloroisophthalonitrile  |  |  |
| Hypocrellin B                 |  |  |
| Acrisorcin                    |  |  |
| <b>Ceftibuten</b>             |  |  |
| Tegaserod maleate             |  |  |
| Acetyl isoallogambogic acid   |  | √                                      |
| Dimethylgambogate             |  | √                                      |
| Pyrrromycin                   |  | √                                      |
| Thiram                        |  |  |
| <b>Erysolin</b>               |  |  |
| Lasalocid sodium              |  |  |
| Plumbagin                     |  |  |
| β-peltatin                    |  |  |

**Table 3.1: Chemicals that induce transcription of a p21 promoter-regulated reporter protein.** The compounds selected for further study are shown in bold.

| <b>Compound</b> | <b>EC<sub>50</sub> (μM)</b> |
|-----------------|-----------------------------|
| 8-azaguanine    | 2.0                         |
| Parbendazole    | 0.05                        |
| Dihydroouabain  | 2.0                         |
| Ceftibuten      | 2.7                         |
| Erysolin        | 3.6                         |
| IC 261          | 2.0                         |
| SKF 96365       | 3.7                         |

**Table 3.2: Efficacies of lead p21-activating compounds.**

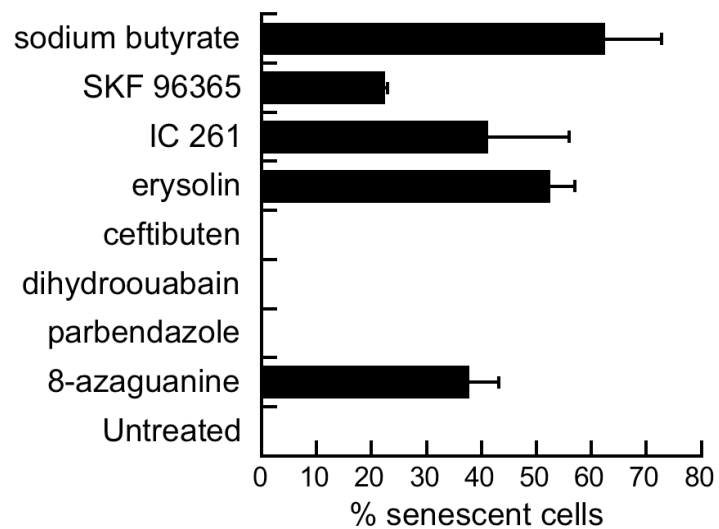


**Figure 3.2: Induction of senescence-associated  $\beta$ -galactosidase activity by p21-activating chemicals.**

T98G cells were exposed to active compounds at concentrations above the measured  $EC_{50}$  for 48 h, allowed to grow in fresh culture medium for a further 3 d, and were stained with X-gal at pH 6.0 (see Section 2.9).

butyrate, an HDAC inhibitor known to induce senescence (238), were senescent. 8-azaguanine, erysolin, IC 261 and SKF 96365 induced senescence in approximately 20-50% of cells (Figure 3.2). These compounds had little apparent toxicity, as at least 75% of cells survived after a 48 h exposure (not shown).

These results indicate that the outlined screen for compounds that induce p21 promoter activity in the absence of p53 has successfully identified compounds that can induce senescence in p53-deficient cancer cells.

### **3.3 Mitotic arrest and slippage in three cancer cell lines**

To determine whether cancer cell lines exhibit differences in mitotic arrest and slippage, a detailed analysis of mitotic arrest and slippage induced by the microtubule-targeting drug paclitaxel was carried out in three human cancer cell lines. MCF-7mp53 breast cancer cells expressing dominant-negative p53, MDA-MB-231 breast cancer cells and T98G glioblastoma cells were exposed to different concentrations of paclitaxel for 24 h and the number of cells arrested at mitosis was determined by quantitative immunofluorescence microscopy using the TG-3 antibody that recognizes mitotically phosphorylated nucleolin (237) and a Cellomics Arrayscan VTI automated fluorescence imager.

After a 24 h exposure, concentration-dependent mitotic arrest was observed at  $\geq 10$  nM paclitaxel for all cell lines (Figure 3.3). However, the extent of mitotic arrest differed for the three cell lines, reaching 70%, 40% and 50% at 100 nM paclitaxel for MCF-7mp53, MDA-MB-231 and T98G cells, respectively. The low percentage of mitotic arrest was not due to insufficiently long cellular exposure to the drug, as the doubling

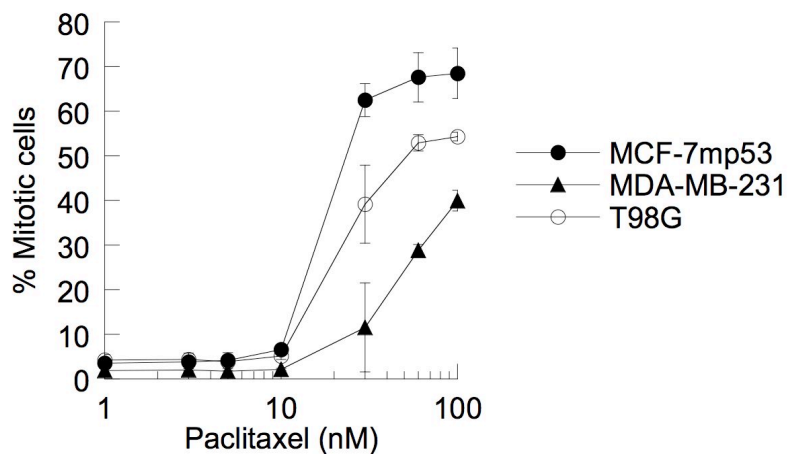


**Figure 3.3: Differential induction of mitotic arrest by paclitaxel in three cancer cell lines.**

MCF-7mp53, MDA-MB-231 and T98G cells were treated with 0-100 nM paclitaxel for 24 h and immunostained with the TG-3 antibody to label cells in mitosis. The proportion of cells in mitosis was determined by quantitation of TG3 fluorescence by automated microscopy (see Section 2.4). Visual inspection of images confirmed that cells had the condensed chromosomes characteristic of mitosis. Error bars represent standard deviation from the mean. Results shown are representative of three independent experiments and all subsequent assays were carried out similarly.

times of these three cell lines are  $\leq 24$  h, sufficiently long to block all cells at mitosis. This observation implied differences in the stability of mitotic arrest among the three cell lines. To characterize the stability of mitotic arrest, cells were exposed to different concentrations of paclitaxel for different times. MCF-7mp53 cells exposed to 30-100 nM paclitaxel showed a linear rate of mitotic accumulation until 16 h, when arrest reached a plateau (Figure 3.4), consistent with stable mitotic arrest and its 16 h doubling time. However, at 10 nM paclitaxel, mitotic accumulation was slower and reached a maximum at 8 h, after which time the proportion of mitotic cells decreased, implying that this low paclitaxel concentration caused transient mitotic arrest. MDA-MB-231 cells exposed to 60 or 100 nM paclitaxel initially arrested linearly at mitosis but accumulation stopped at 14-18 h, short of the 24 h doubling time for this cell line (Figure 3.4). Cells exposed to 30 nM paclitaxel reached a mitotic arrest plateau even earlier, at 8h. These observations implied that mitotic arrest was not stable in MDA-MB-231 cells, even at 100 nM paclitaxel. T98G cells exposed to 30-100 nM paclitaxel showed a linear rate of mitotic accumulation that decreased after 14 h exposure (Figure 3.4). At 10 nM paclitaxel, cells accumulated at mitosis until 8 h, after which the proportion of mitotic cells decreased. Therefore, mitotic arrest was less stable in MDA-MB-231 and T98G cells than in MCF-7mp53 cells.

Cells arrested at mitosis can escape checkpoint arrest and enter interphase without cell division. This response, termed mitotic slippage (see Section 1.6), is characterized by the unique multinucleated ‘grape-like’ nuclear morphology of slipped cells (225). To determine the extent to which mitotic slippage could account for the transient mitotic arrest observed above, the proportion of slipped cells was determined by visual

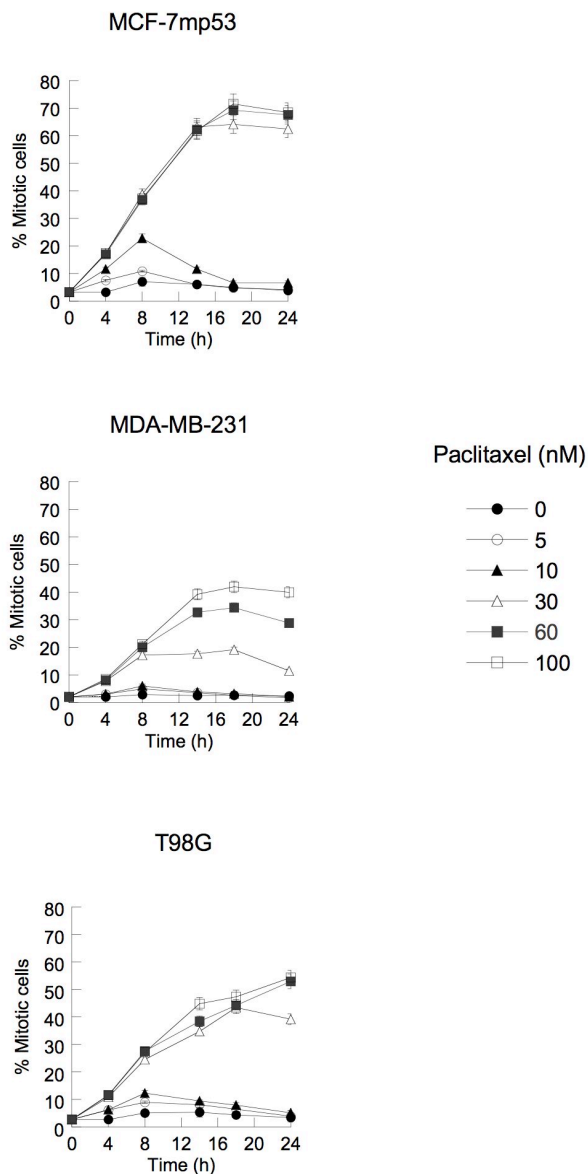


**Figure 3.4: Mitotic accumulation in three cancer cell lines during exposure to paclitaxel.**

MCF-7mp53, MDA-MB-231 and T98G cells were treated with 0-100 nM paclitaxel for up to 24 h and the proportion of mitotic cells was determined by quantitative fluorescence microscopy of the TG3 phosphoepitope (see Section 2.4). Error bars represent standard deviation from the mean.

inspection of nuclei as a function of time and paclitaxel concentration for the three cell lines. MCF-7mp53 cells showed no evidence of mitotic slippage at 30 nM (Figures 3.5A, 3.6) or above (not shown). Interestingly, there was also no evidence of mitotic slippage at 10 nM paclitaxel, a concentration that induced transient mitotic arrest (Figures 3.5A, 3.6).

Examination of populations treated with 10 nM paclitaxel at 8 h and 14 h showed large numbers of cells with metaphase plates (Figure 3.6, asterisks) as well a number of anaphase and telophase cells (Figure 3.6, arrowheads), indicating that cell division was taking place. Moreover, the total number of cells increased markedly between 8 h and 14 h at 10 nM paclitaxel and lower concentrations (not shown), confirming that cell division was taking place. By contrast, cells treated with 30 nM paclitaxel showed scattered condensed chromosomes and no evidence of metaphase plates (Figure 3.6), no cell division and no increase in cell number (not shown). Examination of mitotic slippage in MDA-MB-231 cells revealed a very different situation. MDA-MB-231 cells exposed to 30 nM paclitaxel showed a lower proportion of cells arrested at mitosis than MCF-7mp53 cells. Rather, a large number of cells that had undergone mitotic slippage were observed and this number increased over time to reach 58% of the total cell population at 24 h (Figure 3.5B). Strikingly, cells exposed to 10 nM paclitaxel showed only a maximum of 8% cells arrested at mitosis but the proportion of cells that had undergone mitotic slippage increased over time to reach 85% of the total cell population at 24 h (Figure 3.5B). Examples of images are shown in Figure 3.6, where some of the numerous slipped cells are indicated with arrowheads. There was no evidence of successful completion of mitosis at those concentrations (Figure 3.6) and cell numbers did not increase during the incubation period (not shown). Therefore, a high rate of mitotic slippage accounted for

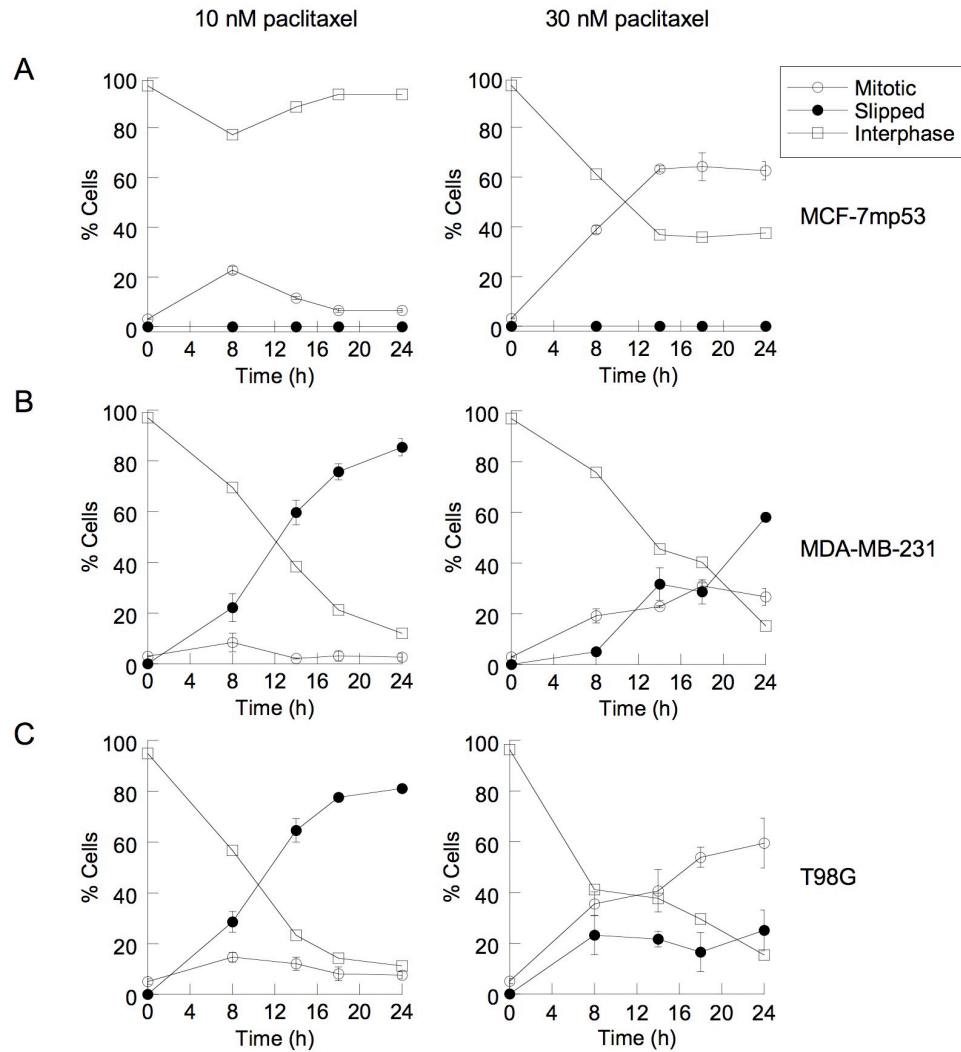


**Figure 3.5: Transient mitotic arrest in MDA-MB-231 and T98G but not MCF-7mp53 cells due to mitotic slippage.**

Cells were treated with 10 or 30 nM paclitaxel for up to 24 h, fixed, and stained with Hoechst 33342 to label nuclei and the TG-3 antibody to label mitotic cells. Automated fluorescence microscopy was used to quantitate the total number of cells and the number of mitotic cells (see Section 2.4) and the images were visually inspected to determine the number of slipped cells based on their characteristic fragmented nuclear morphology.

Error bars represent standard deviation from the mean.

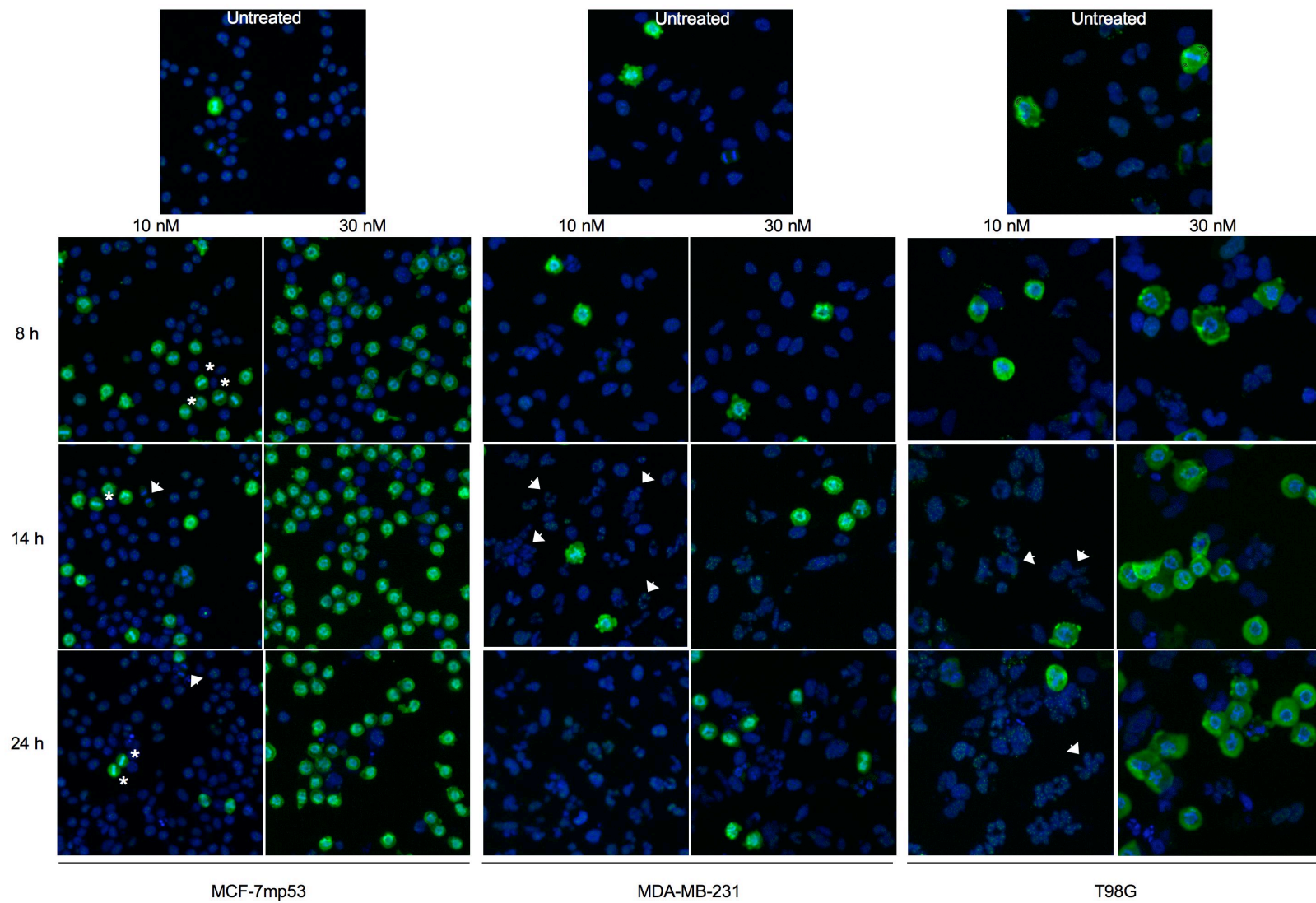


**Figure 3.6: Mitotic arrest and slippage during exposure of MCF-7mp53, MDA-MB-231 and T98G cells to paclitaxel.**

Untreated cells or cells treated with 10 or 30 nM paclitaxel for 8, 14 or 24 h were immunostained with the TG-3 antibody to label cells in mitosis (green), stained with Hoescht 33342 to label nuclei (blue), and imaged using an automated fluorescence microscope (see Section 2.4). Some MCF-7mp53 cells containing metaphase plates are denoted with asterisks (\*) and cells in anaphase or telophase are indicated with arrowheads. Some of the MDA-MB-231 and T98G cells that have undergone mitotic slippage, characterized by a grape-like nuclear morphology, are indicated with arrowheads.

the low proportion of MDA-MB-231 cells arrested at mitosis compared to MCF7-mp53 cells. T98G cells exposed to 10 nM paclitaxel showed a high rate of mitotic slippage, similar to MDA-MB-231 (Figures 3.5C, 3.6). However, at 30 nM paclitaxel, mitotic arrest was more stable in T98G than in MDA-MB-231 cells. There were more T98G cells arrested at mitosis than slipped cells at all time points, unlike MDA-MB-231 cells, where slipped cells became more numerous over time (Figures 3.5B, 3.6).

In summary, these experiments show that three cancer cell lines respond differently to paclitaxel exposure. At a low paclitaxel concentration, MCF-7mp53 cells underwent transient mitotic arrest followed by successful cell division, while at a higher paclitaxel concentration the cells underwent stable mitotic arrest. MCF-7mp53 cells showed no evidence of mitotic slippage at any of the paclitaxel concentrations or exposure times tested. At low paclitaxel concentrations, MDA-MB-231 and T98G cells underwent transient mitotic arrest followed by mitotic slippage without any evidence of successful cell division. At higher paclitaxel concentrations, MDA-MB-231 and T98G cells also underwent transient mitotic arrest followed by mitotic slippage, but the rate of mitotic slippage was higher in MDA-MB-231 cells than in T98G cells. The observation that different cell lines exhibited very different propensities to undergo mitotic slippage prompted me to search for chemicals that inhibit or stimulate mitotic slippage for use as tools to better understand the effect of mitotic slippage in antimetabolic cancer therapy.

### **3.4 Identification of chemical enforcers of mitotic arrest**

A cell-based assay was devised that enabled us to screen for chemicals that prevent mitotic slippage (Figure 3.7). MDA-MB-231 cells were selected because they showed the

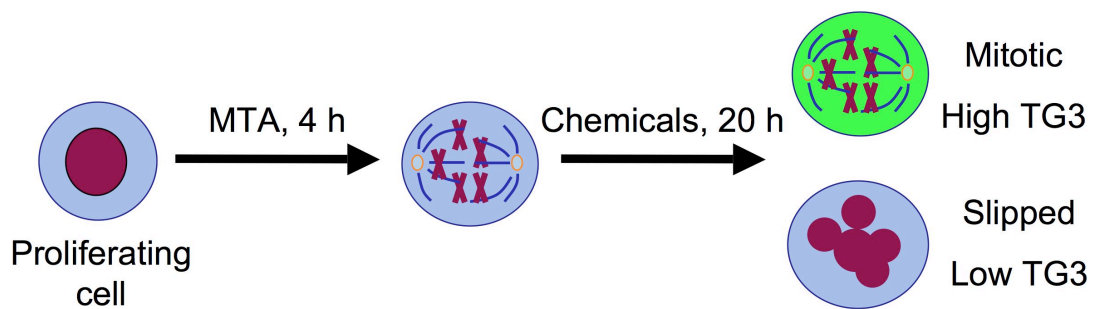


**Figure 3.7: Screen for chemical reinforcers of mitotic arrest.**

MDA-MB-231 cells in 96-well plates were treated with an antimetabolic agent (MTA) for 4 h and screening chemicals were added for a further 20 h before fixing and staining the cells with Hoechst 33342 to label DNA and TG3 to label mitotically phosphorylated nucleolin. The cell number and TG3 fluorescence were then quantified by automated fluorescence microscopy (see Section 2.4).

highest rate of mitotic slippage at 30 nM paclitaxel (Figure 3.5B). Cells were seeded into 96-well plates at 5,000/well and incubated with paclitaxel. After 4 h, chemicals from a collection of 3,584 drugs and pharmacologically active agents were added at a concentration of 15  $\mu$ M. 20 h later, the cells were fixed, immunostained with the TG-3 antibody to label cells arrested at mitosis and counterstained with Hoechst 33342 to label all cell nuclei. The percentage of mitotic cells was determined quantitatively using an automated fluorescence imager. A positive readout (increased mitotic arrest) was selected over a negative readout (decreased slippage) because positive readout assays are less prone to artefactual results from toxic chemicals (239-241). The paclitaxel concentration was selected to provide ~10 % mitotic arrest (20-50 nM), compared to 1-2% for untreated controls (Figure 3.8), to provide a large window to identify chemicals that increase mitotic arrest.

The vast majority of the chemicals tested had no effect, but a small number considerably increased mitotic arrest (Figure 3.8). Nine active chemicals were identified: seven microtubule-targeting agents and derivatives (colchicine, N-formyl-deacetylcolchicine, parbendazole, podophyllotoxin, sanguinarine, vinblastine, vincristine) and the structurally closely related antipsychotic drugs chlorpromazine and triflupromazine (CPZ and TPZ, Figure 3.9). The microtubule-targeting agents were not studied further because experiments described in the previous section had already shown that increasing the concentration of paclitaxel could stabilize mitotic arrest and decrease mitotic slippage, but CPZ and TPZ were analysed in more detail.

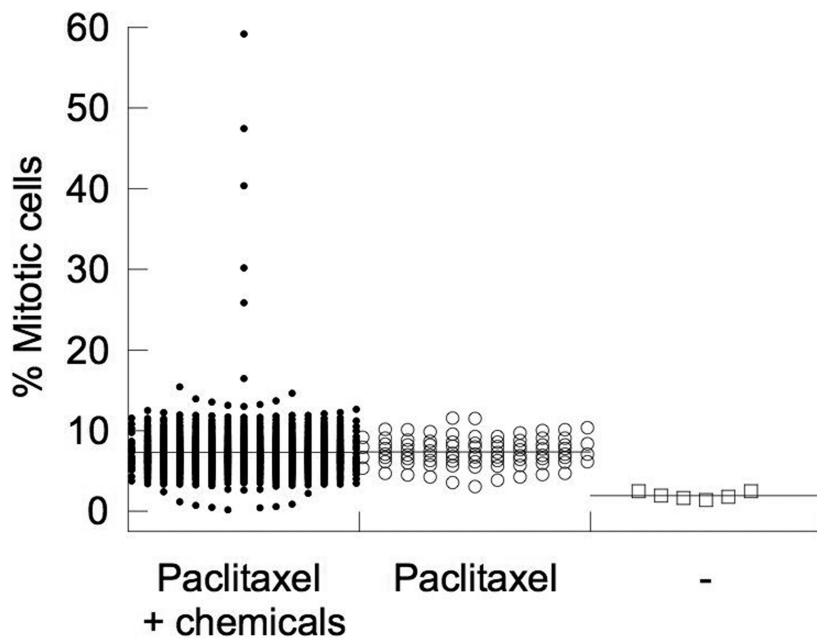


**Figure 3.8: Results of the screen for chemical enforcers of mitotic arrest.**

Example of screening results. MDA-MB-231 cells grown in 96-well plates were left untreated for 24 h (-), treated with paclitaxel for 24 h (paclitaxel) or treated with paclitaxel for 4 h followed by screening chemicals for a further 20 h (see Section 2.4). The proportion of cells in mitosis was determined by quantitative immunofluorescence microscopy.

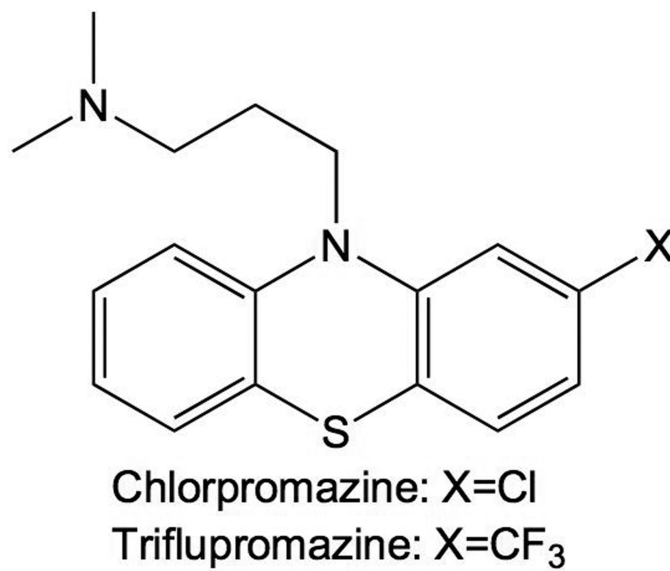


**Figure 3.9: Structures of the chemical reinforcers of mitotic arrest chlorpromazine and triflupromazine.**

Chlorpromazine and triflupromazine, two structurally closely related antipsychotic drugs found to inhibit mitotic slippage.

### **3.4.1 Effect of chlorpromazine and triflupromazine on mitotic slippage**

The effects of CPZ and TPZ on paclitaxel-induced mitotic arrest were tested in the three cell lines. Cells were exposed to different concentrations of CPZ or TPZ 4 h after treatment with 0, 10 or 30 nM paclitaxel and the extent of mitotic arrest was determined after a further 20 h.

Exposure of MDA-MB-231 cells to CPZ or TPZ alone at concentrations  $\leq 10 \mu\text{M}$  did not cause any mitotic arrest (Figure 3.10). Exposure of MDA-MB-231 cells to 10 nM or 30 nM paclitaxel caused 4% and 16% mitotic arrest, respectively, compared to 2% mitotic arrest in untreated populations (Figure 3.10). However, exposure to 10 nM or 30 nM paclitaxel together with 3-10  $\mu\text{M}$  CPZ considerably increased mitotic arrest (Figure 3.10). At higher concentrations, both CPZ and TPZ caused mitotic arrest on their own (Figure 3.10). In the other two cell lines, identical treatment yielded similar results: CPZ and TPZ also caused mitotic arrest at high concentrations, more so in MCF-7mp53 cells than in T98G cells. In combination with paclitaxel, 3-10  $\mu\text{M}$  CPZ and TPZ increased mitotic arrest, particularly when combined with 10 nM paclitaxel (Figure 3.10).

### **3.5 Identification of chemical inducers of mitotic slippage**

To identify chemicals that induce mitotic slippage, T98G was selected as a suitable cell line because it showed a lower spontaneous tendency to undergo mitotic slippage than the MDA-MB-231 cell line, but was able to undergo mitotic slippage, unlike the MCF-7mp53 cell line. The assay took advantage of the observation that mitotic cells adhere only loosely to tissue culture-treated plastic whereas slipped cells attach strongly, providing a positive readout to measure mitotic slippage (Figure 3.11). Adherent

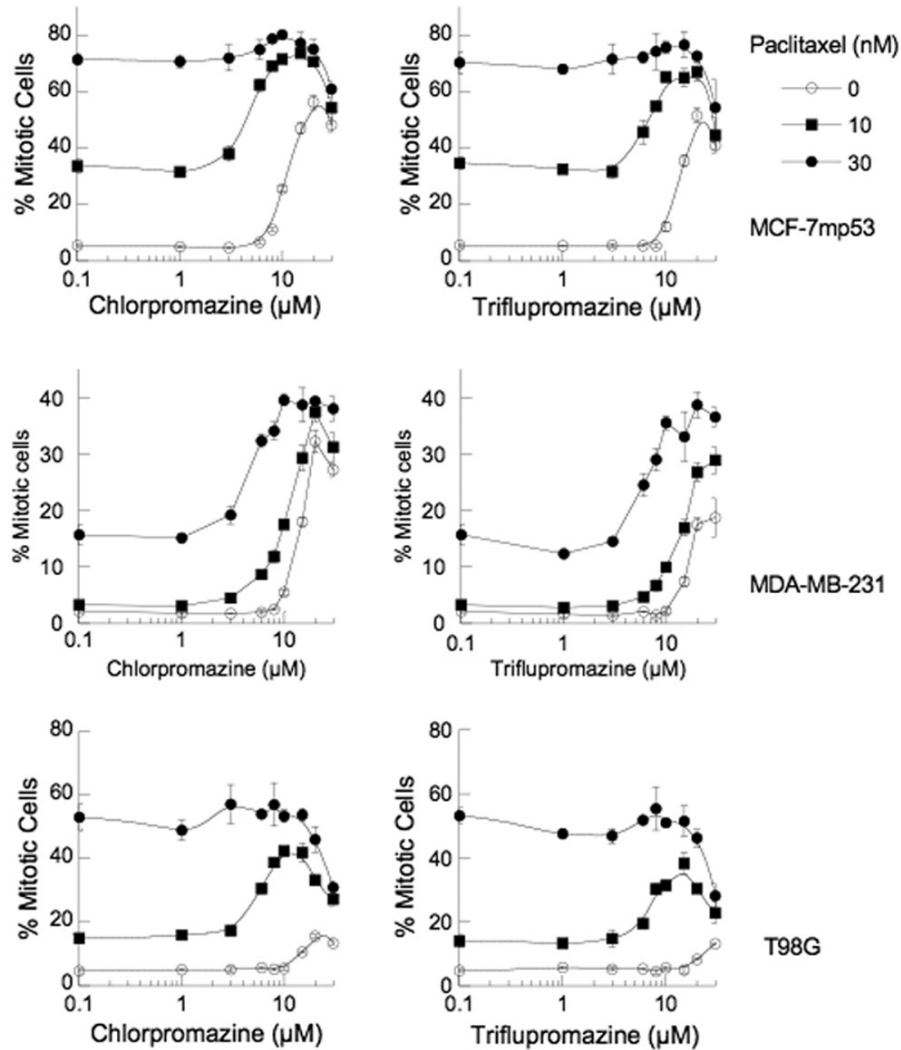


**Figure 3.10: Induction of mitotic arrest by combinations of chlorpromazine and paclitaxel or triflupromazine and paclitaxel.**

MCF-7mp53, MDA-MB-231 and T98G cells were treated with 0, 10 or 30 nM paclitaxel for 4 h followed by the indicated concentrations of chlorpromazine or triflupromazine for 20 h and the proportion of cells in mitosis was determined by quantitative immunofluorescence microscopy (see Section 2.4). Error bars denote standard deviation from the mean.

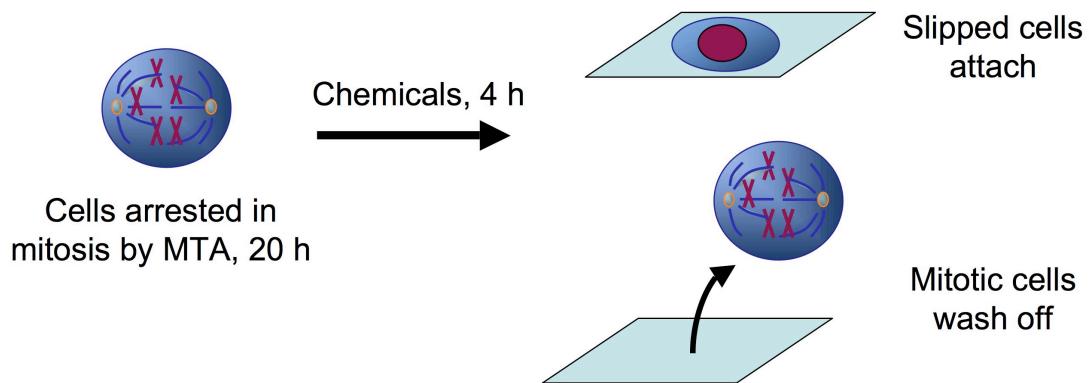


**Figure 3.11: Screen for inducers of mitotic slippage.**

T98G cells arrested in mitosis by an antimetabolic agent were harvested via shake-off, transferred to 96-well plates and exposed to screening chemicals for 4 h. Mitotic cells were then washed away and the nuclei of attached, slipped cells were stained with Hoechst 33342 and quantified by automated fluorescence microscopy (see Section 2.6).

interphase T98G cells were incubated with nocodazole or paclitaxel for 20 h and the cells arrested at mitosis were separated from interphase or slipped cells by shake-off. The mitotic cells were distributed into 96-well plates at 5,000/well in the continued presence of the microtubule-targeting agent. Test chemicals were added and after 4 h, the cells remaining arrested at mitosis were removed by aspiration and the cells that had attached to the plastic surface during the incubation were fixed, their nuclei were stained with Hoechst 33342 to label DNA, and they were counted using an automated fluorescence imager. In controls treated with paclitaxel alone, no more than 10% of the cells became attached during the 4 h incubation (Figure 3.12), whereas 80% of the cells became attached (data not shown) when cells were treated with paclitaxel and 2.5  $\mu$ M ZM447439, an Aurora B inhibitor previously demonstrated to induce mitotic slippage (233).

This assay was used to screen the chemical collection at a concentration of 15  $\mu$ M. Four chemicals induced  $\geq 50\%$  of cells to attach (Figure 3.12). Visual inspection of the images ensured that cells showed the grape-like nuclear morphology characteristic of slipped cells (225) (Figure 3.13) rather than the condensed chromosomes of M-arrested cells. The four active compounds were SU6656, a Src family kinase inhibitor (242); CGP 74514A, a CDK1 inhibitor (126); aklavin (1-deoxypyrrromycin), a DNA-intercalating agent structurally related to the antitumour antibiotic aclarubicin (243); and geraldol, a flavonoid with no known biological activity. The identification of a CDK1 inhibitor as an inducer of mitotic slippage was not unexpected (244), as CDK1 activity is required to maintain mitotic checkpoint activity (224) and loss of CDK1 activity through cyclin B1 degradation precedes the metaphase-to-anaphase transition and triggers exit from

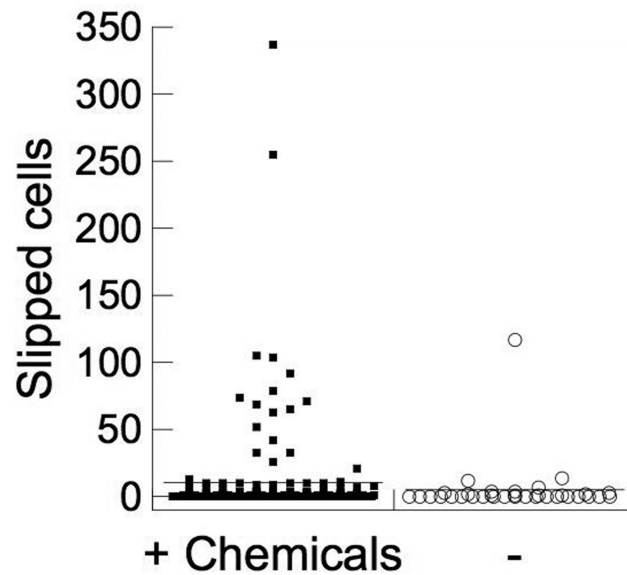


**Figure 3.12: Results of the screen for inducers of mitotic slippage.**

T98G cells were treated with 30 nM paclitaxel for 20 h and mitotic cells were harvested by shake-off and seeded in 96-well plates. The cells were then treated without (-) or with (+) screening chemicals at 15  $\mu$ M for a further 4 h and the attached, slipped cells were fixed, stained with Hoechst 33342 and quantified using automated fluorescence microscopy (see Section 2.6).

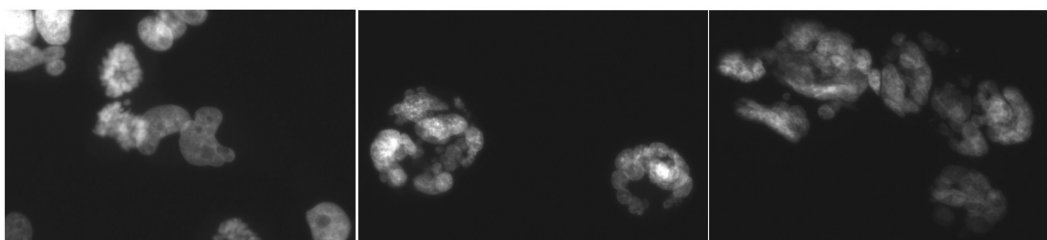


**Figure 3.13: Nuclear morphology of cells induced to undergo mitotic slippage by exposure to paclitaxel and SU6656 or geraldol.**

T98G cells were treated with 30 nM paclitaxel for 20 h and mitotic cells were harvested by shake-off and seeded in 96-well plates. The cells were then treated with SU6656 or geraldol at 15  $\mu$ M for a further 4 h and the attached, slipped cells were fixed, stained with Hoechst 33342 and counted using automated fluorescence microscopy (see Section 2.6).

mitosis (35, 245). Identifying a DNA-damaging agent was also not surprising since activation of the DNA damage checkpoint in cells arrested at mitosis can downregulate CDK1 activity, causing cells to escape mitotic arrest (246). Therefore, SU6656 and geraldol were selected for further study (Figure 3.14).

To verify that the attached cells had indeed escaped mitosis, immunofluorescence microscopy was carried out using the H3P antibody that recognizes histone H3 phosphorylated at Ser10, a widely used mitotic marker (247). Cells arrested at mitosis by paclitaxel showed strong H3P reactivity whereas treatment of cells arrested at mitosis by paclitaxel with SU6656 or geraldol for 4 hours caused an almost complete disappearance of H3P staining (Figure 3.15).

For further characterization of the activity of SU6656 and geraldol, T98G cells were arrested at mitosis by chemicals with different mechanisms of action: the microtubule stabilizing agent paclitaxel, the microtubule depolymerising agent vinblastine, or the kinesin spindle protein (KSP)/Eg5 kinesin inhibitor *S*-trityl-L-cysteine (STLC). They were then exposed to different concentrations of SU6656 or geraldol for 4 h and the proportion of slipped cells was determined. SU6656 and geraldol induced mitotic slippage in cells arrested with any of the three antimitotic agents and they were both active at low micromolar concentrations (Figure 3.16).

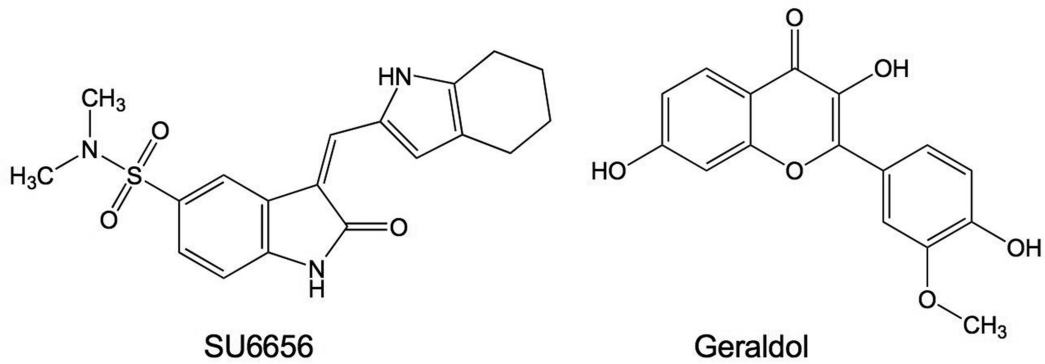


**Figure 3.14: Structures of SU6656 and geraldol.**

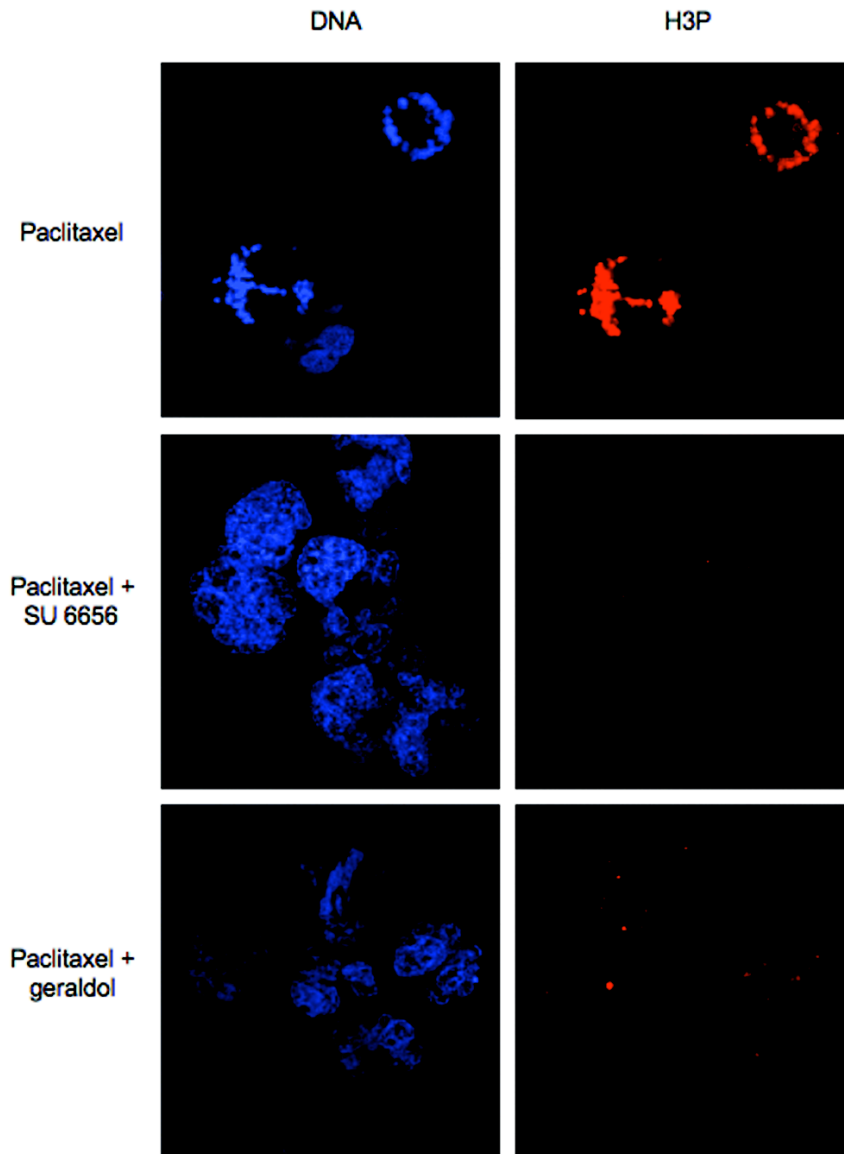


**Figure 3.15: Disappearance of mitotic histone H3 Ser10 phosphorylation in cells treated with SU6656 or geraldol.**

T98G cells arrested at mitosis with 30 nM paclitaxel were exposed, in the continued presence of paclitaxel, to 5  $\mu$ M SU6656 or 5  $\mu$ M geraldol for 4 h. Cells were stained with Hoechst 33342 and anti-phospho-histone H3 (H3P) as described in Section 2.7.

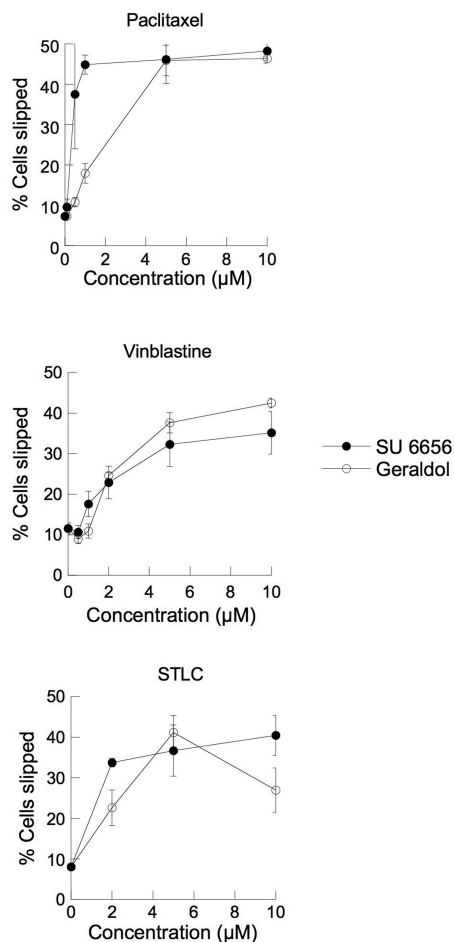


**Figure 3.16: Induction of mitotic slippage after mitotic arrest induced by paclitaxel, vinblastine or *S*-trityl-L-cysteine (STLC).**

T98G cells were treated with 30 nM paclitaxel, 30 nM vinblastine or 1 μM *S*-trityl-L-cysteine for 20 h and mitotic cells were harvested by shake off, seeded in 96-well plates and exposed to 0-10 μM SU6656 or geraldol for 4 h. The nuclei of attached, slipped cells were labelled using Hoechst 33342 and cells were counted using automated fluorescence microscopy (see Section 2.6). Results are shown as a percentage of the number of cells seeded in each well. Error bars denote intervals of 95% confidence, as do all subsequent error bars unless otherwise indicated.

# CHAPTER 4: EFFECTS OF MITOTIC SLIPPAGE ON CELL SURVIVAL AND PROLIFERATION

## 4.1 Synopsis

In this chapter, the effects of inhibition and induction of mitotic slippage by the chemicals identified in Chapter 3 are compared with respect to cell survival. While chlorpromazine and triflupromazine, compounds found to strengthen mitotic arrest, inhibit cell proliferation on their own, they cause an increase in cell survival and proliferation in combination with paclitaxel compared to paclitaxel alone. This result indicates that maintenance of mitotic arrest through prevention of mitotic slippage favours cancer cell survival over death. Conversely, mitotic slippage, either spontaneous or induced by the chemicals SU6656 and geraldol that were identified in Chapter 3, results in cell death over a period of up to 14 days. Death occurs primarily by apoptosis, as evidenced by sub-G1 DNA content. Some cells, after undergoing mitotic slippage, re-replicate their DNA without cell division, become giant and micronucleated, or exhibit senescence-associated  $\beta$ -galactosidase activity before dying. However, this result applies only to mitotic slippage following mitotic arrest induced by microtubule-targeting agents: mitotic slippage following arrest induced by the KSP/Eg5 inhibitor *S*-trityl-L-cysteine results in recovery of normal ploidy and continued cell proliferation. Chlorpromazine and triflupromazine inhibit stimulation of mitotic slippage by SU6656 and geraldol, indicating that mitotic slippage can be prevented by strengthening mitotic arrest.

Comparison of mitotic slippage and cell survival in paired cell lines revealed that loss of securin appears to lower the barrier to mitotic slippage, resulting in an increased frequency of slippage. However, lack of securin activity does not allow a survival advantage, indicating that securin is not important for survival following mitotic slippage.

The results presented in this chapter indicate that outcomes of mitotic slippage result in cell death, favourable for cancer therapy. Therefore, SU6656 and geraldol may have therapeutic potential and are of interest for further study.

#### **4.2 Chlorpromazine and triflupromazine increase survival of paclitaxel-treated cells**

Chlorpromazine and triflupromazine (see Section 3.4.1) were used as tools to examine the effect of strengthening mitotic arrest on cell survival after exposure to paclitaxel. Cells were exposed to 0, 3 or 5 nM paclitaxel and CPZ or TPZ was added at different concentrations 4 h later. After 48 h, the cell culture medium was removed and replaced with fresh medium without any drugs and the cells were cultured for 2-4 additional days. Cell proliferation was then determined using the MTT assay and expressed relative to the effect of paclitaxel alone. On their own, CPZ and TPZ both inhibited proliferation at  $\geq 6$   $\mu\text{M}$  (Figure 4.1). Remarkably, exposure to a combination of paclitaxel and 3-10  $\mu\text{M}$  CPZ or TPZ caused increased cell proliferation compared to exposure to either drug alone. Moreover, cell proliferation increased further in the presence of CPZ or TPZ when the concentration of paclitaxel was increased from 3 nM to 5 nM. At their optimal concentrations, CPZ and TPZ increased the proliferation of MDA-MB-231 cells by nearly 200%, MCF-7-mp53 cells by 150% and T98G cells by 50% (Figure 4.1).

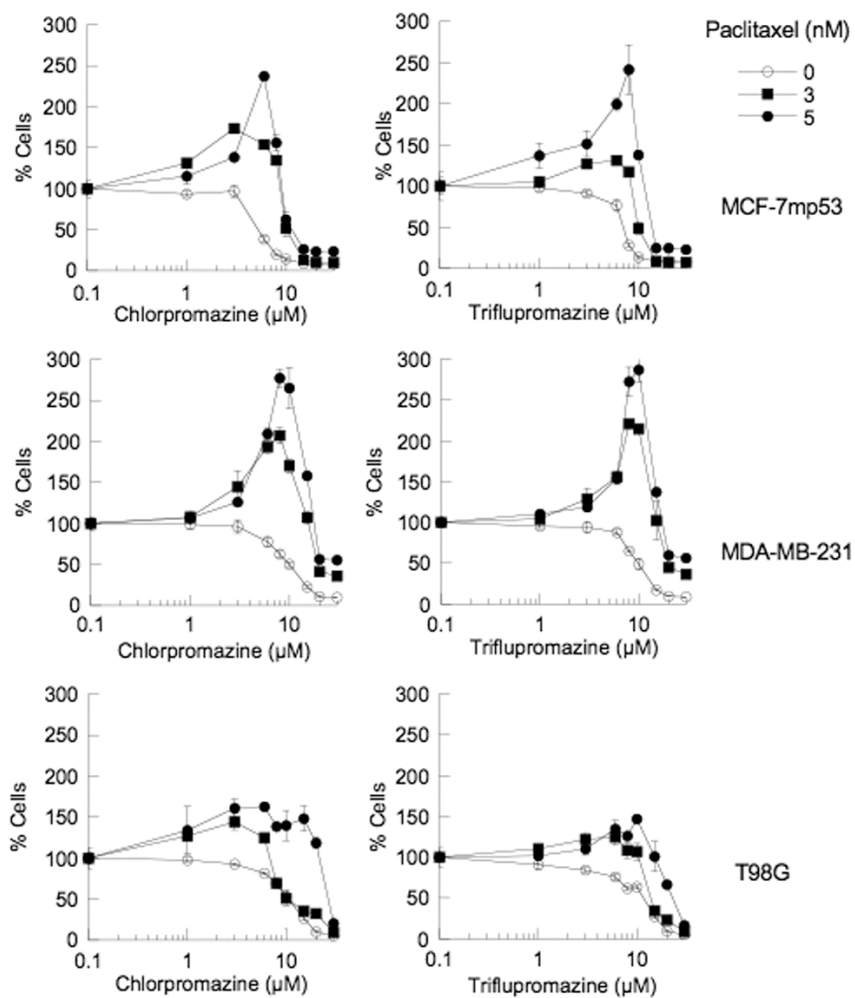


**Figure 4.1: Increase in cell survival caused by combinations of chlorpromazine and paclitaxel or triflupromazine and paclitaxel.**

MCF-7mp53, MDA-MB-231 and T98G cells were treated with 0, 3 or 5 nM paclitaxel for 4 h followed by the indicated concentrations of chlorpromazine or triflupromazine for a further 44 h. The drugs were then washed away and the cells were allowed to grow in fresh culture medium for 2-4 days before the number of live cells was determined using the MTT assay (see Section 2.5). Results are expressed as % live cells compared to treatment without chlorpromazine or triflupromazine. Error bars denote standard deviation from the mean.

CPZ and TPZ retained their toxicity at higher concentrations in the presence of paclitaxel. Therefore, imposing stronger mitotic arrest with CPZ or TPZ, at active but not toxic concentrations, during exposure to paclitaxel enabled cells to better survive and resume proliferation upon drug washout.

### **4.3 Cells forced to undergo mitotic slippage by SU6656 or geraldol experience myriad fates**

The easy separation of cells arrested at mitosis from those that have undergone mitotic slippage afforded by the attachment of the latter to plastic enabled examination of the fate of slipped cells. T98G cells were arrested at mitosis with paclitaxel, vinblastine or *S*-trityl-L-cysteine and incubated without or with SU6656 or geraldol. After 4 h, the drugs were washed away, the attached cells were cultured in fresh medium without drug and their fate was followed for up to 2 weeks using automated microscopy to count cell numbers and flow cytometry of DNA content to measure ploidy.

First, the fate of the cells that spontaneously slipped out of paclitaxel-induced mitotic arrest (DMSO-treated) was examined. Essentially all cells died but this process was protracted, taking up to 14 days (Figure 4.2). The cells that underwent mitotic slippage were unable to divide successfully, as no peak with 2N G1 DNA content (less than the 4N DNA content indicated) appeared (Figure 4.3). Instead, large numbers of cells underwent one round of DNA replication without division, resulting in a peak with twice the G2/M DNA content appearing at days 2-5. A smaller proportion underwent one additional round of DNA replication without cell division by day 5. Microscopic examination at day 5 revealed inordinately large cells with diameters of about 100  $\mu\text{m}$ ,

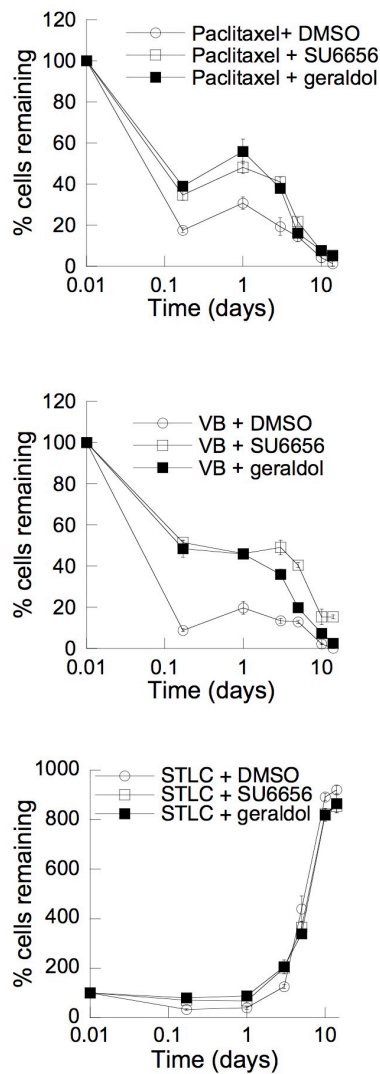


**Figure 4.2: Cell death after exposure to chemical stimulators of mitotic slippage.**

T98G cells were treated with 30 nM paclitaxel, 30 nM vinblastine or 1  $\mu$ M *S*-trityl-L-cysteine (STLC) and mitotic cells were harvested by shake-off, seeded in 96-well plates and treated with 5  $\mu$ M SU6656, 5  $\mu$ M geraldol or DMSO. After 4 h (time = 0), the drugs were washed away and the attached cells were allowed to grow in fresh culture medium for up to two weeks. At various times, cells were fixed, stained with Hoechst 33342 to label nuclei, and counted using an automated fluorescence imager (see Section 2.6).

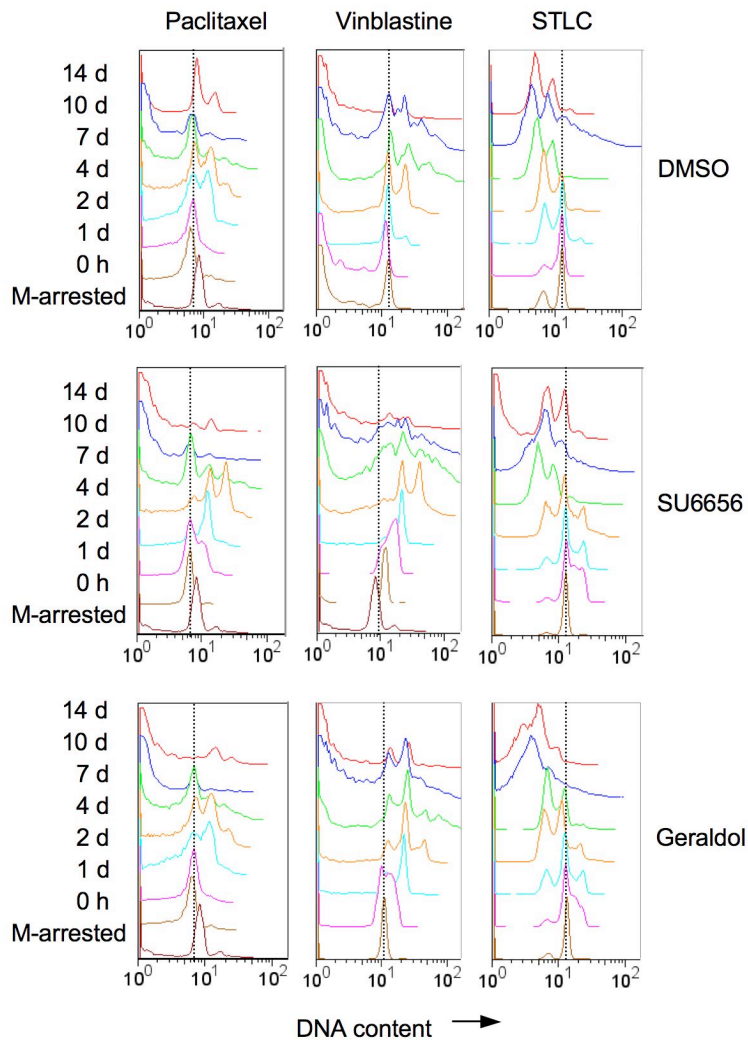


**Figure 4.3: Endoreduplication after mitotic slippage.**

T98G cells were treated with 30 nM paclitaxel, 30 nM vinblastine or 1  $\mu$ M *S*-trityl-L-cysteine (STLC) and mitotic cells were harvested by shake-off, seeded in 96-well plates and treated with 5  $\mu$ M SU6656, 5  $\mu$ M geraldol or DMSO. After 4 h (time = 0), the drugs were washed away and the attached cells were allowed to grow in fresh culture medium for up to two weeks. At various times, cells were fixed, stained with propidium iodide, and their DNA content was analyzed by flow cytometry (see Section 2.8). Dotted lines indicate 4N DNA content (G2/M phase).

containing numerous unequally sized nuclei and an extensive cytoplasmic microtubule network (Figure 4.4). Staining for senescence-associated  $\beta$ -galactosidase activity at day 8 revealed the presence of senescent cells (Figure 4.5). Between days 7 and 14, a large proportion of these cells died, as seen from the appearance of a large sub-G1 DNA peak indicative of apoptosis, a decrease in the higher ploidy peaks and a decrease in cell number (Figure 4.2 and 4.3).

The paclitaxel-arrested cells that were forced to undergo mitotic slippage by exposure to SU6656 or geraldol underwent a largely similar fate. Most of the cells died with kinetics similar to those that underwent slippage spontaneously (Figure 4.2). The fraction of cells treated with SU6656 that underwent two rounds of DNA replication without division was larger than those seen in DMSO- or geraldol-treated cells (Figure 4.3) and there were large numbers of giant cells (Figure 4.4). Many cells showed microtubule bundles reminiscent of interphase cells treated with paclitaxel (Figure 4.4). At day 8, 20-30% of the cells were senescent (Figure 4.5). By day 14, few surviving cells remained (Figure 4.2). In summary, the cells that underwent mitotic slippage after paclitaxel treatment, whether spontaneous or induced, underwent one or more rounds of DNA replication without cell division, became very large and showed signs of senescence, and eventually all died.

The cells that spontaneously slipped out of mitotic arrest imposed by vinblastine or were induced to slip out of mitosis died with kinetics similar to those arrested with paclitaxel (Figure 4.2) and they similarly underwent multiple rounds of DNA replication without intervening cell division (Figure 4.3). Examination of the cells at day 5 also revealed large numbers of giant cells. Interestingly, tubulin immunostaining in these cells

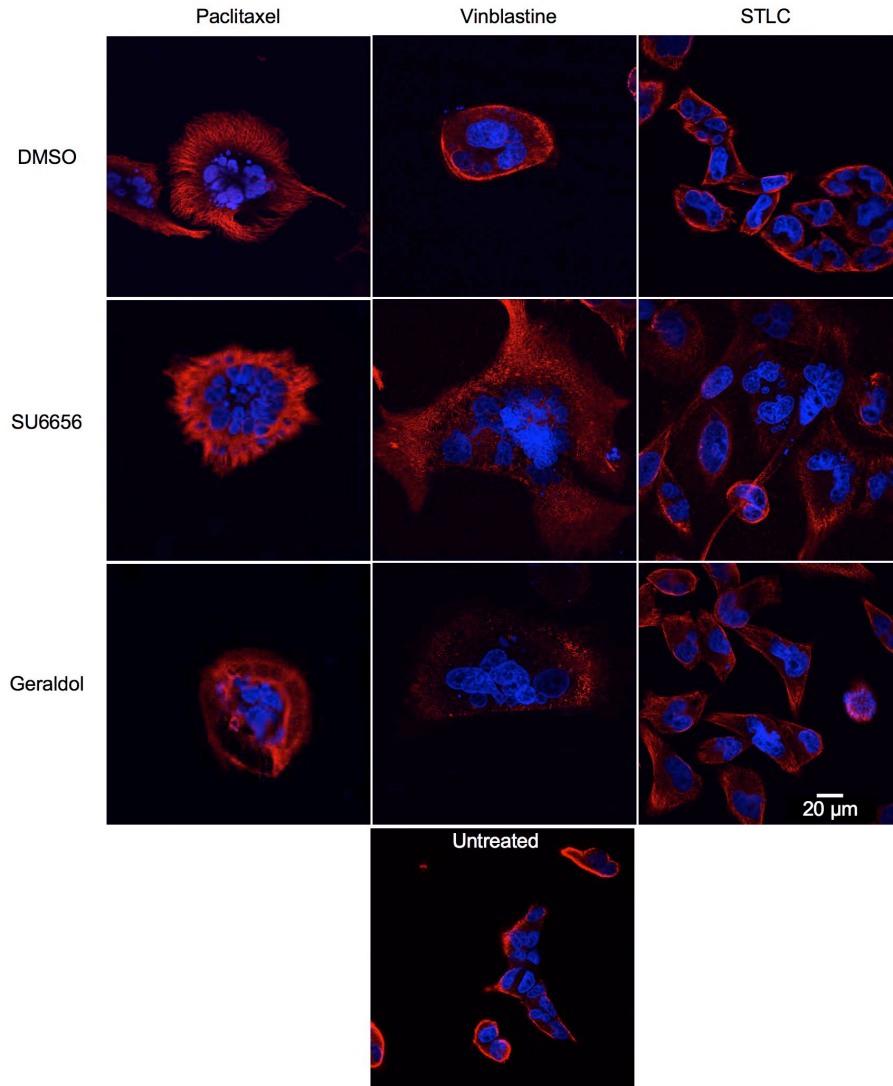


**Figure 4.4: Formation of giant multinucleated cells after mitotic slippage.**

T98G cells arrested at mitosis with 30 nM paclitaxel, 30 nM vinblastine or 1  $\mu$ M *S*-trityl-L-cysteine (STLC) were harvested by shake-off, seeded on coverslips, and treated without (DMSO) or with 5  $\mu$ M SU6656 or 5  $\mu$ M geraldol for 4 h. The chemicals and unattached cells were then washed away and the attached, slipped cells were allowed to grow for 5 days in fresh culture medium, at which time they were stained with Hoechst 33342 to label nuclei (blue) and rabbit  $\alpha$ - $\beta$ -tubulin (red) (see Section 2.7).

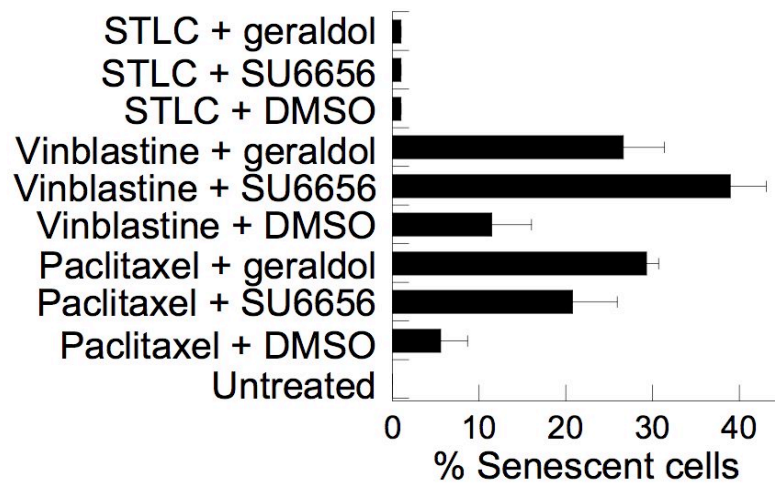


**Figure 4.5: Senescence induction by chemical stimulators of mitotic slippage.**

T98G cells were treated with 30 nM paclitaxel, 30 nM vinblastine or 1  $\mu$ M *S*-trityl-L-cysteine (STLC) and mitotic cells were harvested by shake-off, seeded in 96-well plates and treated with 5  $\mu$ M SU6656, 5  $\mu$ M geraldol or DMSO. After 4 h (time = 0), the drugs were washed away and the attached cells were allowed to grow in fresh culture medium. After 8 days, cells were fixed and stained with X-gal at pH 6 to selectively label senescent cells (see Section 2.9). The number of X-gal-positive cells in 3 fields of view was counted under a bright-field microscope and expressed as a percentage of the total number of cells in those 3 fields.

was punctate and diffuse, showing that the cells had failed to reform a microtubule network (Figure 4.4). There were also large numbers of senescent cells at day 8 (Figure 4.5) and most of the cells were dead by day 14 (Figure 4.2).

The cells that slipped out of mitotic arrest induced by the KSP/Eg5 kinesin inhibitor *S*-trityl-L-cysteine underwent a very different fate. There was little or no evidence of cell death and a high level of cell proliferation was observed after slippage (Figure 4.2). Soon after exposure to DMSO, SU6656 or geraldol, a peak with G1 DNA content appeared (left of the dotted line indicating G2/M DNA content), indicating successful completion of mitosis (Figure 4.3). The cells that had been induced to undergo mitotic slippage by SU6656 or geraldol proliferated, but did so initially as a mixed population containing cells with normal ploidy and cells with double the ploidy of the parental population. By day 7, the population returned to a normal ploidy state, presumably due to the death of the polyploid population (Figure 4.3). At day 5, the cells contained a single nucleus and were of similar size to untreated cells (Figure 4.4). Little or no senescence was observed (Figure 4.5).

SU6656 and geraldol were next used as tools to directly compare the effect of stimulating mitotic slippage on cell survival and proliferation after exposure to paclitaxel with that of inhibiting mitotic slippage. Cells were exposed to combinations of paclitaxel and SU6656 and geraldol and after 48 h the drugs were washed away. Cell viability and proliferation was measured 2-4 days later using the MTT assay. SU6656 inhibited cell proliferation at 1  $\mu$ M or above in all cell lines while geraldol inhibited proliferation much less potently (Figure 4.6). Exposure to a combination of paclitaxel and SU6656 did not lead to a significant change in cell viability over either drug alone (Figure 4.6). Geraldol

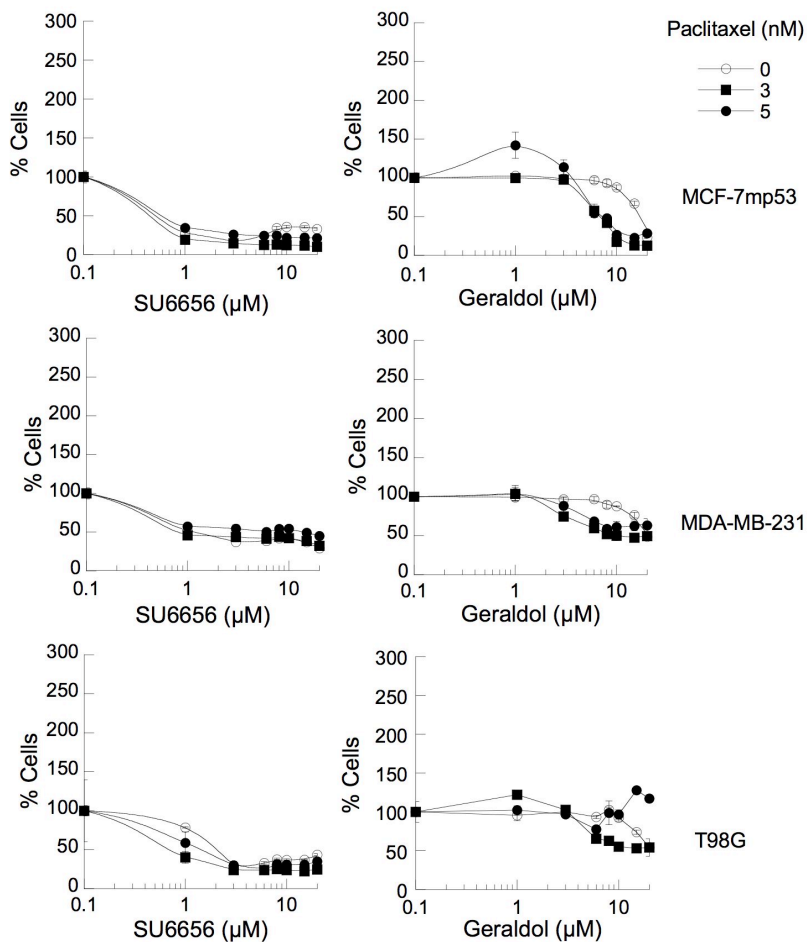


**Figure 4.6: Decrease in cell viability caused by combinations of SU6656 and paclitaxel or geraldol and paclitaxel.**

MCF-7mp53, MDA-MB-231 and T98G cells were treated with 0, 3 or 5 nM paclitaxel for 4 h followed by the indicated concentrations of SU6656 or geraldol for a further 44 h. The drugs were then washed away and the cells were allowed to grow in fresh culture medium for 2-4 days before the number of live cells was determined using the MTT assay (see Section 2.5). Results are expressed as % live cells compared to treatment without SU6656 or geraldol on the same scale as in Figure 4.1 to facilitate direct comparison. Error bars represent standard deviation from the mean.

was slightly more toxic to two of the three cell lines in the presence of paclitaxel than in its absence (Figure 4.6). These results are in sharp contrast to those obtained with the same concentrations of paclitaxel and the mitotic slippage inhibitors CPZ and TPZ, which considerably increased cell survival and proliferation upon exposure to paclitaxel at concentrations that were active in reinforcing mitotic arrest but were not toxic (compare Figures 4.1 and 4.6, shown on the same scale). Therefore, inhibiting mitotic arrest with SU6656 or geraldol during exposure to paclitaxel did not enable cells to better survive and resume proliferation upon drug washout.

#### **4.4 CPZ and TPZ inhibit induction of mitotic slippage by SU6656 and geraldol**

To determine whether enforcing the mitotic checkpoint with CPZ or TPZ would prevent mitotic slippage induced by SU6656 or geraldol, T98G cells were arrested at mitosis with 30 nM paclitaxel and mitotic cells were harvested by shake-off and exposed to SU6656 or geraldol and CPZ or TPZ. After 4 h, the nonadherent cells were washed away and the slipped cells were quantified. Treatment with CPZ or TPZ alone resulted in a low rate of mitotic slippage (Figure 4.7A), approximately equal to that observed upon treatment with paclitaxel alone. When cells were treated with SU6656 in conjunction with CPZ or TPZ, partial inhibition of the action of SU6656 was observed, decreasing the proportion of slipped cells from 50% to 20-25%. CPZ and TPZ also inhibited the effects of geraldol, although to a lesser degree. To ensure that the reduction in the proportion of attached cells was not due to toxicity, the effect of these chemical combinations on cell survival were measured using the MTT assay. SU6656 exhibited slight toxicity, but this effect was not significantly increased by CPZ or TPZ (Figure 4.7B). Geraldol did not

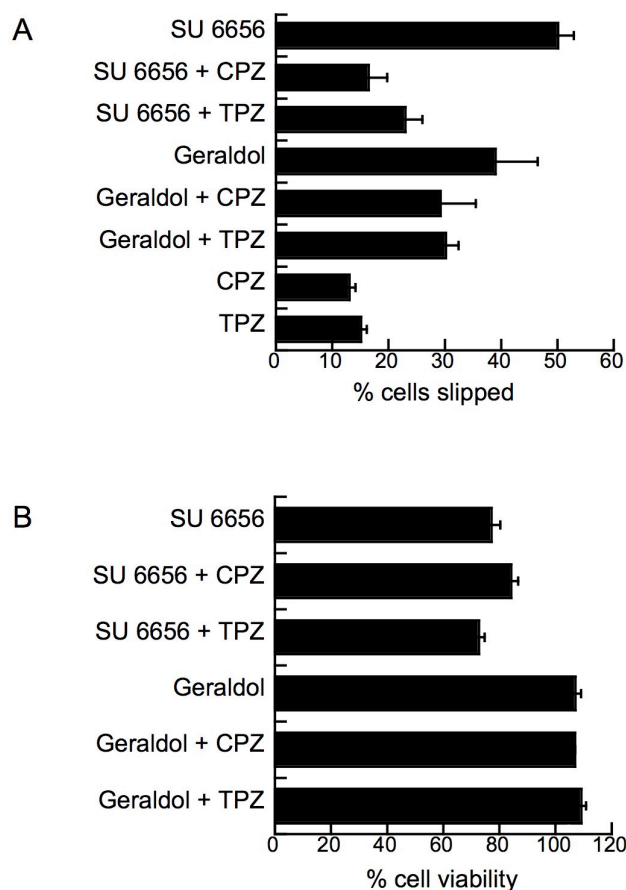


**Figure 4.7: Antagonistic activity of chemical inhibitors and stimulators of mitotic slippage.**

T98G cells were treated with 30 nM paclitaxel for 20 h and mitotic cells were harvested by shake-off, seeded in 96-well plates and treated with the indicated combinations of SU6656 (5  $\mu$ M), geraldol (5  $\mu$ M), chlorpromazine (CPZ, 7  $\mu$ M) or triflupromazine (TPZ, 7  $\mu$ M). The nuclei of attached, slipped cells were stained with Hoechst 33342 and cells were counted using automated fluorescence microscopy (A) (see Section 2.6). Results are expressed as percentages of cells seeded in each well. After incubation with drugs, cell viability was measured using the MTT assay (B) (see Section 2.5). Results are expressed in comparison to cell viability after treatment with paclitaxel alone.

reduce cell viability at all, and this was unchanged by the addition of CPZ or TPZ. Thus, reinforcement of the mitotic checkpoint in T98G cells by CPZ or TPZ is sufficient to at least partially inhibit mitotic slippage induced by SU6656 or geraldol.

#### **4.5 Loss of securin increases the frequency of mitotic slippage**

To determine the contribution to mitotic slippage of other proteins involved in mitosis, paired HCT116 securin<sup>+/+</sup> (wild-type) and securin<sup>-/-</sup> cell lines were assayed for mitotic slippage induction by 5  $\mu$ M SU6656 or 5  $\mu$ M geraldol. Securin is an APC/C<sup>Cdc20</sup> and proteasome substrate that is degraded at the metaphase-to-anaphase transition (36, 248), allowing separate cleavage of cohesin and sister chromatid separation (249). Loss of securin increased spontaneous and induced mitotic slippage two-fold over securin-positive HCT116 cells (Figure 4.8), indicating that securin loss sensitizes cells to mitotic slippage.

The survival of HCT116 wild-type and securin<sup>-/-</sup> cells was compared 7 d following induction of mitotic slippage and drug washout (Figure 4.9). Approximately 10% of wild-type HCT116 cells that had undergone mitotic slippage survived, whether mitotic slippage was spontaneous or induced. The survival rate of HCT116 securin<sup>-/-</sup> cells was not significantly higher than that of wild-type cells, indicating no role for securin in cell survival following an incomplete mitosis.

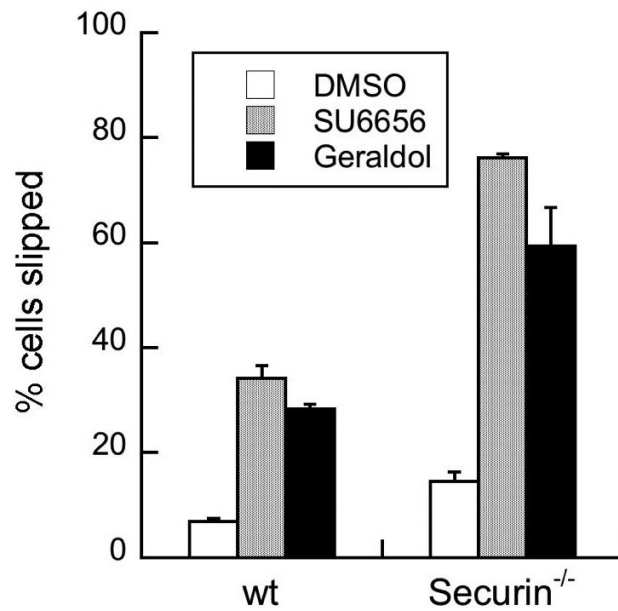


**Figure 4.8: An increase in the frequency of mitotic slippage due to loss of securin.**

HCT116 wt and securin<sup>-/-</sup> cells were exposed to 30 nM paclitaxel for 20 h, harvested by shake-off and incubated with 0.1% DMSO, 5  $\mu$ M SU6656 or 5  $\mu$ M geraldol for 4 h. The attached, slipped cells were then fixed, stained with Hoechst 33342, and quantified by automated fluorescence microscopy (see Section 2.6).

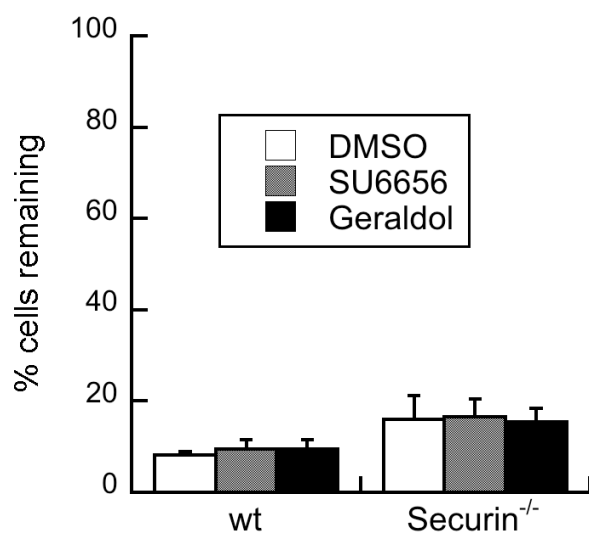


**Figure 4.9: Death of cells lacking securin after mitotic slippage.**

HCT116 wt and securin<sup>-/-</sup> cells were exposed to 30 nM paclitaxel for 20 h, harvested by shake-off and incubated with 0.1% DMSO, 5 μM SU6656 or 5 μM geraldol for 4 h. Both drugs were then washed away and the cells were allowed to grow in fresh cell culture medium for 7 days before staining with Hoechst 33342 and quantification by automated fluorescence microscopy (see Section 2.6).

# **CHAPTER 5: MITOTIC SLIPPAGE VIA PROTEASOME- AND CASPASE-DEPENDENT MITOTIC CHECKPOINT INACTIVATION**

## **5.1 Synopsis**

Work in this chapter aimed to understand the mechanism of action of the mitotic slippage inducers SU6656 and geraldol and apply that knowledge to spontaneously occurring mitotic slippage. Like completion of mitosis, mitotic slippage induced by SU6656 and geraldol is proteasome-dependent and involves degradation of cyclin B1. However, unlike spontaneous mitotic slippage, SU6656 and geraldol stimulate proteasome-dependent degradation of the mitotic checkpoint proteins BubR1, Cdc20 and Mps1. As degradation of BubR1 is sufficient to compromise the mitotic checkpoint, SU6656 and geraldol induce mitotic slippage through mitotic checkpoint inactivation. Stimulation of mitotic slippage is dependent on caspase-3, as shown by prevention of mitotic slippage induction by a caspase-3 inhibitor and in cells that lack caspase-3. Mitotic checkpoint inactivation through degradation of BubR1 is also caspase-3-dependent, as it occurs only in cells expressing caspase-3, while degradation of cyclin B1 and Cdc20 is not, suggesting that cyclin B1 degradation may not be sufficient for mitotic slippage to occur. Additionally, cell attachment and loss of mitotic phosphoepitopes does not occur before 2 h of exposure to geraldol, when BubR1 and Cdc20 are significantly degraded, while cyclin B1 degradation is complete after 30 min of exposure. Despite the clear requirement for caspase-3 for induction of mitotic slippage by SU6656 and

geraldol, caspase-3 is not required for spontaneous mitotic slippage, as mitotic slippage occurs with relatively equal frequencies in cells lacking or expressing caspase-3.

*In vitro* kinase assays revealed that SU6656 and geraldol both inhibit Aurora A and Aurora B, although Aurora B is inhibited more potently, and that geraldol may inhibit a number of additional kinases. However, these compounds likely have additional effects, as induction of mitotic slippage by the well-characterized Aurora B inhibitor ZM447439 is not caspase-3-dependent.

With respect to cell fate after antimitotic treatment and mitotic slippage, loss of caspase-3 does not affect the extensive cell death observed after induction of mitotic slippage. Neither caspase-3 nor p53 affects the similarly extensive cell death observed after exposure to paclitaxel, paclitaxel and SU6656, or paclitaxel and geraldol, implicating cell death pathways other than apoptosis in the outcome of treatment with an antimitotic agent.

## **5.2 Induction of mitotic slippage by SU6656 and geraldol requires proteasomal activity**

When cells spontaneously slip out of mitotic arrest, as well as during normal exit from mitosis, proteasomal activity is required for the degradation of cyclin B1 (226, 227). To determine whether escape from mitotic arrest induced by SU6656 or geraldol similarly requires proteasome activity, mitotic slippage was examined (see Section 2.6) in the presence of the proteasome inhibitor MG-132. In the absence of MG-132, SU6656 or geraldol induced 60-90% of mitotic cells to undergo mitotic slippage. MG-132 reduced the proportion of slipped cells in a concentration-dependent manner (Figure 5.1),

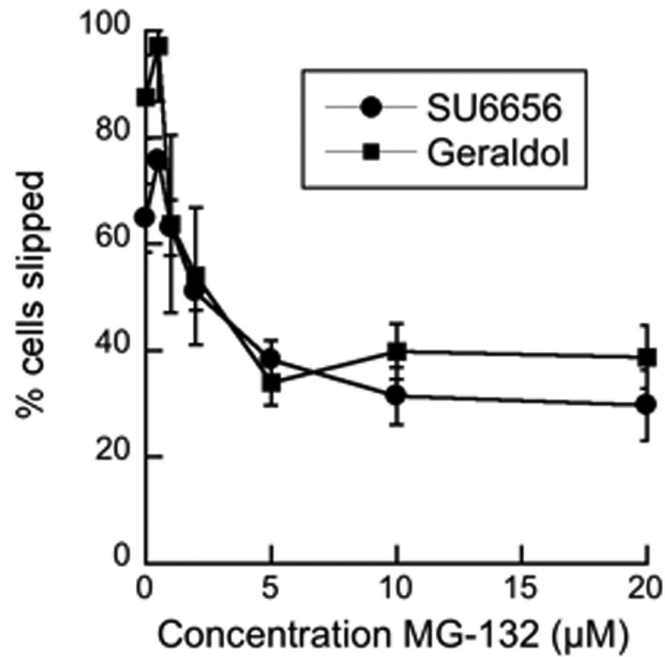


**Figure 5.1: Proteasome-dependent mitotic slippage induction by SU6656 and geraldol.**

T98G cells arrested in mitosis by 30 nM paclitaxel were harvested by shake-off, seeded in 96-well plates and exposed to 5 µM SU6656 or 5 µM geraldol simultaneously with 0-75 µM MG-132. After 4 h, the attached, slipped cells were fixed, stained, and quantified using an automated fluorescence imager (see Section 2.6).

indicating that mitotic slippage induced by both chemicals requires proteasomal protein degradation. Either chemical caused complete disappearance of cyclin B1, as determined by immunoblotting, and this degradation was entirely prevented by co-incubation with MG-132 (Figure 5.2). Therefore, induction of mitotic slippage by these chemicals is similar to normal exit from mitosis and spontaneous slippage with respect to proteasome dependence and cyclin B1 degradation.

### **5.3 Induction of mitotic slippage occurs via proteasome-dependent degradation of mitotic checkpoint proteins**

Although spontaneous mitotic slippage occurs via the ubiquitination of cyclin B1 by APC/C<sup>Cdc20</sup>, it does not involve inactivation of the mitotic checkpoint (226, 227). Using immunoblotting, the effects of SU6656 and geraldol on the cellular levels of the main mitotic checkpoint mediators Cdc20, BubR1, Mad2 and Mps1 were examined.

Interestingly, SU6656 and geraldol caused complete degradation of BubR1 and Cdc20 and a reduction in Mps1 levels. The degradation of these three proteins was prevented by co-incubation with MG-132 (Figure 5.2). Exposure to SU6656, but not geraldol, decreased cellular levels of Mad2 and this depletion was not proteasome-dependent (Figure 5.2).

To determine whether BubR1 is degraded during completion of mitosis, T98G cells were arrested in mitosis by a 12 h exposure to nocodazole and released into drug-free cell culture medium. The cells exited mitosis within 7 h, indicated by the development of a G1 DNA content peak (with lower DNA content than the G2/M peak indicated by a dotted line) measured by flow cytometry (Figure 5.3A). However, BubR1 was not

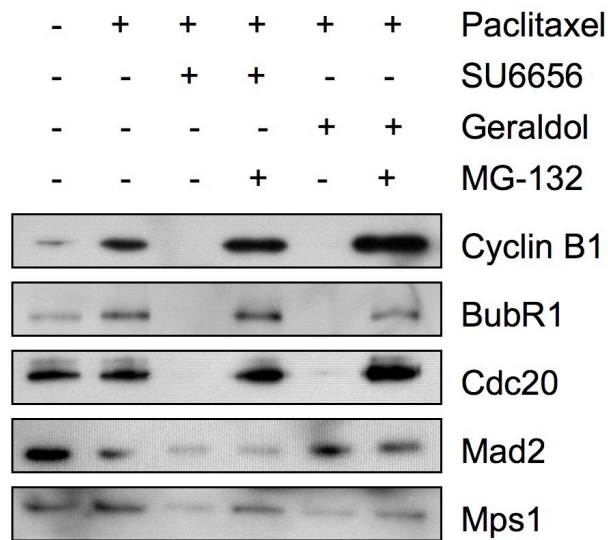


**Figure 5.2: Mitotic slippage induction through proteasome-dependent degradation of mitotic checkpoint proteins.**

Mitotic T98G cells were harvested by shake-off and exposed to 5  $\mu$ M SU6656 or 5  $\mu$ M geraldol without or with 20  $\mu$ M MG-132 for 4 h. Lysates were immunoblotted for the indicated proteins (see Section 2.10). Mitotic cells are enriched in all the indicated proteins due to their upregulation during mitosis.

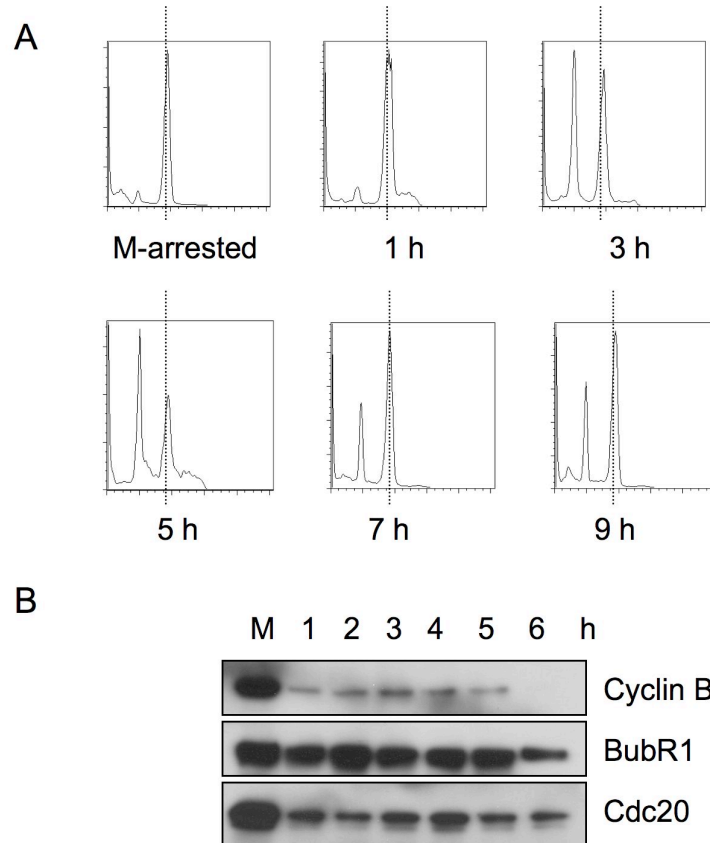


**Figure 5.3: Mitotic checkpoint degradation during mitotic exit.**

T98G cells were arrested in mitosis by exposure to 50 ng/mL nocodazole for 12 h (M), harvested by shake-off, and allowed to exit mitosis in fresh culture medium. To monitor cell division and protein degradation, 0-6 h later cells were permeabilized and stained with propidium iodide and analysed via flow cytometry for DNA content (A) (see Section 2.8) or lysed and immunoblotted (B) (see Section 2.10).

degraded during that time, as shown by immunoblotting (Figure 5.3B), indicating that its degradation in cells induced to undergo mitotic slippage by SU6656 or geraldol is not simply a normal consequence of exiting mitosis. Depletion of BubR1 or Mps1 has previously been shown by multiple groups to be sufficient to inactivate the mitotic checkpoint (109, 125, 126, 250-252). Therefore, these results imply that SU6656 and geraldol induce mitotic slippage through degradation of mitotic checkpoint proteins.

#### **5.4 SU6656 and geraldol do not induce the degradation of cyclin B1, BubR1 and Cdc20 in interphase cells**

To determine whether SU6656 and geraldol induce the proteasome-dependent degradation of cyclin B1, BubR1 and Cdc20 in interphase as well as in mitotic cells, proliferating T98G cells, which comprise 98% interphase cells, were exposed to 5  $\mu$ M SU6656 or 5  $\mu$ M geraldol for 4 h and analysed by immunoblotting. No decrease in the levels of cyclin B1, BubR1 or Cdc20 was observed (Figure 5.4); rather, a slight increase in the levels of all three proteins was observed. Simultaneous treatment with 20  $\mu$ M MG-132 had no additional effect (Figure 5.4). These results indicate that SU6656 and geraldol induce selective degradation of mitotic checkpoint components in cells arrested at mitosis.

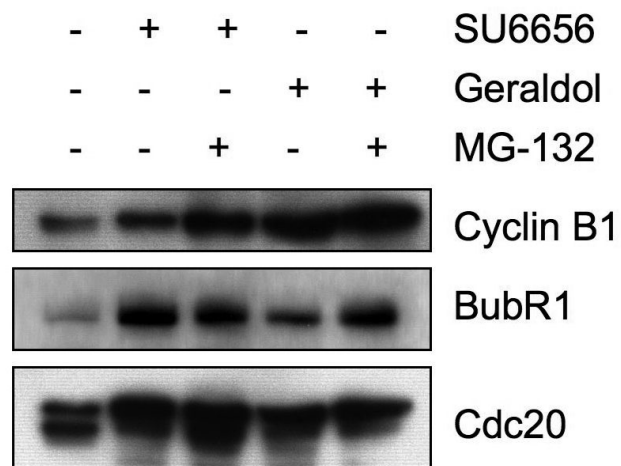


**Figure 5.4: Degradation of mitotic checkpoint proteins in response to SU6656 or geraldol in cycling cells.**

Cycling T98G cells were exposed to 5  $\mu$ M SU6656 or 5  $\mu$ M geraldol for 4 h without or with 20  $\mu$ M MG-132, lysed, and immunoblotted for the indicated proteins as described in Section 2.10.

## **5.5 Mitotic checkpoint inactivation and slippage induction by SU6656 and geraldol require caspase-3**

Caspases have been implicated in mitotic progression (218), and in particular, BubR1 is reportedly degraded by the effector caspase-3 during exit from mitosis (217, 253), although I did not observe this effect in T98G cells (Figure 5.3B). To determine whether mitotic slippage induced by SU6656 and geraldol involves caspase-3, inhibition of SU6656- or geraldol-induced mitotic slippage by the cell-permeable caspase-3 and -7 inhibitor DEVD-CHO was measured. DEVD-CHO prevented induction of mitotic slippage at 50 – 100  $\mu$ M (Figure 5.5), indicating a requirement for caspase activity in mitotic slippage induction by SU6656 and geraldol. Immunoblotting of paclitaxel-arrested T98G cells exposed to SU6656 or geraldol together with 50  $\mu$ M DEVD-CHO revealed that degradation of BubR1 and Cdc20 is caspase-dependent (Figure 5.6) in addition to being proteasome-dependent (Figure 5.2). In contrast, cyclin B1 degradation during induction of mitotic slippage is not dependent on caspase-3 or caspase-7 (Figure 5.6), as co-treatment with DEVD-CHO did not prevent cyclin B1 degradation in response to SU6656 or geraldol.

MCF-7 cells do not express caspase-3 due to a deletion within exon 3 of the CASP-3 gene that results in the introduction of a premature stop codon that completely abrogates translation of the CASP-3 mRNA (254, 255). This observation was utilised to determine whether caspase-3 is required for mitotic slippage induction by SU6656 and geraldol; these chemicals should be unable to stimulate mitotic slippage in MCF-7 cells if caspase-3 is required for this process. Indeed, similarly to MCF-7mp53 cells, SU6656 and geraldol did not induce mitotic slippage in MCF-7 cells (data not shown) or MCF-7 cells stably

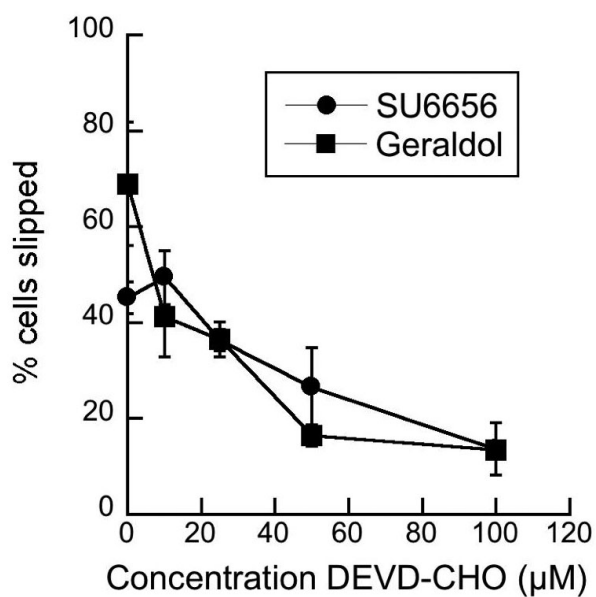


**Figure 5.5: Caspase-dependent mitotic slippage induction by SU6656 and geraldol.**

T98G cells were arrested in mitosis by 30 nM paclitaxel, harvested by shake-off, and seeded in 96-well plates. After exposure to 5 μM SU6656 or 5 μM geraldol simultaneously with 0-100 μM Ac-DEVD-CHO for 4 h, slipped cells were stained with Hoechst 33342 and quantified by automated fluorescence microscopy (see Section 2.6).

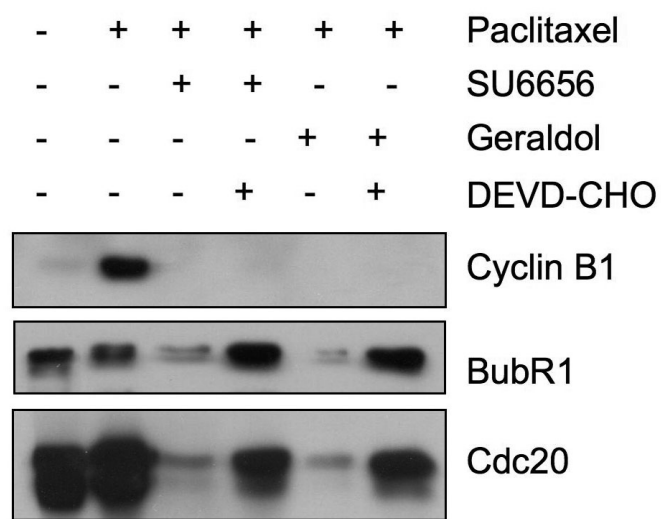


**Figure 5.6: Caspase-dependent mitotic checkpoint protein degradation induced by SU6656 and geraldol.**

Mitotic T98G cells were harvested by shake-off and incubated with 5  $\mu$ M SU6656 or 5  $\mu$ M geraldol without or with 50  $\mu$ M DEVD-CHO for 4 h. Lysates were immunoblotted for the indicated proteins as described in Section 2.10.

transfected with an empty expression vector (MCF-7pcDNA) (Figure 5.7). However, stable transfection of *CASP-3* cDNA into MCF-7 cells (MCF-7casp3), which results in expression of pro-caspase-3 (254), was sufficient to enable cells to undergo robust mitotic slippage in the presence of SU6656 or geraldol (Figure 5.7). Therefore, caspase-3 is required for induction of mitotic slippage by these chemicals.

To assess whether there were differences in the degradation of cyclin B1, BubR1 and Cdc20 in MCF-7pcDNA and MCF-7casp3 cells during exposure to SU6656 and geraldol, paclitaxel-arrested MCF-7pcDNA and MCF-7casp3 cells were harvested via shake-off, exposed to 5  $\mu$ M SU6656 or 5  $\mu$ M geraldol for 4 h and analysed by immunoblotting (Figure 5.8). Cyclin B1 was completely degraded in both cell lines upon exposure to either SU6656 or geraldol. Since MCF-7pcDNA cells do not undergo mitotic slippage under these conditions, while MCF-7casp3 cells do, this result implies that cyclin B1 degradation is not sufficient to induce mitotic slippage. Cdc20 was at least partially degraded in both MCF-7pcDNA and MCF-7casp3 cells. Interestingly, BubR1 was degraded only in MCF-7casp3 cells (Figure 5.8), implying that BubR1 is degraded in a caspase-3-dependent manner during mitotic slippage and that its degradation is required for mitotic slippage induction. The observation by Kim *et al.* that caspase-3 can directly cleave BubR1 during mitotic exit (217) suggests that caspase-3 may degrade BubR1 directly during chemically induced mitotic slippage.

While mitotic slippage induction by SU6656 and geraldol in MCF-7casp3 cells is proteasome-dependent (data not shown), BubR1 degradation in MCF-7casp3 cells was not inhibited by MG-132 (Figure 5.8), further indicating that it is caspase-3 and not the proteasome that is required for the degradation of BubR1 during induction of mitotic

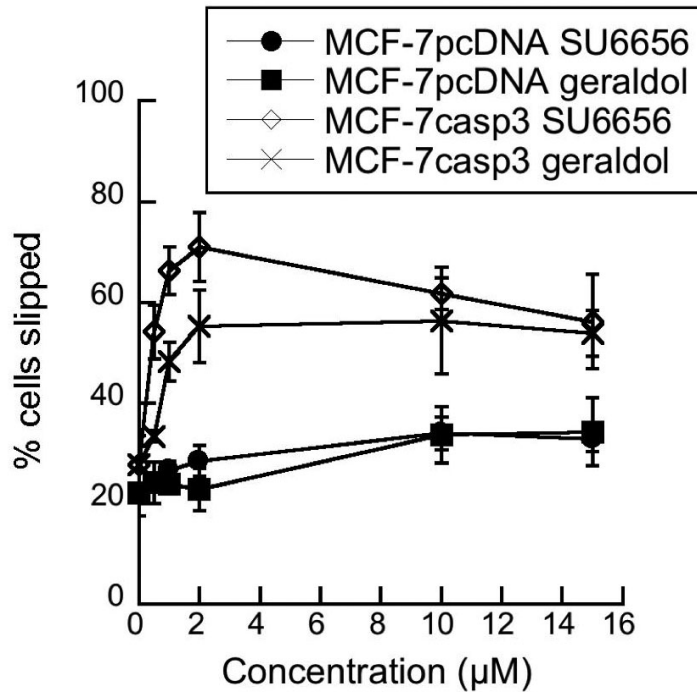


**Figure 5.7: Requirement for caspase-3 for mitotic slippage induction by SU6656 and geraldol.**

MCF-7 cells stably transfected with empty vector (MCF-7pcDNA) or caspase-3 (MCF-7casp3) were arrested in mitosis by 50 nM paclitaxel, harvested by shake-off, and seeded in 96-well plates. 0-15 µM SU6656 or geraldol was added for 4 h and the cells were stained with Hoechst 33342 and quantified using an automated fluorescence imager (see Section 2.6).

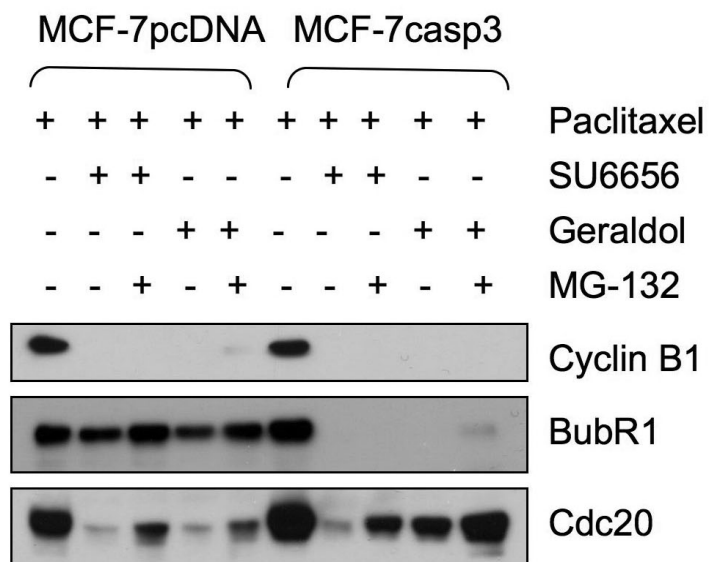


**Figure 5.8: Requirement for caspase-3 for mitotic checkpoint inactivation by SU6656 and geraldol.**

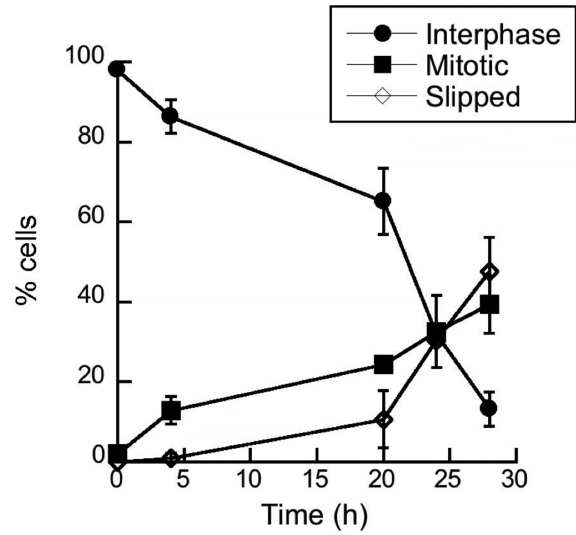
Mitotic MCF-7pcDNA and MCF-7casp3 cells were harvested by shake-off and incubated with 5  $\mu$ M SU6656 or 5  $\mu$ M geraldol without or with 20  $\mu$ M MG-132 for 4 h. Lysates were immunoblotted for the indicated proteins as described in Section 2.10.

slippage. Cdc20 degradation was proteasome-dependent but the degradation of cyclin B1 was not (Figure 5.8). Taken together, these results indicate that SU6656 and geraldol stimulate the degradation of BubR1 by caspase-3, inactivating the mitotic checkpoint and resulting in mitotic slippage.

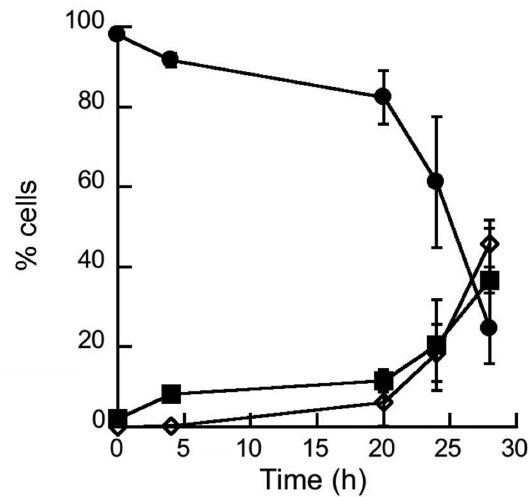
Approximately 20% of MCF-7pcDNA cells underwent mitotic slippage in the absence of SU6656 and geraldol (Figure 5.7), indicating that spontaneous mitotic slippage does not require caspase-3. To extend this observation, mitotic arrest and slippage in MCF-7pcDNA and MCF-7casp3 cells were examined during exposure to paclitaxel. Cells were exposed to 100 nM paclitaxel for up to 28 h and the proportion of interphase, mitotic and slipped cells was determined (Figure 5.9). In both cell lines, mitotic and slipped cells accumulated over time as the proportion of interphase cells declined (Figure 5.9). After 24 h, the proportion of slipped cells became greater than that of mitotic cells. The kinetics of accumulation of mitotic cells and slipped cells were very similar in MCF-7pcDNA and MCF-7casp3 cells (Figure 5.9), confirming that caspase-3 is not required for mitotic arrest or spontaneous slippage in response to paclitaxel. Therefore, while caspase-3 is absolutely required for mitotic slippage induction by SU6656 and geraldol, it is not required for spontaneous mitotic slippage in response to antimetabolic agents.

## **5.6 Mitotic slippage correlates temporally with degradation of BubR1 and Cdc20**

To examine the timing of chemically induced exit from mitosis, paclitaxel-arrested mitotic cells were harvested by shake-off, seeded in 96-well plates and exposed to geraldol for up to 3 h while cell attachment and TG3 fluorescence were measured (see



MCF-7pcDNA



MCF-7casp3

**Figure 5.9: Caspase-3-independence of spontaneous mitotic slippage.**

MCF-7pcDNA or MCF-7casp3 cells were exposed to 30 nM paclitaxel for up to 28 h and nuclei were fixed and stained with Hoechst 33342. The total number of cells was quantified using automated fluorescence microscopy and the images were visually inspected to determine the proportion of slipped and mitotic cells at each time.

Section 2.4) (Figure 5.10). TG3 recognizes nucleolin phosphorylated by CDK1/cyclin B1 and is a marker for mitosis (237). A significant proportion of cells began to attach after 2 h of exposure to geraldol, and the proportion of attached cells continued to increase over time (Figure 5.10A). TG3 fluorescence decreased appreciably within 60 min of exposure to geraldol and continued to decrease over time (Figure 5.10B). These observations were consistent over three separate experiments. TG3 fluorescence during exposure to SU6656 could not be measured due to autofluorescence of the compound. The timing of degradation of cyclin B1, BubR1 and Cdc20 during mitotic slippage was also examined. Paclitaxel-arrested cells were exposed to 5  $\mu$ M SU6656 or 5  $\mu$ M geraldol for 15 min to 3 h. Cyclin B1 disappeared completely within 30 min (Figure 5.11). BubR1 and Cdc20 were partially degraded within 15 min of exposure and almost completely degraded after about 2 h (Figure 5.11), around the time when cells began to attach and lose nucleolin phosphorylation, consistent with a requirement for degradation of BubR1 and Cdc20 for mitotic slippage.

## **5.7 Inhibition of the Aurora kinases by SU6656 and geraldol**

The Aurora kinases play complex roles in metaphase arrest and anaphase initiation, including chromosome congression and interkinetochore tension sensing (256-258). Inhibition of Aurora A or Aurora B in mitotic cells results in mitotic slippage (233, 259). SU6656 was designed as a Src family kinase inhibitor (242), but has since been reported to inhibit Aurora B *in vitro* (260, 261). Geraldol, however, has no known biological activity. Therefore, it was assayed for *in vitro* inhibition of a panel of kinases including Src, Aurora A and Aurora B. Geraldol showed significant inhibition of Aurora A and

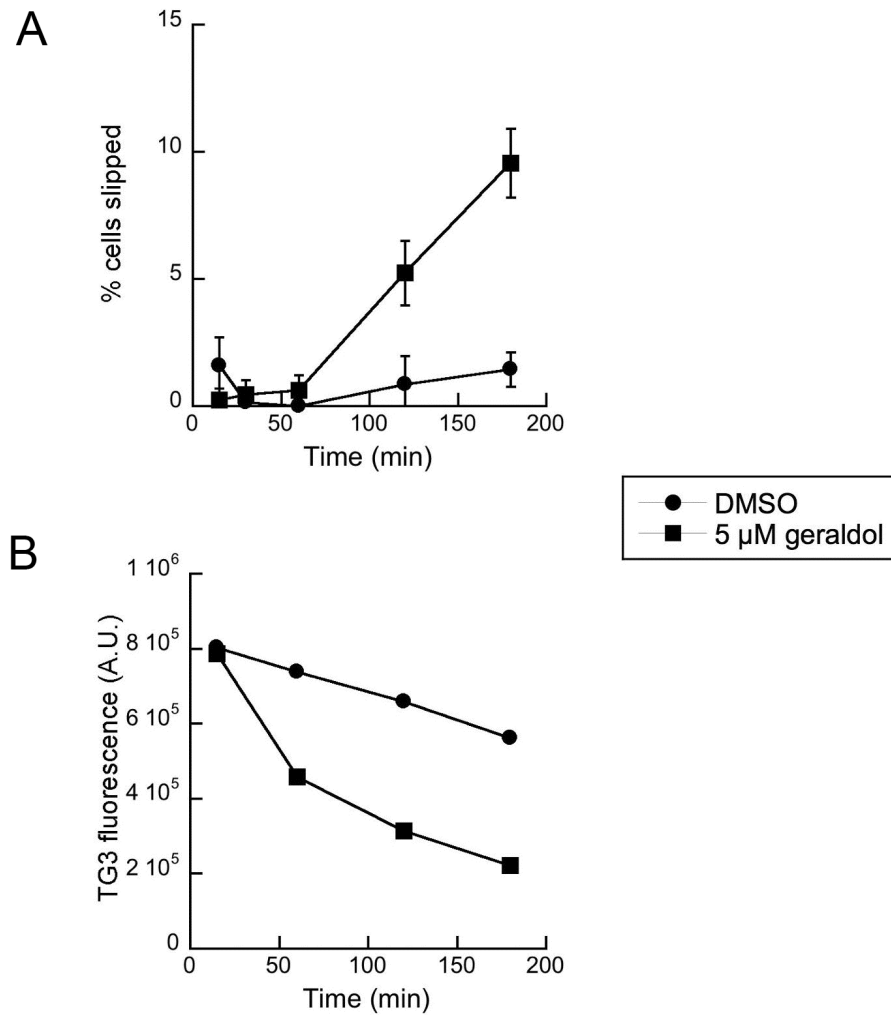


**Figure 5.10: Timeline of mitotic slippage stimulation by geraldol.**

T98G cells arrested in mitosis by 30 nM paclitaxel were harvested by shake-off, seeded in 96-well plates, and incubated with DMSO or 5  $\mu$ M geraldol for 15 min-4 h. Slipped cells were quantified after staining with Hoechst (A) (see Section 2.6) or with mouse TG3 antibody against mitotically phosphorylated nucleolin (B) (see Section 2.4). The proportion of slipped cells was lower than usually observed due to the numerous washes during immunofluorescent staining that removed many attached, slipped cells.

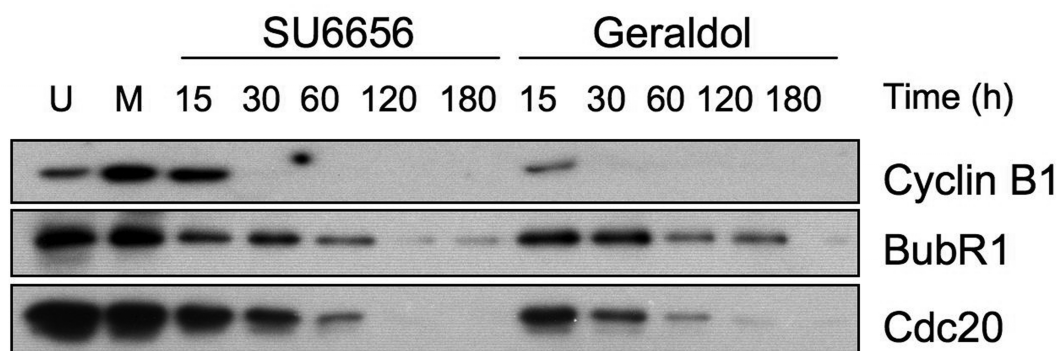


**Figure 5.11: Timeline of mitotic checkpoint inactivation by SU6656 and geraldol.**

Cycling T98G cells (U) were arrested in mitosis by exposure to 30 nM paclitaxel and harvested by shake-off. Mitotic cells (M) were incubated with 5  $\mu$ M SU6656 or 5  $\mu$ M geraldol for 15 min-3 h and lysates were immunoblotted for the indicated proteins as described in Section 2.10.

Aurora B but not Src (Table 5.1). SU6656 and geraldol were then assayed at 0.1-10  $\mu$ M for inhibition of Aurora A and Aurora B kinase activity (Figure 5.12). Both compounds inhibited Aurora A and Aurora B, although Aurora B was inhibited more potently. The intracellular effects of SU6656 and geraldol were compared with those of ZM447439, a well-characterized Aurora B inhibitor that induces mitotic slippage (233). ZM447439 induces 50-60% of mitotic MCF-7 cells to undergo mitotic slippage (Figure 5.13), while SU6656 and geraldol require the introduction of caspase-3 to induce mitotic slippage in MCF-7 cells (Figure 5.7). Thus, mitotic slippage induction through inhibition of Aurora B does not appear to require caspase-3 activation. Therefore, while SU6656 and geraldol may stimulate mitotic slippage in part by inhibition of Aurora B, these compounds probably have additional activities.

### **5.8 Caspase-3 does not significantly impact cell survival after mitotic slippage**

The role of caspase-3 in mitotic slippage induction implies a connection between mitotic slippage and apoptosis, which has also been observed by other groups (171, 184, 262). To investigate the role that caspase-3 might play in the fate of cells that have undergone spontaneous or induced mitotic slippage, the survival of MCF-7pcDNA and MCF-7casp3 cells was compared for up to 14 d after exposure to paclitaxel and DMSO, SU6656, or geraldol and drug washout (Figure 5.14). MCF-7pcDNA and MCF-7casp3 cells arrested at mitosis with paclitaxel were isolated via shake-off and exposed to DMSO, SU6656 or geraldol for 4 h. Unattached mitotic cells were removed and the attached, slipped cells were cultured in the absence of any drugs for up to 14 d while the number of cells remaining at each time was quantified by automated fluorescence

| Target         | % inhibition | Target         | % inhibition | Target         | % inhibition |
|----------------|--------------|----------------|--------------|----------------|--------------|
| ABL1           | 54           | FRK            | 40           | ASK1           | 39           |
| CAMK1 $\delta$ | 55           | LCK            | 59           | JNK1           | 26           |
| MST1           | 81           | LYN B          | 54           | p38 $\alpha$   | 16           |
| AMPK           | 68           | SRC            | -5           | CHK1           | 70           |
| PKC $\alpha$   | 1            | p70S6K         | 62           | CDK1           | 85           |
| PKC $\alpha$   | -1           | PIM1           | 94           | RAF1           | 32           |
| PKD2           | 79           | RSK1           | 91           | PAK4           | 25           |
| CDK2           | 91           | MAPKAPK2       | 24           | FAK            | 11           |
| CDK5           | 96           | FES            | 43           | HER2           | 8            |
| MLCK           | 43           | CK2 $\alpha$ 1 | 46           | JAK2           | -1           |
| NEK2           | 8            | ERK1           | 46           | MET            | 0            |
| KDR            | 46           | FLT3           | 90           | PDGFR $\alpha$ | 42           |
| PLK1           | 32           | BRK            | 18           | PYK2           | 28           |
| GSK3 $\beta$   | 60           | BLK            | -4           | TIE2           | 43           |
| PDK1           | 67           | BMX            | 4            | TRKA           | 64           |
| AKT1           | 42           | EPHB2          | 4            | CDK4           | 50           |
| HCK            | 27           | SYK            | -6           | GRK5           | -14          |
| CSK            | 0            | ZAP70          | 3            | RIPK2          | 92           |
| FGFR1          | 47           | SGK1           | 41           | Aurora B       | 89           |
| FGR            | 67           | Aurora A       | 62           | RAF1<br>(EE)   | 52           |

**Table 5.1: Geraldol *in vitro* kinase inhibition.**

The purified kinases were incubated with 10  $\mu$ M geraldol, appropriate peptide substrates and  $^{33}$ P-ATP for 20 – 30 min at room temperature as described in Section 2.11. 10  $\mu$ L of the reaction mixture was spotted on a phosphocellulose plate and  $\gamma$ - $^{33}$ P-ATP incorporated was quantified by scintillation counting. Assays were performed by Signalchem Inc. and the values shown are means of three separate experiments.

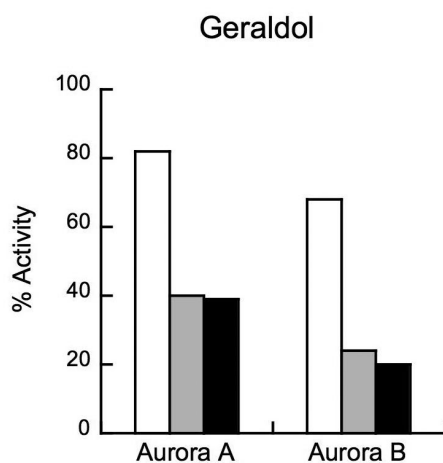
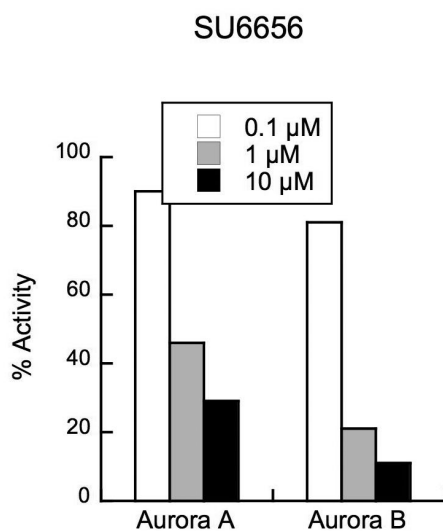


**Figure 5.12: Inhibition of Aurora A and Aurora B by SU6656 and geraldol.**

SU6656 and geraldol were assayed for *in vitro* inhibition of Aurora A and Aurora B activity on myelin basic protein, measured by  $^{33}\text{P}$ -phosphate incorporation as described in Section 2.11. Assays were performed by Signalchem Inc. and values shown are representative of three separate experiments.

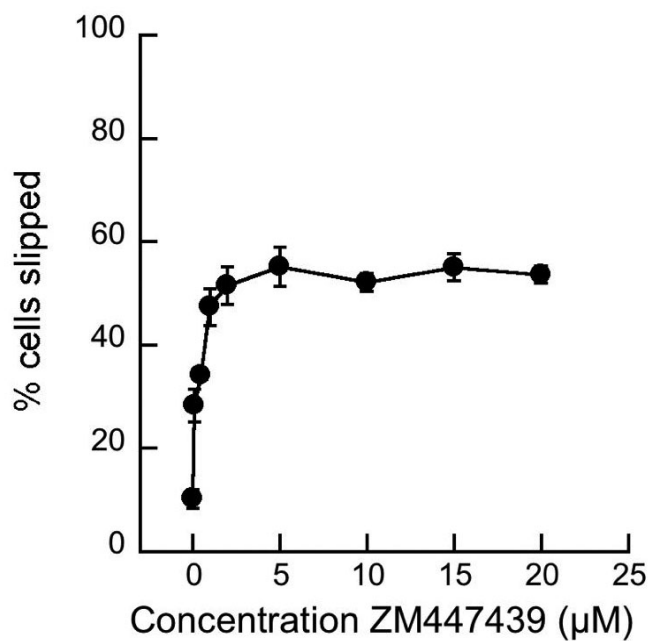


**Figure 5.13: Caspase-independent induction of mitotic slippage by ZM447439.**

MCF-7 cells were arrested in mitosis by 50 nM paclitaxel for 20 h, harvested by shake-off, seeded in 96-well plates and incubated with 0.1-20 µM ZM447439 for 4 h. Cells were fixed, stained with Hoechst 33342 and imaged by automated fluorescence microscopy (see Section 2.6).

microscopy (Figure 5.14). Extensive cell death occurred in both cell lines such that, 14 d after mitotic slippage, fewer than 20% of the initial number of mitotic cells remained. Therefore, caspase-3 does not appear to play a major role in cell death after mitotic slippage.

### **5.9 Caspase-3 and p53 are not essential for cell death subsequent to antimetabolic treatment**

To extend the evaluation of the role apoptosis plays in cell fate after mitotic slippage to include the entire cell population exposed to an antimetabolic agent, the fate of the entire cell population after exposure to paclitaxel and SU6656 or geraldol was also examined and compared between cells lacking caspase-3 or p53 and vehicle-transfected cells. MCF-7pcDNA cells, MCF-7casp3 cells and MCF-7 cells stably transfected with dominant-negative p53 (MCF-7mp53) were exposed to paclitaxel for 20 h and DMSO, SU6656 or geraldol was added for a further 4 h before both drugs were washed away. The cells were then allowed to grow in fresh cell culture medium for up to 10 d prior to staining and quantification. Initially, a small increase in cell number was observed, indicating that some cells recovered and were able to divide (Figure 5.15). However, extensive cell death began to occur 5 d following drug treatment and the majority of cells died before day 10 (Figure 5.15). Caspase-3 expression or loss of p53 activity did not alter this response.

After undergoing mitotic slippage, cells remained metabolically active for up to several days and underwent one or more rounds of DNA replication without cell division before undergoing apoptosis (Section 4.3). To examine metabolic activity of the entire

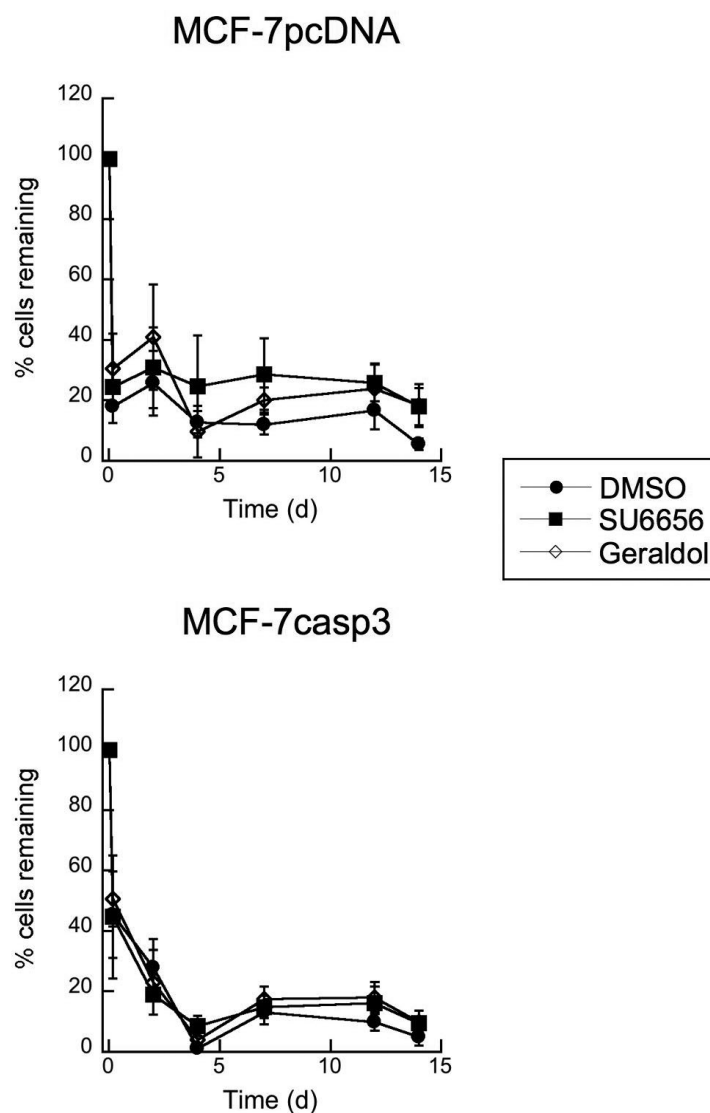


**Figure 5.14: Cell death after mitotic slippage with or without caspase-3 activity.**

MCF-7pcDNA and MCF-7casp3 cells were exposed to 30 nM paclitaxel for 20 h, harvested by shake-off and seeded in 96-well plates. After exposure to 0.1% DMSO, 5  $\mu$ M SU6656 or 5  $\mu$ M geraldol for 4 h, mitotic cells were removed and the attached, slipped cells were allowed to grow in fresh culture medium for up to 14 d before staining with Hoechst and quantification as a proportion of mitotic cells by automated fluorescence microscopy (see Section 2.6).

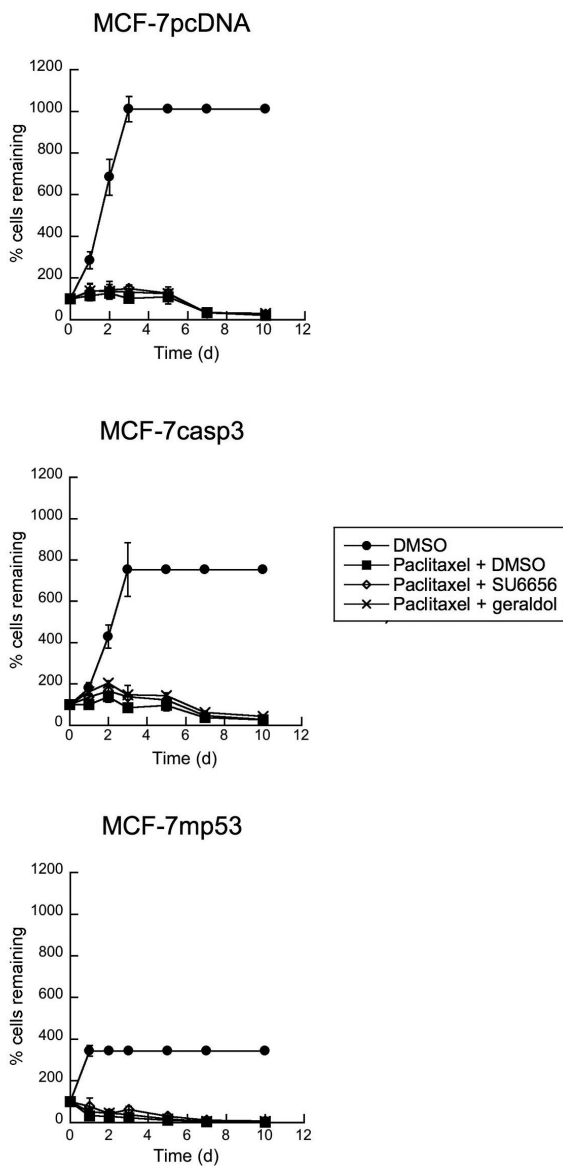


**Figure 5.15: Cell death after exposure to combinations of paclitaxel and SU6656 or paclitaxel and geraldol with or without caspase-3 or p53 activity.**

MCF-7pcDNA, MCF-7casp3 or MCF-7mp53 cells in 96-well plates were exposed to 0.1% DMSO or 30 nM paclitaxel for 20 h and then 0.1% DMSO, 5  $\mu$ M SU6656 or 5  $\mu$ M geraldol for a further 4 h. Drugs were washed away and the cells were allowed to grow in fresh culture medium for up to 10 d before staining with Hoechst 33342 and quantification by automated fluorescence microscopy (see Section 2.6).

cell population after exposure to paclitaxel or paclitaxel and SU6656 or geraldol, MCF-7pcDNA, MCF-7casp3 and MCF-7mp53 cells were treated as above and metabolic activity was measured using the MTT assay. The metabolic activity of treated cells in both cell lines increased during the first three days to roughly the same extent as untreated cells (Figure 5.16), although untreated cells proliferated rapidly during that time and there was a minimal increase in number of treated cells (Figure 5.15). Metabolic activity reached a plateau after 3 d and decreased considerably after 7 d, a response not altered by caspase-3 expression or p53 mutation. This result indicates that, for 3 d after treatment with paclitaxel without or with SU6656 or geraldol, little or no cell proliferation or death took place, but cells continued to grow in size. Cell growth was arrested between 3 and 7 d before extensive cell death took place after day 7.

The majority of cells that undergo mitotic slippage die within 4 d, and, curiously, this result appears to have little dependence on an intact apoptotic pathway, as both the MCF-7casp3 and MCF-7pcDNA cell lines exhibit extensive cell death following mitotic slippage (Section 5.8). This similarity is also reflected in the fate of all cells after exposure to a microtubule-targeting agent without or with SU6656 or geraldol. MCF-7mp53 cells, which do not undergo mitotic slippage (Section 3.3) and which lack the cell cycle arrest/apoptotic stimulus of p53, appear to be more susceptible to cell death following exposure to a microtubule-targeting agent than MCF-7pcDNA or MCF-7casp3 cells, suggesting the involvement of other cell death pathways in the response to antimitotic agents.

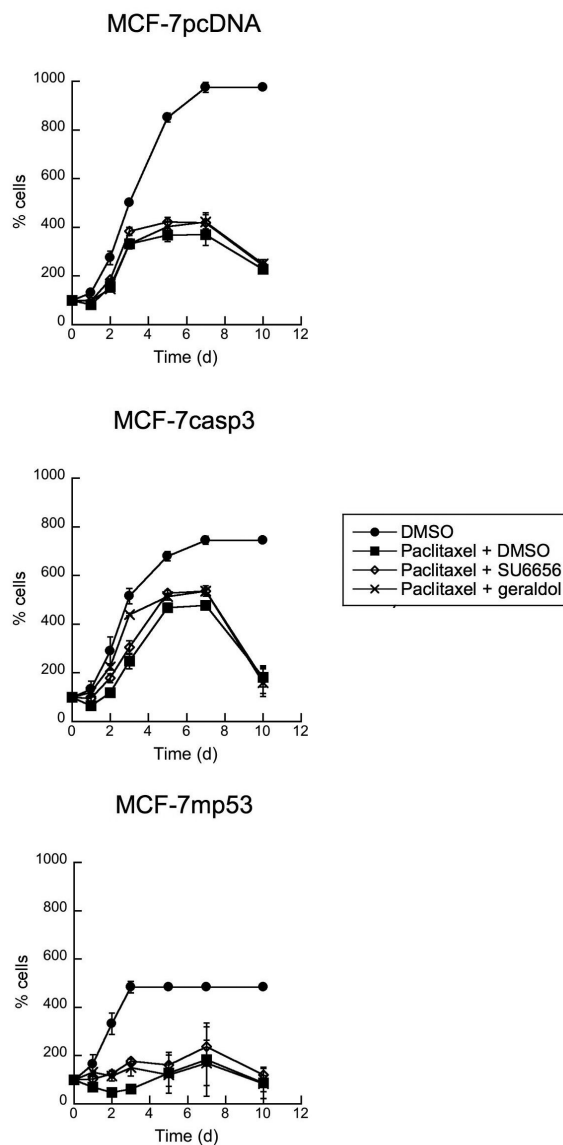


**Figure 5.16: Decrease in cell viability after exposure to combinations of paclitaxel and SU6656 or paclitaxel and geraldol with or without caspase-3 or p53 activity.**

MCF-7pcDNA or MCF-7casp3 cells in 96-well plates were exposed to 0.1% DMSO or 30 nM paclitaxel for 20 h and then 0.1% DMSO, 5  $\mu$ M SU6656 or 5  $\mu$ M geraldol for a further 4 h. Drugs were washed away and the cells were allowed to grow in fresh culture medium for up to 14 d before analysis of cell viability by the MTT assay as described in Section 2.5.

## CHAPTER 6: CONCLUSION

### 6.1 Chemical inducers of senescence

#### 6.1.1 Discussion

Senescence is a state of permanent growth arrest in response to DNA damage that is thought to be a barrier to tumorigenesis (see Section 1.3.3). Chapter 3 presents a novel screen for chemicals that induce senescence independently of p53, which is normally a crucial component of pathways leading to senescence (137, 263, 264). While several classes of drugs, including DNA-damaging agents (265-267), and, to a lesser extent, antimetabolic agents (268), have been observed to induce senescence in a subset of treated cells, this screen represents one of the first efforts to screen for compounds that induce senescence. I identified four chemicals that induce senescence in T98G cells: 8-azaguanine, erysolin, IC 261 and SKF 96365. These chemicals induce senescence through increased activity in the promoter region of p21, a CDK inhibitor that can cause growth arrest at G1 or G2 (269, 270). This is a novel function for all four small molecules, although they had previously described biological activities. 8-azaguanine is a guanine analogue that is incorporated into nucleic acids (271) and has known antimetabolic (272) and anticancer activity. Erysolin is an isothiocyanate that induces apoptosis in cells through the generation of reactive oxygen species (273, 274). IC 261 affects mitotic spindle formation through inhibition of casein kinase 1- $\delta$  and  $-\epsilon$  (275, 276) and causes a p53-dependent post-mitotic arrest (276). SKF 96365 blocks receptor-mediated calcium entry (277).

The significance of this discovery is twofold: first, a recent increase in interest in senescence as a phenotype important in cancer (278, 279) points to a function for these chemicals in studies to better understand senescence, and second, senescence-inducing chemicals have demonstrated therapeutic potential.

### **6.1.2 Future perspectives**

There are several potential pathways to senescence, and it has been shown that upregulation of only one of these silent pathways in cancer is sufficient to re-activate the senescent phenotype (280). Both of the most prominent pathways to senescence involve the DNA damage response, either through single-stranded DNA exposed at short telomeres (133, 135, 138) or through DNA breaks caused by the hyper-replication associated with oncogene overexpression (140). Cells can overcome senescence through mutation or loss of p53 or pRb, attenuating this DNA damage response (137, 148). 8-azaguanine, erysolin, IC 261 and SKF 96365 could be used to induce senescence in untransformed or in cancer cells, allowing study of the effects of senescence in cancer, regarding which there are many unanswered questions. For instance, while replicative senescence is irreversible (281), senescence induced by drugs may not be. They could also be used to determine the effect of senescence on the tumour microenvironment: senescent cells have been found to secrete pro-inflammatory cytokines that may promote proliferation in surrounding cells (282), although this has not been observed in drug-induced senescence. Many other questions regarding senescence remain: what role does it play in tumour development? What is the relationship, if any, between apoptosis and senescence? Given that there are few chemicals known to induce senescence, and the

ones that are known also induce apoptosis, these compounds could be of considerable use in expanding our knowledge of this phenomenon.

Besides their function as chemical tools to study senescence, these compounds could have therapeutic use in tumours that have lost p53 function, a proportion that may be higher than 50% (283), and in tumours that are otherwise resistant to apoptosis. The development of drugs that increase p53 activity, for instance through preventing the inhibitory association of p53 with Mdm2 (284, 285), has been of interest for some years. Recent work in models of tumours with inactivated apoptotic pathways has indicated that senescence stimulation can lead to improved survival rates (286). Induction of senescence by low doses of some anticancer therapeutics has been reported to reduce toxicity-related side effects (287) and to increase the immune response directed towards the tumour (288, 289). Chemicals that initiate senescence may also find applications in treatment of premalignant or early cancers, consistent with the view of senescence as a tumour suppressor. For instance, retinoids that are used in chemoprevention have been observed to induce senescence (290). It would also be of interest to use the chemicals I have identified in *in vitro* cell culture and *in vivo* animal models of cancer to clarify whether induction of senescence in tumours can halt tumour progression and improve prognosis. The need for efficient senescence-inducing agents has been highlighted by a recent review (291), and these chemicals may satisfy this need. Despite the potential of these compounds to illuminate our understanding of senescence, I chose to focus this thesis on mitotic slippage and therefore did not pursue answers to these questions.

## 6.2 Chemical modulators of mitotic slippage

### 6.2.1 Discussion

Mitotic slippage (reviewed in Section 1.6) occurs when cells bypass mitotic arrest and exit mitosis without separating their chromosomes and enter a G1-like state characterized by polyploidy and a ‘grape-like’ nuclear morphology (225). This work initially characterizes mitotic arrest and slippage in three cell lines in response to the anticancer drug paclitaxel, a microtubule-stabilizing agent that blocks cells at mitosis. The paclitaxel concentrations selected correspond to the 5-200 nM plasma concentration range, of which  $\geq 90\%$  is protein bound, observed during typical administration for cancer treatment by infusion over several hours (292-294). At the lower end of this concentration range, paclitaxel caused transient mitotic arrest followed by successful cell division or by mitotic slippage, depending on the cell line. Higher concentrations of paclitaxel increased the length of mitotic arrest in all cell lines, but a significant fraction of MDA-MB-231 and T98G cells underwent mitotic slippage during exposure to 10-30 nM paclitaxel. Mitotic slippage has similarly been observed to vary between different cell types and upon treatment with different antimetabolic agents (185, 188, 226, 295).

The prevalence of mitotic slippage in two of the cancer cell lines prompted me to study its relevance to cell survival and proliferation. To address this issue, screening assays were conceived for chemical inhibitors and stimulators of mitotic slippage. Both assays were designed such that active chemicals would cause an increase in detection signal rather than a decrease. The inclusion of a positive readout in cell-based screening is an effective way to filter out compounds acting non-specifically (239-241). In independent work, DeMoe *et al.*, Salmela *et al.* and Stolz *et al.* reported similar screens

for chemical inducers of mitotic slippage using different cell lines and chemical collections (296-298).

The screen for inhibitors of mitotic slippage identified several microtubule-targeting agents, which was not surprising given the observation that increasing the concentration of paclitaxel strengthened mitotic arrest. The identification of chlorpromazine and trifluorpromazine as inhibitors of mitotic slippage was more unexpected. These two closely related drugs approved for use in humans are believed to exert their antipsychotic action by blocking dopamine receptors in the brain (299). CPZ has multiple other effects, including anticancer activity (41, 300) and inhibition of bacterial antibiotic resistance (301). In 1983 it was reported to cause accumulation of cells in mitosis (302) and it was recently found to inhibit the mitotic kinesin KSP/Eg5, causing mitotic arrest with monopolar spindles, an effect characteristic of mitotic kinesin inhibitors (41). CPZ indeed caused mitotic arrest at high concentrations in the three cell lines studied. However, lower concentrations of CPZ and TPZ that did not themselves cause mitotic arrest were able to strengthen mitotic arrest by low concentrations of paclitaxel (Figure 3.10). In all cases, increasing the concentration of an antimitotic agent causes increased mitotic arrest and inhibition of cell proliferation.

Remarkably, although cellular exposure to a combination of low concentrations of paclitaxel and CPZ or TPZ increased mitotic arrest, it strongly increased cell survival upon drug washout (Figure 4.1). MCF-7mp53 cells exposed to low paclitaxel concentrations cells arrest only transiently at mitosis and successfully divide; this result indicates that low paclitaxel concentrations can activate the mitotic checkpoint without functionally inactivating the mitotic spindle itself. With respect to the scheme outlined in

Figure 1.5, the results indicate that enforcing mitotic arrest by a mechanism that does not further damage the mitotic spindle can increase cell survival and proliferation following drug removal. These observations are in agreement with the classical view articulated by Hartwell and Weinert that checkpoints serve to promote cell survival in response to various insults (303).

The screen for stimulators of mitotic slippage identified two structurally unrelated chemicals: the synthetic kinase inhibitor SU6656 and the naturally occurring flavonoid geraldol. Both chemicals were active in cells arrested at mitosis by the microtubule-stabilizing drug paclitaxel, the microtubule-depolymerizing drug vinblastine, and the KSP/Eg5 inhibitor *S*-trityl-L-cysteine, indicating broad applicability (Figure 3.16). SU6656 was originally developed as a Src kinase inhibitor (242) but has since been shown to inhibit additional kinases (260, 261). At the time it was identified, nothing was known about cellular targets for geraldol. Fisetin, a structurally similar but less potent flavonoid (not shown) was later found to inhibit Aurora B and induce mitotic slippage (298).

It has until now been difficult to study the fate of cells after mitotic slippage. Most approaches have used time-lapse microscopy to follow individual cells, typically for up to one day (226, 304-306). The identification of chemicals that stimulate mitotic slippage and the ability to isolate these cells in large numbers enabled me to follow their fate over an extended time period. The effect of mitotic slippage on cell fate was studied in detail in the T98G cell line. Cells that underwent spontaneous or chemically induced slippage after mitotic arrest induced by a microtubule-targeting agent experienced a similar complex fate. My results show that all cells eventually died but that this process took up

to 2 weeks (Figure 4.2). During this time, a large proportion of the cells replicated their DNA up to three times without intervening cell division, resulting in a large increase in ploidy (Figure 4.3). Since T98G cells are hyperpentaploid, some of the cells acquired 40 times the 2N ploidy of normal cells. These cells were flattened and enormous, with diameters exceeding 100  $\mu\text{m}$  (Figure 4.4). A large proportion of these cells expressed a senescence marker about one week after undergoing mitotic slippage (Figure 4.5). Cell death was observed throughout the two-week observation period, indicating that cells died at different stages of this process. These results are in general agreement with those of Chan *et al.*, Salmela *et al.*, and Stolz *et al.*, who observed independently that cells treated with microtubule-targeting agents and the CDK1 inhibitors roscovitine or RO3306 (307) or the proposed Aurora inhibitors fisetin (298) or Gö6976 (297) underwent mitotic slippage and DNA endoreduplication before dying by apoptosis several days later.

The inability of slipped cells to survive and proliferate could be an intrinsic property of slipped cells, or it could be a consequence of irreversible damage to the microtubule network inflicted by the microtubule-targeting drugs. The observation that large numbers of cells that slipped out of mitotic arrest imposed by the KSP/Eg5 kinesin inhibitor *S*-trityl-L-cysteine were able to survive and proliferate with normal ploidy (Figures 4.2, 4.3) shows that mitotic slippage does not necessarily cause cell death. The microtubule network of cells that slipped out of mitosis after treatment with paclitaxel or vinblastine was abnormal (Figure 4.4), and video microscopy analysis revealed that interphase slipped cells entered mitosis and unsuccessfully attempted to segregate chromosomes before exiting mitosis and re-entering interphase (not shown). This result contrasts with

Tao *et al.*'s report that inhibition of KSP causes mitotic slippage and apoptosis (171). However, Tao *et al.* found that many cells re-entered the cell cycle after treatment with a KSP inhibitor, in agreement with my findings, and that while induction of mitotic slippage after treatment with a KSP inhibitor increased cell death, the apoptotic fraction of cells was small and many cells divided and re-entered the cell cycle, again in agreement with my findings (171). As my studies of mitotic arrest in three cell lines show, response to treatment with an antimitotic agent also varies with cell line.

However, these results demonstrating that mitotic slippage can lead to cell death indicate that inducing mitotic slippage may represent a strategy to increase the efficacy of antimitotic cancer therapies. As such, it is essential to better understand the pathways leading to mitotic slippage through the use of chemicals.

SU6656 and geraldol induce the proteasome-dependent degradation of cyclin B1 as occurs during exit from mitosis (Figure 5.2) (23, 185, 308). However, unlike during the metaphase-to-anaphase transition, these chemicals inactivate the mitotic checkpoint through the proteasome-dependent degradation of BubR1 (Figure 5.2) that is sufficient to compromise the mitotic checkpoint (126, 309, 310). Degradation of Mad2, the other component of the MCC that can inhibit APC/C<sup>Cdc20</sup> directly (311), is not significant and occurs only in response to SU6656 in a non-proteasome-dependent manner (Figure 5.2). This effect occurs only in mitotic cells (Figure 5.4), and BubR1 is not degraded during completion of mitosis in T98G cells (Figure 5.3B). These results suggest that, rather than accelerating spontaneous mitotic slippage, SU6656 and geraldol activate an alternate pathway leading to mitotic slippage through BubR1 degradation.

Examination of the timing of mitotic checkpoint inactivation and slippage revealed that mitotic slippage, defined in this experiment by cell attachment and loss of the mitotic phosphoepitope recognized by the TG3 antibody, begins to occur 2 h following exposure to geraldol, while cyclin B1 degradation is complete 30 min after drug treatment (Figures 5.10, 5.11). BubR1 and Cdc20 degradation occur more slowly (Figure 5.11) and approximately correlate with mitotic slippage, indicating a possible requirement for checkpoint inactivation prior to mitotic slippage, even in the absence of CDK1/cyclin B1 activity. In agreement with this observation, cyclin B1 is also completely degraded in MCF-7 cells in response to SU6656 and geraldol, although mitotic slippage cannot be induced (Figures 5.7, 5.8). It is not known whether the degradation of other APC/C substrates or dephosphorylation of mitotic checkpoint kinase substrates might be involved in mitotic slippage. While I show that loss of the APC/C substrate securin increases the frequency of mitotic slippage (Figure 4.8), although not cellular survival subsequent to mitotic slippage (Figure 4.9), it is not clear whether securin degradation is required for mitotic slippage.

Caspase-3 is upregulated during mitosis (218, 312, 313) and has been demonstrated to increase the formation of micronuclei in response to antimitotic agents (262), but a role for caspase-3 in mitosis remains undefined. This work reveals a novel role for caspase-3: mitotic slippage induced by SU6656 and geraldol is caspase-3-dependent. Co-treatment of mitotic cells with SU6656 or geraldol and the caspase-3 and -7 inhibitor DEVD-CHO prevented mitotic slippage and checkpoint inactivation (Figures 5.5, 5.6). While introduction of caspase-3 into MCF-7 cells does not affect the frequency of spontaneous mitotic slippage in response to paclitaxel (Figure 5.9), mitotic slippage can be induced by

SU6656 and geraldol in MCF-7 cells only when exogenous caspase-3 is expressed (Figure 5.7), indicating that caspase-3 is absolutely required for induction of mitotic slippage by SU6656 and geraldol.

This requirement for caspase-3 is likely due to its role in inactivation of the mitotic checkpoint; mitotic slippage and BubR1 degradation occur in MCF-7 cells with active caspase-3 but not in MCF-7 cells lacking caspase-3 (Figures 5.7, 5.8). BubR1 degradation is sufficient to inactivate the mitotic checkpoint (109, 125, 126) and, further, BubR1 depletion has been implicated in the development of polyploidy (309, 314). Several factors can influence the degradation of BubR1 during mitosis. Choi *et al.* observed that BubR1 deacetylation at metaphase results in abrogation of its anaphase inhibition effects and in its degradation by APC/C<sup>Cdc20</sup> (110). Co-treatment of mitotic cells with SU6656 or geraldol and the deacetylase inhibitor trichostatin A did not prevent chemical induction of mitotic slippage (data not shown), indicating that SU6656 and geraldol do not induce premature deacetylation of BubR1. While a small proteasome-dependent decrease in BubR1 was observed in MCF-7pcDNA cells in response to SU6656 and geraldol (Figure 5.8), this is not sufficient for mitotic slippage to occur and is probably due to some deacetylation and proteasome-dependent degradation of BubR1. Kim *et al.* observed cleavage of BubR1 by caspase-3 during mitosis, which also led to exit from mitosis (217). BubR1 is degraded in a caspase-3 but not proteasome-dependent manner in MCF-7 cells (Figure 5.7), indicating that caspase-3 initiates mitotic slippage through cleavage of BubR1.

However, caspase-3 does not appear to be required for cell death following paclitaxel treatment (Figures 5.14, 5.15, 5.16). While caspase-3 is required for DNA fragmentation

during apoptosis (254), cells that lack caspase-3 can nevertheless undergo apoptosis. The important role of p53 in apoptosis is well established (211, 315), but p53 activity is not required for apoptotic cell death (316, 317) and I show that it is not required for cell death in response to paclitaxel treatment (Figures 5.15, 5.16). Other cell death pathways may also be involved in the fate of cells following exposure to an antimitotic agent: for instance, necrosis and autophagy have both been implicated in cell death following antimitotic therapy (180-183, 318).

Spontaneous mitotic slippage has been described to occur through slow ubiquitylation of cyclin B1 by APC/C<sup>Cdc20</sup> and subsequent proteasome-dependent degradation despite mitotic checkpoint activity (226, 227). I propose a model (Figure 6.1) for mitotic slippage where decreased CDK1 activity due to slow cyclin B1 depletion, combined with phosphatase activity, results in loss of the mitosis-specific CDK1/cyclin B1 inhibitory phosphorylation on caspase-9 (184). Active caspase-9 may then cleave procaspase-3, and activated caspase-3 can cleave BubR1, resulting in inactivation of the mitotic checkpoint and activation of APC/C<sup>Cdc20</sup>. This event would lead to further ubiquitylation and degradation of cyclin B1, combining to force exit from mitosis through mitotic slippage. Exactly where SU6656 and geraldol may act in this cascade is unclear, as there could be many possible upstream events influencing the activation of caspase-9 that I propose as the first step in this process.

In summary, these results show that during exposure of cancer cells to low nanomolar concentrations of paclitaxel that approximate plasma drug concentrations achieved during treatment of patients, enforcing mitotic arrest with an inhibitor of mitotic slippage can promote cell survival and proliferation. Conversely, cells that undergo mitotic slippage or

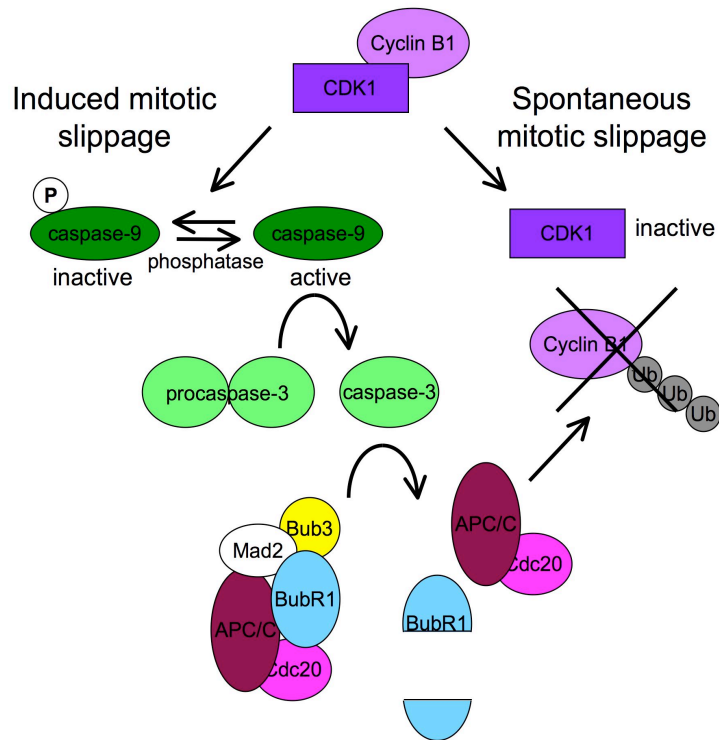


**Figure 6.1: Model for spontaneous and induced mitotic slippage.**

Mitotic slippage may occur through slow proteasome-dependent degradation of cyclin B1 in the presence of an active mitotic checkpoint or through chemically stimulated caspase activation and subsequent inactivation of the mitotic checkpoint.

checkpoint adaptation, whether spontaneous or induced, will likely fail to proliferate and will die. With respect to the different cell fates described in Figure 1.5, I show that inhibiting mitotic slippage can result in successful completion of cell division and continued proliferation, while inducing cells to slip out of mitotic arrest stimulated by a microtubule-targeting agent invariably results in cell death. Results from my studies of small-molecule inducers of mitotic slippage imply that when tumour cells treated with a microtubule-targeting agent such as the taxanes or the *Vinca* alkaloids undergo mitotic slippage, the ultimate outcome is cell death and potential tumour regression. However, when tumour cells treated with kinesin inhibitors slip out of mitotic arrest, they can continue to proliferate. Therefore, induction of mitotic slippage may represent a strategy to increase the antitumour effects of microtubule-targeting drugs.

The chemical inducers of mitotic slippage SU6656 and geraldol cause proteasome- and caspase-dependent inactivation of the mitotic checkpoint, in contrast to the accepted model for spontaneous mitotic slippage. Caspase-3 is required for mitotic slippage induction and checkpoint inactivation through degradation of BubR1, although not for cell death in response to antimetabolic agents. I propose a model for induced mitotic slippage that includes an important role for caspases in modulation of mitotic arrest. In response to the cellular stress presented by a prolonged mitotic arrest, caspases may contribute to the outcome of antimetabolic cancer therapy through mitotic slippage as well as through apoptosis.

### 6.2.2 Future perspectives

There remains much about mitotic slippage that is not clearly understood, and given its influential role in the cellular response to antimitotic cancer therapies, it is important that factors influencing mitotic slippage are clearly elucidated.

First, what genetic factors influence a particular cell type to fail to maintain mitotic arrest and undergo mitotic slippage? Or, put simply in the terms of this thesis, why do MDA-MB-231 cells undergo mitotic slippage in response to paclitaxel while MCF-7mp53 cells undergo stable mitotic arrest? Caspase-3 is not required for spontaneous mitotic slippage (Figure 5.9), so the factors underlying the robust mitotic arrest observed in MCF-7mp53 cells remain mysterious. If the mitotic checkpoint were non-functional in cells that undergo mitotic slippage, then they would not arrest in mitosis at all and would die (319). Therefore, there must be other protein expression changes or mutations that govern the likelihood of mitotic slippage as a response to antimitotic agents.

Understanding the factors in tumour cells that influence mitotic arrest and mitotic slippage would enable better prediction of tumour response to antimitotic drugs and greater efficacy of chemotherapy.

My observation that inhibition of mitotic slippage leads to increased cell survival and proliferation in comparison with induction of mitotic arrest alone was somewhat surprising. With respect to the outcomes of antimitotic therapy as outlined in Figure 1.6, given that antimitotic therapy is successful in the clinic, it would have been supposed that inhibiting mitotic slippage would drive cells toward mitotic death. However, this was clearly not the case, and why reinforcement of mitotic arrest increases cell survival is a question of interest.

Together with this effort comes a better understanding of the molecular mechanism of mitotic slippage. I postulate that it can occur either through slow cyclin B1 degradation in the presence of an active mitotic checkpoint or through caspase-mediated inactivation of the mitotic checkpoint (Figure 6.1). However, more evidence is required to show that mitotic slippage can occur through the latter pathway, and determine what signals result in the activation of caspase-9 that initiates caspase-mediated mitotic slippage. The direct targets of SU6656 and geraldol remain a mystery, as there are many factors that can influence caspase activation.

The role of the Aurora kinases in mitotic slippage is incompletely understood, although many of the chemicals that induce mitotic slippage, including SU6656 and geraldol, inhibit either Aurora A (259) or Aurora B (233, 297, 298). Elucidating how lack of Aurora kinase activity during prometaphase arrest leads to the inability to maintain that arrest will contribute to our knowledge of mitosis and to therapeutic uses for this class of compounds, as several Aurora kinase inhibitors are currently undergoing clinical trials (320-322).

I show results that imply that cyclin B1 degradation may not be sufficient for mitotic slippage to occur. This should be investigated further to complete our understanding of how mitotic slippage occurs – if cyclin B1 degradation is not all that is required for mitotic slippage, then what other processes are required?

Cells are known to be especially vulnerable to DNA damage while chromosomes are condensed, and DNA damage during mitosis has been indicated to cause mitotic slippage (246); however, this connection is not well understood. I report the identification of the DNA topoisomerase inhibitor aklavin, which is closely structurally related to aclarubicin,

idarubicin, doxorubicin and daunorubicin, as an inducer of mitotic slippage. How a DNA-damaging agent can induce mitotic slippage is an interesting question remaining to be answered, especially considering that many chemotherapy regimens involve both DNA topoisomerase inhibitors and antimetabolic agents. Also for this reason, it is important to discover the outcome with respect to cell fate of mitotic slippage induced by DNA-damaging agents. Studies of the doxorubicin family of DNA topoisomerase inhibitors and mitotic slippage are currently undergoing in the Roberge laboratory.

While I and others (297, 298, 304, 307, 323) show that mitotic slippage, whether spontaneous or stimulated by chemicals, results in cell death in cell culture, mitotic slippage has not been sufficiently studied in *in vivo* tumour models to allow understanding of the contribution slippage makes to cancer cell death within tumours. Antimetabolic agents are usually administered intravenously over several hours, so tumour cells may be exposed to drugs at low or varying concentrations and for short periods of time. Mitotic slippage may therefore be more prevalent in tumours, as it occurs more frequently when cells are exposed to low concentrations of antimetabolic agents (Section 3.3) (185, 295). Additionally, the polyploidy ensuing from mitotic slippage may be tolerated differently *in vivo*, and if polyploid cells are able to undergo cell division, they may give rise to aneuploid cells that are known to contribute to drug resistance and relapse (120, 127, 131). Regardless, it remains to be established whether the cell death observed after mitotic slippage in cell culture occurs *in vivo*, and the effect of mitotic slippage on overall tumour shrinkage and progression needs to be determined. If mitotic slippage is shown to result in cancer cell death *in vivo*, then agents that induce mitotic

slippage could be of interest as part of a combination therapy to increase cell killing by antimetabolic agents.

## BIBLIOGRAPHY

1. Workman P, Collins I. Probing the probes: fitness factors for small molecule tools. *Chem Biol.* 2010;17:561-77.
2. Taylor S, Peters JM. Polo and Aurora kinases: lessons derived from chemical biology. *Curr Opin Cell Biol.* 2008;20:77-84.
3. Burkard ME, Randall CL, Laroche S, Zhang C, Shokat KM, Fisher RP, Jallepalli PV. Chemical genetics reveals the requirement for Polo-like kinase 1 activity in positioning RhoA and triggering cytokinesis in human cells. *Proc Natl Acad Sci U S A.* 2007;104:4383-8.
4. Brennan IM, Peters U, Kapoor TM, Straight AF. Polo-like kinase controls vertebrate spindle elongation and cytokinesis. *PLoS One.* 2007;2:e409.
5. Petronczki M, Glotzer M, Kraut N, Peters JM. Polo-like kinase 1 triggers the initiation of cytokinesis in human cells by promoting recruitment of the RhoGEF Ect2 to the central spindle. *Dev Cell.* 2007;12:713-25.
6. Santamaria A, Neef R, Eberspacher U, Eis K, Husemann M, Mumberg D, Prechtel S, Schulze V, Siemeister G, Wortmann L, Barr FA, Nigg EA. Use of the novel Plk1 inhibitor ZK-thiazolidinone to elucidate functions of Plk1 in early and late stages of mitosis. *Mol Biol Cell.* 2007;18:4024-36.
7. Sebastian M, Reck M, Waller CF, Kortsik C, Frickhofen N, Schuler M, Fritsch H, Gaschler-Markefski B, Hanft G, Munzert G, von Pawel J. The efficacy and safety of BI 2536, a novel Plk-1 inhibitor, in patients with stage IIIB/IV non-small cell lung cancer who had relapsed after, or failed, chemotherapy: results from an open-label, randomized phase II clinical trial. *J Thorac Oncol.* 2010;5:1060-7.
8. Schoffski P, Blay JY, De Greve J, Brain E, Machiels JP, Soria JC, Sleijfer S, Wolter P, Ray-Coquard I, Fontaine C, Munzert G, Fritsch H, Hanft G, Aerts C, Rapion J, Allgeier A, Bogaerts J, Lacombe D. Multicentric parallel phase II trial of the polo-like kinase 1 inhibitor BI 2536 in patients with advanced head and neck cancer, breast cancer, ovarian cancer, soft tissue sarcoma and melanoma. The first protocol of the European Organization for Research and Treatment of Cancer (EORTC) Network Of Core Institutes (NOCI). *Eur J Cancer.* 2010;46:2206-15.
9. Hofheinz RD, Al-Batran SE, Hochhaus A, Jager E, Reichardt VL, Fritsch H, Trommeshauser D, Munzert G. An open-label, phase I study of the polo-like kinase-1 inhibitor, BI 2536, in patients with advanced solid tumors. *Clin Cancer Res.* 2010;16:4666-74.
10. Crews CM, Shotwell JB. Small-molecule inhibitors of the cell cycle: an overview. In: Meijer L, Jezequel A, Roberge M, editors. *Progress in Cell Cycle Research*; 2003. p. 125-33.
11. Inglese J, Johnson RL, Simeonov A, Xia M, Zheng W, Austin CP, Auld DS. High-throughput screening assays for the identification of chemical probes. *Nat Chem Biol.* 2007;3:466-79.
12. Fox S, Farr-Jones S, Sopchak L, Boggs A, Nicely HW, Khoury R, Biro M. High-throughput screening: update on practices and success. *J Biomol Screen.* 2006;11:864-9.
13. An WF, Tolliday N. Cell-based assays for high-throughput screening. *Mol Biotechnol.* 2010;45:180-6.

14. Jain RB. A recursive version of Grubbs' test for detecting multiple outliers in environmental and chemical data. *Clin Biochem.* 2010;43:1030-3.
15. Rausch O. High content cellular screening. *Curr Opin Chem Biol.* 2006;10:316-20.
16. Shelat AA, Guy RK. The interdependence between screening methods and screening libraries. *Curr Opin Chem Biol.* 2007;11:244-51.
17. Hann MM, Leach AR, Harper G. Molecular complexity and its impact on the probability of finding leads for drug discovery. *J Chem Inf Comput Sci.* 2001;41:856-64.
18. Carpenter AE. Image-based chemical screening. *Nat Chem Biol.* 2007;3:461-5.
19. Kolb HC, Sharpless KB. The growing impact of click chemistry on drug discovery. *Drug Discov Today.* 2003;8:1128-37.
20. Nomura DK, Dix MM, Cravatt BF. Activity-based protein profiling for biochemical pathway discovery in cancer. *Nat Rev Cancer.* 2010;10:630-8.
21. Draetta G, Piwnica-Worms H, Morrison D, Druker B, Roberts T, Beach D. Human cdc2 protein kinase is a major cell-cycle regulated tyrosine kinase substrate. *Nature.* 1988;336:738-44.
22. Dunphy WG, Brizuela L, Beach D, Newport J. The *Xenopus* cdc2 protein is a component of MPF, a cytoplasmic regulator of mitosis. *Cell.* 1988;54:423-31.
23. Draetta G, Luca F, Westendorf J, Brizuela L, Ruderman J, Beach D. Cdc2 protein kinase is complexed with both cyclin A and B: evidence for proteolytic inactivation of MPF. *Cell.* 1989;56:829-38.
24. Cogswell JP, Godlevski MM, Bonham M, Bisi J, Babiss L. Upstream stimulatory factor regulates expression of the cell cycle-dependent cyclin B1 gene promoter. *Mol Cell Biol.* 1995;15:2782-90.
25. Desai D, Gu Y, Morgan DO. Activation of human cyclin-dependent kinases in vitro. *Mol Biol Cell.* 1992;3:571-82.
26. Morla AO, Draetta G, Beach D, Wang JY. Reversible tyrosine phosphorylation of cdc2: dephosphorylation accompanies activation during entry into mitosis. *Cell.* 1989;58:193-203.
27. Moreno S, Hayles J, Nurse P. Regulation of p34cdc2 protein kinase during mitosis. *Cell.* 1989;58:361-72.
28. Riabowol K, Draetta G, Brizuela L, Vandre D, Beach D. The cdc2 kinase is a nuclear protein that is essential for mitosis in mammalian cells. *Cell.* 1989;57:393-401.
29. Luscher B, Brizuela L, Beach D, Eisenman RN. A role for the p34cdc2 kinase and phosphatases in the regulation of phosphorylation and disassembly of lamin B2 during the cell cycle. *EMBO J.* 1991;10:865-75.
30. Rieder CL, Cole RW, Khodjakov A, Sluder G. The checkpoint delaying anaphase in response to chromosome monoorientation is mediated by an inhibitory signal produced by unattached kinetochores. *J Cell Biol.* 1995;130:941-8.
31. Nicklas RB, Ward SC, Gorbsky GJ. Kinetochore chemistry is sensitive to tension and may link mitotic forces to a cell cycle checkpoint. *J Cell Biol.* 1995;130:929-39.
32. Cohen-Fix O, Peters JM, Kirschner MW, Koshland D. Anaphase initiation in *Saccharomyces cerevisiae* is controlled by the APC-dependent degradation of the anaphase inhibitor Pds1p. *Genes Dev.* 1996;10:3081-93.
33. Bastians H, Topper LM, Gorbsky GL, Ruderman JV. Cell cycle-regulated proteolysis of mitotic target proteins. *Mol Biol Cell.* 1999;10:3927-41.

34. Shirayama M, Toth A, Galova M, Nasmyth K. APC(Cdc20) promotes exit from mitosis by destroying the anaphase inhibitor Pds1 and cyclin Clb5. *Nature*. 1999;402:203-7.
35. Wheatley SP, Hinchcliffe EH, Glotzer M, Hyman AA, Sluder G, Wang Y. CDK1 inactivation regulates anaphase spindle dynamics and cytokinesis in vivo. *J Cell Biol*. 1997;138:385-93.
36. Zou H, McGarry TJ, Bernal T, Kirschner MW. Identification of a vertebrate sister-chromatid separation inhibitor involved in transformation and tumorigenesis. *Science*. 1999;285:418-22.
37. Woodruff JB, Drubin DG, Barnes G. Mitotic spindle disassembly occurs via distinct subprocesses driven by the anaphase-promoting complex, Aurora B kinase, and kinesin-8. *J Cell Biol*. 2010;191:795-808.
38. Gorbsky GJ, Sammak PJ, Borisy GG. Chromosomes move poleward in anaphase along stationary microtubules that coordinately disassemble from their kinetochore ends. *J Cell Biol*. 1987;104:9-18.
39. Sluder G. Centrosomes and the cell cycle. *J Cell Sci Suppl*. 1989;12:253-75.
40. Mitchison T, Evans L, Schulze E, Kirschner M. Sites of microtubule assembly and disassembly in the mitotic spindle. *Cell*. 1986;45:515-27.
41. Lee L, Tirnauer JS, Li J, Schuyler SC, Liu JY, Pellman D. Positioning of the mitotic spindle by a cortical-microtubule capture mechanism. *Science*. 2000;287:2260-2.
42. Tyson JJ, Novak B. Temporal organization of the cell cycle. *Curr Biol*. 2008;18:R759-R68.
43. Shiloh Y. The ATM-mediated DNA-damage response: taking shape. *Trends Biochem Sci*. 2006;31:402-10.
44. Zou L. Single- and double-stranded DNA: building a trigger of ATR-mediated DNA damage response. *Genes Dev*. 2007;21:879-85.
45. Buscemi G, Perego P, Carenini N, Nakanishi M, Chessa L, Chen J, Khanna K, Delia D. Activation of ATM and Chk2 kinases in relation to the amount of DNA strand breaks. *Oncogene*. 2004;23:7691-700.
46. Bekker-Jensen S, Lukas C, Kitagawa R, Melander F, Kastan MB, Bartek J, Lukas J. Spatial organization of the mammalian genome surveillance machinery in response to DNA strand breaks. *J Cell Biol*. 2006;173:195-206.
47. Turenne GA, Paul P, Laflair L, Price BD. Activation of p53 transcriptional activity requires ATM's kinase domain and multiple N-terminal serine residues of p53. *Oncogene*. 2001;20:5100-10.
48. Mailand N, Falck J, Lukas C, Syljuasen RG, Welcker M, Bartek J, Lukas J. Rapid destruction of human Cdc25A in response to DNA damage. *Science*. 2000;288:1425-9.
49. Gire V, Roux P, Wynford-Thomas D, Brondello JM, Dulic V. DNA damage checkpoint kinase Chk2 triggers replicative senescence. *EMBO J*. 2004;23:2554-63.
50. Dulic V, Beney GE, Frebourg G, Drullinger LF, Stein GH. Uncoupling between phenotypic senescence and cell cycle arrest in aging p21-deficient fibroblasts. *Mol Cell Biol*. 2000;20:6741-54.
51. Zhang H, Cohen SN. Smurf2 up-regulation activates telomere-dependent senescence. *Genes Dev*. 2004;18:3028-40.
52. Taylor WR, Stark GR. Regulation of the G2/M transition by p53. *Oncogene*. 2001;20:1803-15.

53. Afshari CA, Nichols MA, Xiong Y, Mudryj M. A role for a p21-E2F interaction during senescence arrest of normal human fibroblasts. *Cell Growth Differ.* 1996;7:979-88.
54. Xiao Z, Chen Z, Gunasekera AH, Sowin TJ, Rosenberg SH, Fesik S, Zhang H. Chk1 mediates S and G2 arrests through Cdc25A degradation in response to DNA-damaging agents. *J Biol Chem.* 2003;278:21767-73.
55. Strausfeld U, Fernandez A, Capony JP, Girard F, Lautredou N, Derancourt J, Labbe JC, Lamb NJ. Activation of p34cdc2 protein kinase by microinjection of human cdc25C into mammalian cells. Requirement for prior phosphorylation of cdc25C by p34cdc2 on sites phosphorylated at mitosis. *J Biol Chem.* 1994;269:5989-6000.
56. Chen F, Zhang Z, Bower J, Lu Y, Leonard SS, Ding M, Castranova V, Piwnicka-Worms H, Shi X. Arsenite-induced Cdc25C degradation is through the KEN-box and ubiquitin-proteasome pathway. *Proc Natl Acad Sci U S A.* 2002;99:1990-5.
57. Dirick L, Bohm T, Nasmyth K. Roles and regulation of Cln-Cdc28 kinases at the start of the cell cycle of *Saccharomyces cerevisiae*. *EMBO J.* 1995;14:4803-13.
58. Blow JJ, Hodgson B. Replication licensing--defining the proliferative state? *Trends Cell Biol.* 2002;12:72-8.
59. Kato J, Matsushime H, Hiebert SW, Ewen ME, Sherr CJ. Direct binding of cyclin D to the retinoblastoma gene product (pRb) and pRb phosphorylation by the cyclin D-dependent kinase CDK4. *Genes Dev.* 1993;7:331-42.
60. Bates S, Bonetta L, MacAllan D, Parry D, Holder A, Dickson C, Peters G. CDK6 (PLSTIRE) and CDK4 (PSK-J3) are a distinct subset of the cyclin-dependent kinases that associate with cyclin D1. *Oncogene.* 1994;9:71-9.
61. Meyerson M, Harlow E. Identification of G1 kinase activity for cdk6, a novel cyclin D partner. *Mol Cell Biol.* 1994;14:2077-86.
62. Chellappan SP, Hiebert S, Mudryj M, Horowitz JM, Nevins JR. The E2F transcription factor is a cellular target for the RB protein. *Cell.* 1991;65:1053-61.
63. Shirodkar S, Ewen M, DeCaprio JA, Morgan J, Livingston DM, Chittenden T. The transcription factor E2F interacts with the retinoblastoma product and a p107-cyclin A complex in a cell cycle-regulated manner. *Cell.* 1992;68:157-66.
64. Weintraub SJ, Prater CA, Dean DC. Retinoblastoma protein switches the E2F site from positive to negative element. *Nature.* 1992;358:259-61.
65. Harper JW, Adami GR, Wei N, Keyomarsi K, Elledge SJ. The p21 Cdk-interacting protein Cip1 is a potent inhibitor of G1 cyclin-dependent kinases. *Cell.* 1993;75:805-16.
66. Polyak K, Kato JY, Solomon MJ, Sherr CJ, Massague J, Roberts JM, Koff A. p27Kip1, a cyclin-Cdk inhibitor, links transforming growth factor-beta and contact inhibition to cell cycle arrest. *Genes Dev.* 1994;8:9-22.
67. Vlach J, Hennecke S, Amati B. Phosphorylation-dependent degradation of the cyclin-dependent kinase inhibitor p27. *EMBO J.* 1997;16:5334-44.
68. Won KA, Reed SI. Activation of cyclin E/CDK2 is coupled to site-specific autophosphorylation and ubiquitin-dependent degradation of cyclin E. *EMBO J.* 1996;15:4182-93.
69. Parry D, Bates S, Mann DJ, Peters G. Lack of cyclin D-Cdk complexes in Rb-negative cells correlates with high levels of p16INK4/MTS1 tumour suppressor gene product. *EMBO J.* 1995;14:503-11.

70. Reynisdottir I, Polyak K, Iavarone A, Massague J. Kip/Cip and Ink4 Cdk inhibitors cooperate to induce cell cycle arrest in response to TGF-beta. *Genes Dev.* 1995;9:1831-45.
71. Brown VD, Phillips RA, Gallie BL. Cumulative effect of phosphorylation of pRB on regulation of E2F activity. *Mol Cell Biol.* 1999;19:3246-56.
72. Harbour JW, Luo RX, Dei Santi A, Postigo AA, Dean DC. Cdk phosphorylation triggers sequential intramolecular interactions that progressively block Rb functions as cells move through G1. *Cell.* 1999;98:859-69.
73. Dutta A, Stillman B. cdc2 family kinases phosphorylate a human cell DNA replication factor, RPA, and activate DNA replication. *EMBO J.* 1992;11:2189-99.
74. Pospiech H, Grosse F, Pisani FM. The initiation step of eukaryotic DNA replication. *Subcell Biochem.* 2010;50:79-104.
75. Rosenblatt J, Gu Y, Morgan DO. Human cyclin-dependent kinase 2 is activated during the S and G2 phases of the cell cycle and associates with cyclin A. *Proc Natl Acad Sci U S A.* 1992;89:2824-8.
76. Pagano M, Draetta G, Jansen-Durr P. Association of cdk2 kinase with the transcription factor E2F during S phase. *Science.* 1992;255:1144-7.
77. Pardee AB. A restriction point for control of normal animal cell proliferation. *Proc Natl Acad Sci U S A.* 1974;71:1286-90.
78. Huang S, Ingber DE. A discrete cell cycle checkpoint in late G(1) that is cytoskeleton-dependent and MAP kinase (Erk)-independent. *Exp Cell Res.* 2002;275:255-64.
79. Crissman HA, Gadbois DM, Tobey RA, Bradbury EM. Transformed mammalian cells are deficient in kinase-mediated control of progression through the G1 phase of the cell cycle. *Proc Natl Acad Sci U S A.* 1991;88:7580-4.
80. Olivetto M, Caldini R, Chevanne M, Cipolleschi MG. The respiration-linked limiting step of tumor cell transition from the non-cycling to the cycling state: its inhibition by oxidizable substrates and its relationships to purine metabolism. *J Cell Physiol.* 1983;116:149-58.
81. Malumbres M, Carnero A. Cell cycle deregulation: a common motif in cancer. *Prog Cell Cycle Res.* 2003;5:5-18.
82. Williams JP, Stewart T, Li B, Mulloy R, Dimova D, Classon M. The retinoblastoma protein is required for Ras-induced oncogenic transformation. *Mol Cell Biol.* 2006;26:1170-82.
83. Hernando E, Nahle Z, Juan G, Diaz-Rodriguez E, Alaminos M, Hemann M, Michel L, Mittal V, Gerald W, Benezra R, Lowe SW, Cordon-Cardo C. Rb inactivation promotes genomic instability by uncoupling cell cycle progression from mitotic control. *Nature.* 2004;430:797-802.
84. O'Connell CB, Khodjakov AL. Cooperative mechanisms of mitotic spindle formation. *J Cell Sci.* 2007;120:1717-22.
85. Rieder CL, Schultz A, Cole R, Sluder G. Anaphase onset in vertebrate somatic cells is controlled by a checkpoint that monitors sister kinetochore attachment to the spindle. *J Cell Biol.* 1994;127:1301-10.
86. Musacchio A, Salmon ED. The spindle-assembly checkpoint in space and time. *Nat Rev Mol Cell Biol.* 2007;8:379-93.

87. Ganem NJ, Storchova Z, Pellman D. Tetraploidy, aneuploidy and cancer. *Curr Opin Genet Dev.* 2007;17:157-62.
88. To-Ho KW, Cheung HW, Ling MT, Wong YC, Wang X. MAD2DeltaC induces aneuploidy and promotes anchorage-independent growth in human prostate epithelial cells. *Oncogene.* 2008;27:347-57.
89. Schiff PB, Fant J, Horwitz SB. Promotion of microtubule assembly in vitro by taxol. *Nature.* 1979;277:665-7.
90. Jordan MA, Thrower D, Wilson L. Mechanism of inhibition of cell proliferation by Vinca alkaloids. *Cancer Res.* 1991;51:2212-22.
91. Kelling J, Sullivan K, Wilson L, Jordan MA. Suppression of centromere dynamics by Taxol in living osteosarcoma cells. *Cancer Res.* 2003;63:2794-801.
92. Fang G, Yu H, Kirschner MW. Direct binding of CDC20 protein family members activates the anaphase-promoting complex in mitosis and G1. *Mol Cell.* 1998;2:163-71.
93. Malureanu LA, Jeganathan KB, Hamada M, Wasilewski L, Davenport J, van Deursen JM. BubR1 N terminus acts as a soluble inhibitor of cyclin B degradation by APC/C(Cdc20) in interphase. *Dev Cell.* 2009;16:118-31.
94. King RW, Peters JM, Tugendreich S, Rolfe M, Hieter P, Kirschner MW. A 20S complex containing CDC27 and CDC16 catalyzes the mitosis-specific conjugation of ubiquitin to cyclin B. *Cell.* 1995;81:279-88.
95. Yu H, King RW, Peters JM, Kirschner MW. Identification of a novel ubiquitin-conjugating enzyme involved in mitotic cyclin degradation. *Current Biology.* 1996;6:455-66.
96. Visintin R, Prinz S, Amon A. CDC20 and CDH1: a family of substrate-specific activators of APC-dependent proteolysis. *Science.* 1997;278:460-3.
97. Floyd S, Pines J, Lindon C. APC/C Cdh1 targets aurora kinase to control reorganization of the mitotic spindle at anaphase. *Curr Biol.* 2008;18:1649-58.
98. Song L, Rape M. Regulated degradation of spindle assembly factors by the anaphase-promoting complex. *Mol Cell.* 2010;38:369-82.
99. van Zon W, Wolthuis RM. Cyclin A and Nek2A: APC/C-Cdc20 substrates invisible to the mitotic spindle checkpoint. *Biochem Soc Trans.* 2010;38:72-7.
100. Sudakin V, Chan GK, Yen TJ. Checkpoint inhibition of the APC/C in HeLa cells is mediated by a complex of BUBR1, BUB3, CDC20, and MAD2. *J Cell Biol.* 2001;154:925-36.
101. Wu H, Lan Z, Li W, Wu S, Weinstein J, Sakamoto KM, Dai W. p55CDC/hCDC20 is associated with BUBR1 and may be a downstream target of the spindle checkpoint kinase. *Oncogene.* 2000;19:4557-62.
102. Tang Z, Bharadwaj R, Li B, Yu H. Mad2-Independent inhibition of APCCdc20 by the mitotic checkpoint protein BubR1. *Dev Cell.* 2001;1:227-37.
103. Hwang LH, Lau LF, Smith DL, Mistrot CA, Hardwick KG, Hwang ES, Amon A, Murray AW. Budding yeast Cdc20: a target of the spindle checkpoint. *Science.* 1998;279:1041-4.
104. Kallio M, Weinstein J, Daum JR, Burke DJ, Gorbsky GJ. Mammalian p55CDC mediates association of the spindle checkpoint protein Mad2 with the cyclosome/anaphase-promoting complex, and is involved in regulating anaphase onset and late mitotic events. *J Cell Biol.* 1998;141:1393-406.

105. Fang G. Checkpoint protein BubR1 acts synergistically with Mad2 to inhibit anaphase-promoting complex. *Mol Biol Cell*. 2002;13:755-66.
106. Davenport J, Harris LD, Goorha R. Spindle checkpoint function requires Mad2-dependent Cdc20 binding to the Mad3 homology domain of BubR1. *Exp Cell Res*. 2006;312:1831-42.
107. Nilsson J, Yekezare M, Minshull J, Pines J. The APC/C maintains the spindle assembly checkpoint by targeting Cdc20 for destruction. *Nat Cell Biol*. 2008;10:1411-20.
108. Ge S, Skaar JR, Pagano M. APC/C- and Mad2-mediated degradation of Cdc20 during spindle checkpoint activation. *Cell Cycle*. 2009;8:167-71.
109. Chan GK, Jablonski SA, Sudakin V, Hittle JC, Yen TJ. Human BUBR1 is a mitotic checkpoint kinase that monitors CENP-E functions at kinetochores and binds the cyclosome/APC. *J Cell Biol*. 1999;146:941-54.
110. Choi E, Choe H, Min J, Choi JY, Kim J, Lee H. BubR1 acetylation at prometaphase is required for modulating APC/C activity and timing of mitosis. *EMBO J*. 2009;28:2077-89.
111. Vanoosthuyse V, Meadows JC, van der Sar SJ, Millar JB, Hardwick KG. Bub3p facilitates spindle checkpoint silencing in fission yeast. *Mol Biol Cell*. 2009;20:5096-105.
112. Lampson MA, Renduchitala K, Khodjakov A, Kapoor TM. Correcting improper chromosome-spindle attachments during cell division. *Nat Cell Biol*. 2004;6:232-7.
113. Thompson SL, Compton DA. Examining the link between chromosomal instability and aneuploidy in human cells. *J Cell Biol*. 2008;180:665-72.
114. Cimini D. Merotelic kinetochore orientation, aneuploidy, and cancer. *Biochim Biophys Acta*. 2008;1786:32-40.
115. Kelly AE, Funabiki H. Correcting aberrant kinetochore microtubule attachments: an Aurora B-centric view. *Curr Opin Cell Biol*. 2009;21:51-8.
116. King EM, Rachidi N, Morrice N, Hardwick KG, Stark MJ. Ipl1p-dependent phosphorylation of Mad3p is required for the spindle checkpoint response to lack of tension at kinetochores. *Genes Dev*. 2007;21:1163-8.
117. Lok W, Klein RQ, Saif MW. Aurora kinase inhibitors as anti-cancer therapy. *Anticancer Drugs*. 2010;21:339-50.
118. Galipeau PC, Cowan DS, Sanchez CA, Barrett MT, Emond MJ, Levine DS, Rabinovitch PS, Reid BJ. 17p (p53) allelic losses, 4N (G2/tetraploid) populations, and progression to aneuploidy in Barrett's esophagus. *Proc Natl Acad Sci U S A*. 1996;93:7081-4.
119. Olaharski AJ, Sotelo R, Solorza-Luna G, Gonsebatt ME, Guzman P, Mohar A, Eastmond DA. Tetraploidy and chromosomal instability are early events during cervical carcinogenesis. *Carcinogenesis*. 2006;27:337-43.
120. Fujiwara T, Bandi M, Nitta M, Ivanova EV, Bronson RT, Pellman D. Cytokinesis failure generating tetraploids promotes tumorigenesis in p53-null cells. *Nature*. 2005;437:1043-7.
121. Roh M, Franco OE, Hayward SW, van der Meer R, Abdulkadir SA. A role for polyploidy in the tumorigenicity of Pim-1-expressing human prostate and mammary epithelial cells. *PLoS One*. 2008;3:e2572.
122. Meraldi P, Honda R, Nigg EA. Aurora-A overexpression reveals tetraploidization as a major route to centrosome amplification in p53<sup>-/-</sup> cells. *EMBO J*. 2002;21:483-92.

123. Zhang D, Hirota T, Marumoto T, Shimizu M, Kunitoku N, Sasayama T, Arima Y, Feng L, Suzuki M, Takeya M, Saya H. Cre-loxP-controlled periodic Aurora-A overexpression induces mitotic abnormalities and hyperplasia in mammary glands of mouse models. *Oncogene*. 2004;23:8720-30.
124. Hanks S, Coleman K, Reid S, Plaja A, Firth H, Fitzpatrick D, Kidd A, Mehes K, Nash R, Robin N, Shannon N, Tolmie J, Swansbury J, Irrthum A, Douglas J, Rahman N. Constitutional aneuploidy and cancer predisposition caused by biallelic mutations in BUB1B. *Nat Genet*. 2004;36:1159-61.
125. Millband DN, Hardwick KG. Fission yeast Mad3p is required for Mad2p to inhibit the anaphase-promoting complex and localizes to kinetochores in a Bub1p-, Bub3p-, and Mph1p-dependent manner. *Mol Cell Biol*. 2002;22:2728-42.
126. Dai W, Wang Q, Liu T, Swamy M, Fang Y, Xie S, Mahmood R, Yang YM, Xu M, Rao CV. Slippage of mitotic arrest and enhanced tumor development in mice with BubR1 haploinsufficiency. *Cancer Res*. 2004;64:440-5.
127. Holland AJ, Cleveland DW. Boveri revisited: chromosomal instability, aneuploidy and tumorigenesis. *Nat Rev Mol Cell Biol*. 2009;10:478-87.
128. Weaver BA, Cleveland DW. Does aneuploidy cause cancer? *Curr Opin Cell Biol*. 2006;18:658-67.
129. Sotillo R, Hernando E, Diaz-Rodriguez E, Teruya-Feldstein J, Cordon-Cardo C, Lowe SW, Benzra R. Mad2 overexpression promotes aneuploidy and tumorigenesis in mice. *Cancer Cell*. 2007;11:9-23.
130. Mondal G, Sengupta S, Panda CK, Gollin SM, Saunders WS, Roychoudhury S. Overexpression of Cdc20 leads to impairment of the spindle assembly checkpoint and aneuploidization in oral cancer. *Carcinogenesis*. 2007;28:81-92.
131. Sotillo R, Schvartzman JM, Socci ND, Benzra R. Mad2-induced chromosome instability leads to lung tumour relapse after oncogene withdrawal. *Nature*. 2010;464:436-40.
132. d'Adda di Fagagna F. Living on a break: cellular senescence as a DNA-damage response. *Nat Rev Cancer*. 2008;8:512-22.
133. Vaziri H, Dragowska W, Allsopp RC, Thomas TE, Harley CB, Lansdorp PM. Evidence for a mitotic clock in human hematopoietic stem cells: loss of telomeric DNA with age. *Proc Natl Acad Sci U S A*. 1994;91:9857-60.
134. Kruk PA, Rampino NJ, Bohr VA. DNA damage and repair in telomeres: relation to aging. *Proc Natl Acad Sci U S A*. 1995;92:258-62.
135. Hubbard K, Dhanaraj SN, Sethi KA, Rhodes J, Wilusz J, Small MB, Ozer HL. Alteration of DNA and RNA binding activity of human telomere binding proteins occurs during cellular senescence. *Exp Cell Res*. 1995;218:241-7.
136. Rochette PJ, Brash DE. Human telomeres are hypersensitive to UV-induced DNA Damage and refractory to repair. *PLoS Genet*. 2010;6:e1000926.
137. Bond J, Houghton M, Blaydes J, Gire V, Wynford-Thomas D, Wyllie F. Evidence that transcriptional activation by p53 plays a direct role in the induction of cellular senescence. *Oncogene*. 1996;13:2097-104.
138. Vaziri H, West MD, Allsopp RC, Davison TS, Wu YS, Arrowsmith CH, Poirier GG, Benchimol S. ATM-dependent telomere loss in aging human diploid fibroblasts and DNA damage lead to the post-translational activation of p53 protein involving poly(ADP-ribose) polymerase. *EMBO J*. 1997;16:6018-33.

139. Takai H, Smogorzewska A, de Lange T. DNA damage foci at dysfunctional telomeres. *Curr Biol*. 2003;13:1549-56.
140. Di Micco R, Fumagalli M, Cicalese A, Piccinin S, Gasparini P, Luise C, Schurra C, Garre M, Nuciforo PG, Bensimon A, Maestro R, Pelicci PG, d'Adda di Fagagna F. Oncogene-induced senescence is a DNA damage response triggered by DNA hyper-replication. *Nature*. 2006;444:638-42.
141. Hayflick L. The Limited in Vitro Lifetime of Human Diploid Cell Strains. *Exp Cell Res*. 1965;37:614-36.
142. Goldstein S. Replicative senescence: the human fibroblast comes of age. *Science*. 1990;249:1129-33.
143. Dimri GP, Lee X, Basile G, Acosta M, Scott G, Roskelley C, Medrano EE, Linskens M, Rubelj I, Pereira-Smith O, et al. A biomarker that identifies senescent human cells in culture and in aging skin in vivo. *Proc Natl Acad Sci U S A*. 1995;92:9363-7.
144. Parkinson EK, Munro J, Steeghs K, Morrison V, Ireland H, Forsyth N, Fitzsimmons S, Bryce S. Replicative senescence as a barrier to human cancer. *Biochem Soc Trans*. 2000;28:226-33.
145. Bartkova J, Rezaei N, Liontos M, Karakaidos P, Kletsas D, Issaeva N, Vassiliou LV, Kolettas E, Niforou K, Zoumpourlis VC, Takaoka M, Nakagawa H, Tort F, Fugger K, Johansson F, Sehested M, Andersen CL, Dyrskjot L, Orntoft T, Lukas J, Kittas C, Helleday T, Halazonetis TD, Bartek J, Gorgoulis VG. Oncogene-induced senescence is part of the tumorigenesis barrier imposed by DNA damage checkpoints. *Nature*. 2006;444:633-7.
146. Nuciforo PG, Luise C, Capra M, Pelosi G, d'Adda di Fagagna F. Complex engagement of DNA damage response pathways in human cancer and in lung tumor progression. *Carcinogenesis*. 2007;28:2082-8.
147. Greenman C, Stephens P, Smith R, Dalgliesh GL, Hunter C, Bignell G, Davies H, Teague J, Butler A, Stevens C, Edkins S, O'Meara S, Vastrik I, Schmidt EE, Avis T, Barthorpe S, Bhamra G, Buck G, Choudhury B, Clements J, Cole J, Dicks E, Forbes S, Gray K, Halliday K, Harrison R, Hills K, Hinton J, Jenkinson A, Jones D, Menzies A, Mironenko T, Perry J, Raine K, Richardson D, Shepherd R, Small A, Tofts C, Varian J, Webb T, West S, Widaa S, Yates A, Cahill DP, Louis DN, Goldstraw P, Nicholson AG, Basseur F, Looijenga L, Weber BL, Chiew YE, DeFazio A, Greaves MF, Green AR, Campbell P, Birney E, Easton DF, Chenevix-Trench G, Tan MH, Khoo SK, Teh BT, Yuen ST, Leung SY, Wooster R, Futreal PA, Stratton MR. Patterns of somatic mutation in human cancer genomes. *Nature*. 2007;446:153-8.
148. Metz T, Harris AW, Adams JM. Absence of p53 allows direct immortalization of hematopoietic cells by the myc and raf oncogenes. *Cell*. 1995;82:29-36.
149. Gascoigne KE, Taylor SS. How do anti-mitotic drugs kill cancer cells? *J Cell Sci*. 2009;122:2579-85.
150. Manfredi JJ, Parness J, Horwitz SB. Taxol binds to cellular microtubules. *J Cell Biol*. 1982;94:688-96.
151. Jordan MA, Toso RJ, Thrower D, Wilson L. Mechanism of mitotic block and inhibition of cell proliferation by taxol at low concentrations. *Proc Natl Acad Sci U S A*. 1993;90:9552-6.

152. Nogales E. Structural insights into microtubule function. *Annu Rev Biochem.* 2000;69:277-302.
153. Jordan MA, Wendell K, Gardiner S, Derry WB, Copp H, Wilson L. Mitotic block induced in HeLa cells by low concentrations of paclitaxel (Taxol) results in abnormal mitotic exit and apoptotic cell death. *Cancer Res.* 1996;56:816-25.
154. Rai SS, Wolff J. Localization of the vinblastine-binding site on beta-tubulin. *J Biol Chem.* 1996;271:14707-11.
155. Perez EA. Microtubule inhibitors: Differentiating tubulin-inhibiting agents based on mechanisms of action, clinical activity, and resistance. *Mol Cancer Ther.* 2009;8:2086-95.
156. Rowinsky EK, Chaudhry V, Cornblath DR, Donehower RC. Neurotoxicity of Taxol. *J Natl Cancer Inst Monogr.* 1993:107-15.
157. Morris PG, Fornier MN. Microtubule active agents: beyond the taxane frontier. *Clin Cancer Res.* 2008;14:7167-72.
158. McGrogan BT, Gilmartin B, Carney DN, McCann A. Taxanes, microtubules and chemoresistant breast cancer. *Biochim Biophys Acta.* 2008;1785:96-132.
159. Gottesman MM, Fojo T, Bates SE. Multidrug resistance in cancer: role of ATP-dependent transporters. *Nat Rev Cancer.* 2002;2:48-58.
160. Giannakakou P, Sackett DL, Kang YK, Zhan Z, Buters JT, Fojo T, Poruchynsky MS. Paclitaxel-resistant human ovarian cancer cells have mutant beta-tubulins that exhibit impaired paclitaxel-driven polymerization. *J Biol Chem.* 1997;272:17118-25.
161. Kamath K, Wilson L, Cabral F, Jordan MA. BetaIII-tubulin induces paclitaxel resistance in association with reduced effects on microtubule dynamic instability. *J Biol Chem.* 2005;280:12902-7.
162. Mozzetti S, Ferlini C, Concolino P, Filippetti F, Raspaglio G, Prislei S, Gallo D, Martinelli E, Ranelletti FO, Ferrandina G, Scambia G. Class III beta-tubulin overexpression is a prominent mechanism of paclitaxel resistance in ovarian cancer patients. *Clin Cancer Res.* 2005;11:298-305.
163. Alli E, Bash-Babula J, Yang JM, Hait WN. Effect of stathmin on the sensitivity to antimicrotubule drugs in human breast cancer. *Cancer Res.* 2002;62:6864-9.
164. Zhang CC, Yang JM, White E, Murphy M, Levine A, Hait WN. The role of MAP4 expression in the sensitivity to paclitaxel and resistance to vinca alkaloids in p53 mutant cells. *Oncogene.* 1998;16:1617-24.
165. Verrills NM, Po'uha ST, Liu ML, Liaw TY, Larsen MR, Ivery MT, Marshall GM, Gunning PW, Kavallaris M. Alterations in gamma-actin and tubulin-targeted drug resistance in childhood leukemia. *J Natl Cancer Inst.* 2006;98:1363-74.
166. Pusztai L. Markers predicting clinical benefit in breast cancer from microtubule-targeting agents. *Ann Oncol.* 2007;18 Suppl 12:xii15-20.
167. Perez EA. Impact, mechanisms, and novel chemotherapy strategies for overcoming resistance to anthracyclines and taxanes in metastatic breast cancer. *Breast Cancer Res Treat.* 2009;114:195-201.
168. Sawin KE, LeGuellec K, Philippe M, Mitchison TJ. Mitotic spindle organization by a plus-end-directed microtubule motor. *Nature.* 1992;359:540-3.
169. Valentine MT, Fordyce PM, Krzyziak TC, Gilbert SP, Block SM. Individual dimers of the mitotic kinesin motor Eg5 step processively and support substantial loads in vitro. *Nat Cell Biol.* 2006;8:470-6.

170. Mayer TU, Kapoor TM, Haggarty SJ, King RW, Schreiber SL, Mitchison TJ. Small molecule inhibitor of mitotic spindle bipolarity identified in a phenotype-based screen. *Science*. 1999;286:971-4.
171. Tao W, South VJ, Zhang Y, Davide JP, Farrell L, Kohl NE, Sepp-Lorenzino L, Lobell RB. Induction of apoptosis by an inhibitor of the mitotic kinesin KSP requires both activation of the spindle assembly checkpoint and mitotic slippage. *Cancer Cell*. 2005;8:49-59.
172. Vijapurkar U, Wang W, Herbst R. Potentiation of kinesin spindle protein inhibitor-induced cell death by modulation of mitochondrial and death receptor apoptotic pathways. *Cancer Res*. 2007;67:237-45.
173. DeBonis S, Skoufias DA, Lebeau L, Lopez R, Robin G, Margolis RL, Wade RH, Kozielski F. In vitro screening for inhibitors of the human mitotic kinesin Eg5 with antimetabolic and antitumor activities. *Mol Cancer Ther*. 2004;3:1079-90.
174. Lad L, Luo L, Carson JD, Wood KW, Hartman JJ, Copeland RA, Sakowicz R. Mechanism of inhibition of human KSP by ispinesib. *Biochemistry*. 2008;47:3576-85.
175. Huszar D, Theoclitou ME, Skolnik J, Herbst R. Kinesin motor proteins as targets for cancer therapy. *Cancer Metastasis Rev*. 2009;28:197-208.
176. Harrison MR, Holen KD, Liu G. Beyond taxanes: a review of novel agents that target mitotic tubulin and microtubules, kinases, and kinesins. *Clin Adv Hematol Oncol*. 2009;7:54-64.
177. Panvichian R, Orth K, Day ML, Day KC, Pilat MJ, Pienta KJ. Paclitaxel-associated multinucleation is permitted by the inhibition of caspase activation: a potential early step in drug resistance. *Cancer Res*. 1998;58:4667-72.
178. Chen JG, Horwitz SB. Differential mitotic responses to microtubule-stabilizing and -destabilizing drugs. *Cancer Res*. 2002;62:1935-8.
179. Niikura Y, Dixit A, Scott R, Perkins G, Kitagawa K. BUB1 mediation of caspase-independent mitotic death determines cell fate. *Journal of Cell Biology*. 2007;178:283-96.
180. Gorka M, Daniewski WM, Gajkowska B, Lusakowska E, Godlewski MM, Motyl T. Autophagy is the dominant type of programmed cell death in breast cancer MCF-7 cells exposed to AGS 115 and EFDAC, new sesquiterpene analogs of paclitaxel. *Anticancer Drugs*. 2005;16:777-88.
181. Portugal J, Bataller M, Mansilla S. Cell death pathways in response to antitumor therapy. *Tumori*. 2009;95:409-21.
182. Tang D, Kang R, Cheh CW, Livesey KM, Liang X, Schapiro NE, Benschop R, Sparvero LJ, Amoscato AA, Tracey KJ, Zeh HJ, Lotze MT. HMGB1 release and redox regulates autophagy and apoptosis in cancer cells. *Oncogene*. 2010.
183. Furuya T, Kim M, Lipinski M, Li J, Kim D, Lu T, Shen Y, Rameh L, Yankner B, Tsai LH, Yuan J. Negative regulation of Vps34 by Cdk mediated phosphorylation. *Mol Cell*. 2010;38:500-11.
184. Allan LA, Clarke PR. Phosphorylation of caspase-9 by CDK1/cyclin B1 protects mitotic cells against apoptosis. *Mol Cell*. 2007;26:301-10.
185. Gascoigne KE, Taylor SS. Cancer cells display profound intra- and interline variation following prolonged exposure to antimetabolic drugs. *Cancer Cell*. 2008;14:111-22.

186. Brito DA, Yang Z, Rieder CL. Microtubules do not promote mitotic slippage when the spindle assembly checkpoint cannot be satisfied. *J Cell Biol.* 2008;182:623-9.
187. Chan YW, On KF, Chan WM, Wong W, Siu HO, Hau PM, Poon RY. The kinetics of p53 activation versus cyclin E accumulation underlies the relationship between the spindle-assembly checkpoint and the postmitotic checkpoint. *J Biol Chem.* 2008;283:15716-23.
188. Orth JD, Tang Y, Shi J, Loy CT, Amendt C, Wilm C, Zenke FT, Mitchison TJ. Quantitative live imaging of cancer and normal cells treated with Kinesin-5 inhibitors indicates significant differences in phenotypic responses and cell fate. *Mol Cancer Ther.* 2008;7:3480-9.
189. Symmans WF, Volm MD, Shapiro RL, Perkins AB, Kim AY, Demaria S, Yee HT, McMullen H, Oratz R, Klein P, Formenti SC, Muggia F. Paclitaxel-induced apoptosis and mitotic arrest assessed by serial fine-needle aspiration: implications for early prediction of breast cancer response to neoadjuvant treatment. *Clin Cancer Res.* 2000;6:4610-7.
190. Degtrev A, Yuan J. Expansion and evolution of cell death programmes. *Nat Rev Mol Cell Biol.* 2008;9:378-90.
191. Clarke PG. Developmental cell death: morphological diversity and multiple mechanisms. *Anat Embryol (Berl).* 1990;181:195-213.
192. Hofmann ER, Milstein S, Boulton SJ, Ye M, Hofmann JJ, Stergiou L, Gartner A, Vidal M, Hengartner MO. *Caenorhabditis elegans* HUS-1 is a DNA damage checkpoint protein required for genome stability and EGL-1-mediated apoptosis. *Curr Biol.* 2002;12:1908-18.
193. Tait SW, de Vries E, Maas C, Keller AM, D'Santos CS, Borst J. Apoptosis induction by Bid requires unconventional ubiquitination and degradation of its N-terminal fragment. *J Cell Biol.* 2007;179:1453-66.
194. Konishi Y, Lehtinen M, Donovan N, Bonni A. Cdc2 phosphorylation of BAD links the cell cycle to the cell death machinery. *Mol Cell.* 2002;9:1005-16.
195. Zha J, Weiler S, Oh KJ, Wei MC, Korsmeyer SJ. Posttranslational N-myristoylation of BID as a molecular switch for targeting mitochondria and apoptosis. *Science.* 2000;290:1761-5.
196. Li H, Zhu H, Xu CJ, Yuan J. Cleavage of BID by caspase 8 mediates the mitochondrial damage in the Fas pathway of apoptosis. *Cell.* 1998;94:491-501.
197. Youle RJ, Strasser A. The BCL-2 protein family: opposing activities that mediate cell death. *Nat Rev Mol Cell Biol.* 2008;9:47-59.
198. Scorrano L, Korsmeyer SJ. Mechanisms of cytochrome c release by proapoptotic BCL-2 family members. *Biochem Biophys Res Commun.* 2003;304:437-44.
199. Wei MC, Lindsten T, Mootha VK, Weiler S, Gross A, Ashiya M, Thompson CB, Korsmeyer SJ. tBID, a membrane-targeted death ligand, oligomerizes BAK to release cytochrome c. *Genes Dev.* 2000;14:2060-71.
200. Zou H, Li Y, Liu X, Wang X. An APAF-1/cytochrome c multimeric complex is a functional apoptosome that activates procaspase-9. *J Biol Chem.* 1999;274:11549-56.
201. Cain K, Bratton SB, Langlais C, Walker G, Brown DG, Sun XM, Cohen GM. Apaf-1 oligomerizes into biologically active approximately 700-kDa and inactive approximately 1.4-MDa apoptosome complexes. *J Biol Chem.* 2000;275:6067-70.

202. Degtarev A, Boyce M, Yuan J. A decade of caspases. *Oncogene*. 2003;22:8543-67.
203. Tang D, Kidd VJ. Cleavage of DFF-45/ICAD by multiple caspases is essential for its function during apoptosis. *J Biol Chem*. 1998;273:28549-52.
204. Woo M, Hakem R, Soengas MS, Duncan GS, Shahinian A, Kagi D, Hakem A, McCurrach M, Khoo W, Kaufman SA, Senaldi G, Howard T, Lowe SW, Mak TW. Essential contribution of caspase 3/CPP32 to apoptosis and its associated nuclear changes. *Genes Dev*. 1998;12:806-19.
205. Rao RV, Hermel E, Castro-Obregon S, del Rio G, Ellerby LM, Ellerby HM, Bredesen DE. Coupling endoplasmic reticulum stress to the cell death program. Mechanism of caspase activation. *J Biol Chem*. 2001;276:33869-74.
206. Cheng EH, Kirsch DG, Clem RJ, Ravi R, Kastan MB, Bedi A, Ueno K, Hardwick JM. Conversion of Bcl-2 to a Bax-like death effector by caspases. *Science*. 1997;278:1966-8.
207. Schulze-Osthoff K, Ferrari D, Los M, Wesselborg S, Peter ME. Apoptosis signaling by death receptors. *Eur J Biochem*. 1998;254:439-59.
208. Micheau O, Tschopp J. Induction of TNF receptor I-mediated apoptosis via two sequential signaling complexes. *Cell*. 2003;114:181-90.
209. Scaffidi C, Fulda S, Srinivasan A, Friesen C, Li F, Tomaselli KJ, Debatin KM, Krammer PH, Peter ME. Two CD95 (APO-1/Fas) signaling pathways. *EMBO J*. 1998;17:1675-87.
210. Barnhart BC, Lee JC, Alappat EC, Peter ME. The death effector domain protein family. *Oncogene*. 2003;22:8634-44.
211. Baptiste-Okoh N, Barsotti AM, Prives C. A role for caspase 2 and PIDD in the process of p53-mediated apoptosis. *Proc Natl Acad Sci U S A*. 2008;105:1937-42.
212. Gao Z, Shao Y, Jiang X. Essential roles of the Bcl-2 family of proteins in caspase-2-induced apoptosis. *J Biol Chem*. 2005;280:38271-5.
213. Peterson D, Lee J, Lei XC, Forrest WF, Davis DP, Jackson PK, Belmont LD. A chemosensitization screen identifies TP53RK, a kinase that restrains apoptosis after mitotic stress. *Cancer Res*. 2010;70:6325-35.
214. Li F, Ambrosini G, Chu EY, Plescia J, Tognin S, Marchisio PC, Altieri DC. Control of apoptosis and mitotic spindle checkpoint by survivin. *Nature*. 1998;396:580-4.
215. Mita AC, Mita MM, Nawrocki ST, Giles FJ. Survivin: key regulator of mitosis and apoptosis and novel target for cancer therapeutics. *Clin Cancer Res*. 2008;14:5000-5.
216. Shi YH, Ding WX, Zhou J, He JY, Xu Y, Gambotto AA, Rabinowich H, Fan J, Yin XM. Expression of X-linked inhibitor-of-apoptosis protein in hepatocellular carcinoma promotes metastasis and tumor recurrence. *Hepatology*. 2008;48:497-507.
217. Kim M, Murphy K, Liu F, Parker SE, Dowling ML, Baff W, Kao GD. Caspase-mediated specific cleavage of BubR1 is a determinant of mitotic progression. *Mol Cell Biol*. 2005;25:9232-48.
218. Hashimoto T, Yamauchi L, Hunter T, Kikkawa U, Kamada S. Possible involvement of caspase-7 in cell cycle progression at mitosis. *Genes Cells*. 2008;13:609-21.
219. Andreassen PR, Martineau SN, Margolis RL. Chemical induction of mitotic checkpoint override in mammalian cells results in aneuploidy following a transient tetraploid state. *Mutat Res*. 1996;372:181-94.

220. Jin L, Williamson A, Banerjee S, Philipp I, Rape M. Mechanism of ubiquitin-chain formation by the human anaphase-promoting complex. *Cell*. 2008;133:653-65.
221. Jin HS, Lee TH. Cell cycle-dependent expression of cIAP2 at G2/M phase contributes to survival during mitotic cell cycle arrest. *Biochem J*. 2006;399:335-42.
222. Prescott DM, Bender MA. Synthesis of RNA and protein during mitosis in mammalian tissue culture cells. *Exp Cell Res*. 1962;26:260-8.
223. Blagosklonny MV. Mitotic arrest and cell fate: why and how mitotic inhibition of transcription drives mutually exclusive events. *Cell Cycle*. 2007;6:70-4.
224. Rudner AD, Hardwick KG, Murray AW. Cdc28 activates exit from mitosis in budding yeast. *J Cell Biol*. 2000;149:1361-76.
225. Elhajouji A, Cunha M, Kirsch-Volders M. Spindle poisons can induce polyploidy by mitotic slippage and micronucleate mononucleates in the cytokinesis-block assay. *Mutagenesis*. 1998;13:193-8.
226. Brito DA, Rieder CL. Mitotic checkpoint slippage in humans occurs via cyclin B destruction in the presence of an active checkpoint. *Curr Biol*. 2006;16:1194-200.
227. Lee J, Kim JA, Margolis RL, Fotedar R. Substrate degradation by the anaphase promoting complex occurs during mitotic slippage. *Cell Cycle*. 2010;9:1792-801.
228. Senovilla L, Vitale I, Galluzzi L, Vivet S, Joza N, Younes AB, Rello-Varona S, Castedo M, Kroemer G. p53 represses the polyploidization of primary mammary epithelial cells by activating apoptosis. *Cell Cycle*. 2009;8:1380-5.
229. Huang HC, Shi J, Orth JD, Mitchison TJ. Evidence that mitotic exit is a better cancer therapeutic target than spindle assembly. *Cancer Cell*. 2009;16:347-58.
230. Listovsky T, Zor A, Laronne A, Brandeis M. Cdk1 is essential for mammalian cyclosome/APC regulation. *Exp Cell Res*. 2000;255:184-91.
231. Vassilev LT, Tovar C, Chen S, Knezevic D, Zhao X, Sun H, Heimbrook DC, Chen L. Selective small-molecule inhibitor reveals critical mitotic functions of human CDK1. *Proc Natl Acad Sci U S A*. 2006;103:10660-5.
232. Wesierska-Gadek J, Krystof V. Selective cyclin-dependent kinase inhibitors discriminating between cell cycle and transcriptional kinases: future reality or utopia? *Ann N Y Acad Sci*. 2009;1171:228-41.
233. Ditchfield C, Johnson VL, Tighe A, Ellston R, Haworth C, Johnson T, Mortlock A, Keen N, Taylor SS. Aurora B couples chromosome alignment with anaphase by targeting BubR1, Mad2, and Cenp-E to kinetochores. *J Cell Biol*. 2003;161:267-80.
234. Place RF, Noonan EJ, Giardina C. HDACs and the senescent phenotype of WI-38 cells. *BMC Cell Biol*. 2005;6:37.
235. Okamoto H, Fujioka Y, Takahashi A, Takahashi T, Taniguchi T, Ishikawa Y, Yokoyama M. Trichostatin A, an inhibitor of histone deacetylase, inhibits smooth muscle cell proliferation via induction of p21(WAF1). *J Atheroscler Thromb*. 2006;13:183-91.
236. Beumer JH, Tawbi H. Role of histone deacetylases and their inhibitors in cancer biology and treatment. *Curr Clin Pharmacol*. 2010;5:196-208.
237. Anderson HJ, de Jong G, Vincent I, Roberge M. Flow cytometry of mitotic cells. *Exp Cell Res*. 1998;238:498-502.
238. Terao Y, Nishida J, Horiuchi S, Rong F, Ueoka Y, Matsuda T, Kato H, Furugen Y, Yoshida K, Kato K, Wake N. Sodium butyrate induces growth arrest and senescence-like phenotypes in gynecologic cancer cells. *Int J Cancer*. 2001;94:257-67.
239. Zaman GJ. Cell-based screening. *Drug Discov Today*. 2004;9:828-30.

240. Milstein S, Vidal M. Perturbing interactions. *Nat Methods*. 2005;2:412-4.
241. Schriemer DC, Kemmer D, Roberge M. Design of phenotypic screens for bioactive chemicals and identification of their targets by genetic and proteomic approaches. *Comb Chem High Throughput Screen*. 2008;11:610-6.
242. Blake RA, Broome MA, Liu X, Wu J, Gishizky M, Sun L, Courtneidge SA. SU6656, a selective src family kinase inhibitor, used to probe growth factor factor signaling. *Molecular and Cellular Biology*. 2000;20:9018-27.
243. Andreassi C, Jarecki J, Zhou J, Coovert DD, Monani UR, Chen X, Whitney M, Pollok B, Zhang M, Androphy E, Burghes AH. Aclarubicin treatment restores SMN levels to cells derived from type I spinal muscular atrophy patients. *Hum Mol Genet*. 2001;10:2841-9.
244. Tsuiki H, Nitta M, Tada M, Inagaki M, Ushio Y, Saya H. Mechanism of hyperploid cell formation induced by microtubule inhibiting drug in glioma cell lines. *Oncogene*. 2001;20:420-9.
245. Wasch R, Cross FR. APC-dependent proteolysis of the mitotic cyclin Clb2 is essential for mitotic exit. *Nature*. 2002;418:556-62.
246. Badie C, Itzhaki JE, Sullivan MJ, Carpenter AJ, Porter AC. Repression of CDK1 and other genes with CDE and CHR promoter elements during DNA damage-induced G(2)/M arrest in human cells. *Mol Cell Biol*. 2000;20:2358-66.
247. Juan G, Traganos F, James WM, Ray JM, Roberge M, Sauve DM, Anderson H, Darzynkiewicz Z. Histone H3 phosphorylation and expression of cyclins A and B1 measured in individual cells during their progression through G2 and mitosis. *Cytometry*. 1998;32:71-7.
248. Hilioti Z, Chung YS, Mochizuki Y, Hardy CF, Cohen-Fix O. The anaphase inhibitor Pds1 binds to the APC/C-associated protein Cdc20 in a destruction box-dependent manner. *Curr Biol*. 2001;11:1347-52.
249. Waizenegger IC, Hauf S, Meinke A, Peters JM. Two distinct pathways remove mammalian cohesin from chromosome arms in prophase and from centromeres in anaphase. *Cell*. 2000;103:399-410.
250. Stucke VM, Sillje HH, Arnaud L, Nigg EA. Human Mps1 kinase is required for the spindle assembly checkpoint but not for centrosome duplication. *EMBO J*. 2002;21:1723-32.
251. Fisk HA, Mattison CP, Winey M. Human Mps1 protein kinase is required for centrosome duplication and normal mitotic progression. *Proc Natl Acad Sci U S A*. 2003;100:14875-80.
252. Schmidt M, Budirahardja Y, Klompaker R, Medema RH. Ablation of the spindle assembly checkpoint by a compound targeting Mps1. *EMBO Rep*. 2005;6:866-72.
253. Baek KH, Shin HJ, Jeong SJ, Park JW, McKeon F, Lee CW, Kim CM. Caspases-dependent cleavage of mitotic checkpoint proteins in response to microtubule inhibitor. *Oncol Res*. 2005;15:161-8.
254. Janicke RU, Sprengart ML, Wati MR, Porter AG. Caspase-3 is required for DNA fragmentation and morphological changes associated with apoptosis. *J Biol Chem*. 1998;273:9357-60.
255. Janicke RU. MCF-7 breast carcinoma cells do not express caspase-3. *Breast Cancer Res Treat*. 2009;117:219-21.

256. Kim Y, Holland AJ, Lan W, Cleveland DW. Aurora kinases and protein phosphatase 1 mediate chromosome congression through regulation of CENP-E. *Cell*. 2010;142:444-55.
257. Maia AF, Feijao T, Vromans MJ, Sunkel CE, Lens SM. Aurora B kinase cooperates with CENP-E to promote timely anaphase onset. *Chromosoma*. 2010;119:405-13.
258. Liu D, Vader G, Vromans MJ, Lampson MA, Lens SM. Sensing chromosome bi-orientation by spatial separation of aurora B kinase from kinetochore substrates. *Science*. 2009;323:1350-3.
259. Wysong DR, Chakravarty A, Hoar K, Ecsedy JA. The inhibition of Aurora A abrogates the mitotic delay induced by microtubule perturbing agents. *Cell Cycle*. 2009;8:876-88.
260. Bain J, McLauchlan H, Elliott M, Cohen P. The specificities of protein kinase inhibitors: an update. *Biochem J*. 2003;371:199-204.
261. Bain J, Plater L, Elliott M, Shpiro N, Hastie CJ, McLauchlan H, Klevernic I, Arthur JS, Alessi DR, Cohen P. The selectivity of protein kinase inhibitors: a further update. *Biochem J*. 2007;408:297-315.
262. Decordier I, Cundari E, Kirsch-Volders M. Survival of aneuploid, micronucleated and/or polyploid cells: crosstalk between ploidy control and apoptosis. *Mutat Res*. 2008;651:30-9.
263. Shay JW, Pereira-Smith OM, Wright WE. A role for both RB and p53 in the regulation of human cellular senescence. *Exp Cell Res*. 1991;196:33-9.
264. Serrano M, Lin AW, McCurrach ME, Beach D, Lowe SW. Oncogenic ras provokes premature cell senescence associated with accumulation of p53 and p16INK4a. *Cell*. 1997;88:593-602.
265. Gewirtz DA, Holt SE, Elmore LW. Accelerated senescence: an emerging role in tumor cell response to chemotherapy and radiation. *Biochem Pharmacol*. 2008;76:947-57.
266. Roberson RS, Kussick SJ, Vallieres E, Chen SY, Wu DY. Escape from therapy-induced accelerated cellular senescence in p53-null lung cancer cells and in human lung cancers. *Cancer Res*. 2005;65:2795-803.
267. te Poele RH, Okorokov AL, Jardine L, Cummings J, Joel SP. DNA damage is able to induce senescence in tumor cells in vitro and in vivo. *Cancer Res*. 2002;62:1876-83.
268. Chang BD, Broude EV, Dokmanovic M, Zhu H, Ruth A, Xuan Y, Kandel ES, Lausch E, Christov K, Roninson IB. A senescence-like phenotype distinguishes tumor cells that undergo terminal proliferation arrest after exposure to anticancer agents. *Cancer Res*. 1999;59:3761-7.
269. el-Deiry WS, Harper JW, O'Connor PM, Velculescu VE, Canman CE, Jackman J, Pietenpol JA, Burrell M, Hill DE, Wang Y, et al. WAF1/CIP1 is induced in p53-mediated G1 arrest and apoptosis. *Cancer Res*. 1994;54:1169-74.
270. Agarwal ML, Agarwal A, Taylor WR, Stark GR. p53 controls both the G2/M and the G1 cell cycle checkpoints and mediates reversible growth arrest in human fibroblasts. *Proc Natl Acad Sci U S A*. 1995;92:8493-7.
271. Mandel HG, Carlo PE, Smith PK. The incorporation of 8-azaguanine into nucleic acids of tumor-bearing mice. *J Biol Chem*. 1954;206:181-9.

272. Finkelstein M, Winters WD, Thomas PA, Davison C, Smith PK. The effect of 8-azaguanine on tissue metabolism in mice bearing sarcoma 37. *Cancer Res.* 1951;11:807-10.
273. Doudican NA, Bowling B, Orlow SJ. Enhancement of arsenic trioxide cytotoxicity by dietary isothiocyanates in human leukemic cells via a reactive oxygen species-dependent mechanism. *Leuk Res.* 2010;34:229-34.
274. Kim MJ, Kim SH, Lim SJ. Comparison of the apoptosis-inducing capability of sulforaphane analogues in human colon cancer cells. *Anticancer Res.* 2010;30:3611-9.
275. Stoter M, Bamberger AM, Aslan B, Kurth M, Speidel D, Loning T, Frank HG, Kaufmann P, Lohler J, Henne-Bruns D, Deppert W, Knippschild U. Inhibition of casein kinase I delta alters mitotic spindle formation and induces apoptosis in trophoblast cells. *Oncogene.* 2005;24:7964-75.
276. Behrend L, Milne DM, Stoter M, Deppert W, Campbell LE, Meek DW, Knippschild U. IC261, a specific inhibitor of the protein kinases casein kinase 1-delta and -epsilon, triggers the mitotic checkpoint and induces p53-dependent postmitotic effects. *Oncogene.* 2000;19:5303-13.
277. Merritt JE, Armstrong WP, Benham CD, Hallam TJ, Jacob R, Jaxa-Chamiec A, Leigh BK, McCarthy SA, Moores KE, Rink TJ. SK&F 96365, a novel inhibitor of receptor-mediated calcium entry. *Biochem J.* 1990;271:515-22.
278. Kuilman T, Michaloglou C, Mooi WJ, Peeper DS. The essence of senescence. *Genes Dev.* 2010;24:2463-79.
279. Saretzki G. Cellular senescence in the development and treatment of cancer. *Curr Pharm Des.* 2010;16:79-100.
280. Smith JR, Ning Y, Pereira-Smith OM. Why are transformed cells immortal? Is the process reversible? *Am J Clin Nutr.* 1992;55:1215S-21S.
281. Takahashi A, Ohtani N, Hara E. Irreversibility of cellular senescence: dual roles of p16INK4a/Rb-pathway in cell cycle control. *Cell Div.* 2007;2:10.
282. Coppe JP, Patil CK, Rodier F, Sun Y, Munoz DP, Goldstein J, Nelson PS, Desprez PY, Campisi J. Senescence-associated secretory phenotypes reveal cell-nonautonomous functions of oncogenic RAS and the p53 tumor suppressor. *PLoS Biol.* 2008;6:2853-68.
283. Hollstein M, Sidransky D, Vogelstein B, Harris CC. p53 mutations in human cancers. *Science.* 1991;253:49-53.
284. Momand J, Zambetti GP, Olson DC, George D, Levine AJ. The mdm-2 oncogene product forms a complex with the p53 protein and inhibits p53-mediated transactivation. *Cell.* 1992;69:1237-45.
285. Vassilev LT, Vu BT, Graves B, Carvajal D, Podlaski F, Filipovic Z, Kong N, Kammlott U, Lukacs C, Klein C, Fotouhi N, Liu EA. In vivo activation of the p53 pathway by small-molecule antagonists of MDM2. *Science.* 2004;303:844-8.
286. Schmitt CA, Fridman JS, Yang M, Lee S, Baranov E, Hoffman RM, Lowe SW. A senescence program controlled by p53 and p16INK4a contributes to the outcome of cancer therapy. *Cell.* 2002;109:335-46.
287. Schwarze SR, Fu VX, Desotelle JA, Kenowski ML, Jarrard DF. The identification of senescence-specific genes during the induction of senescence in prostate cancer cells. *Neoplasia.* 2005;7:816-23.

288. Petti C, Molla A, Vegetti C, Ferrone S, Anichini A, Sensi M. Coexpression of NRASQ61R and BRAFV600E in human melanoma cells activates senescence and increases susceptibility to cell-mediated cytotoxicity. *Cancer Res.* 2006;66:6503-11.
289. Xue W, Zender L, Miething C, Dickins RA, Hernando E, Krizhanovsky V, Cordon-Cardo C, Lowe SW. Senescence and tumour clearance is triggered by p53 restoration in murine liver carcinomas. *Nature.* 2007;445:656-60.
290. Roninson IB, Dokmanovic M. Induction of senescence-associated growth inhibitors in the tumor-suppressive function of retinoids. *J Cell Biochem.* 2003;88:83-94.
291. Ewald JA, Desotelle JA, Wilding G, Jarrard DF. Therapy-induced senescence in cancer. *J Natl Cancer Inst.* 2010;102:1536-46.
292. Karlsson MO, Molnar V, Freijs A, Nygren P, Bergh J, Larsson R. Pharmacokinetic models for the saturable distribution of paclitaxel. *Drug Metab Dispos.* 1999;27:1220-3.
293. Brouwer E, Verweij J, De Bruijn P, Loos WJ, Pillay M, Buijs D, Sparreboom A. Measurement of fraction unbound paclitaxel in human plasma. *Drug Metab Dispos.* 2000;28:1141-5.
294. Veltkamp SA, Thijssen B, Garrigue JS, Lambert G, Lallemand F, Binlich F, Huitema AD, Nuijen B, Nol A, Beijnen JH, Schellens JH. A novel self-microemulsifying formulation of paclitaxel for oral administration to patients with advanced cancer. *Br J Cancer.* 2006;95:729-34.
295. Demidenko ZN, Kalurupalle S, Hanco C, Lim CU, Broude E, Blagosklonny MV. Mechanism of G1-like arrest by low concentrations of paclitaxel: next cell cycle p53-dependent arrest with sub G1 DNA content mediated by prolonged mitosis. *Oncogene.* 2008;27:4402-10.
296. DeMoe JH, Santaguida S, Daum JR, Musacchio A, Gorbsky GJ. A high throughput, whole cell screen for small molecule inhibitors of the mitotic spindle checkpoint identifies OM137, a novel Aurora kinase inhibitor. *Cancer Res.* 2009;69:1509-16.
297. Stolz A, Vogel C, Schneider V, Ertych N, Kienitz A, Yu H, Bastians H. Pharmacologic abrogation of the mitotic spindle checkpoint by an indolocarbazole discovered by cellular screening efficiently kills cancer cells. *Cancer Res.* 2009;69:3874-83.
298. Salmela AL, Pouwels J, Varis A, Kukkonen AM, Toivonen P, Halonen PK, Perala M, Kallioniemi O, Gorbsky GJ, Kallio MJ. Dietary flavonoid fisetin induces a forced exit from mitosis by targeting the mitotic spindle checkpoint. *Carcinogenesis.* 2009;30:1032-40.
299. York DH. Dopamine receptor blockade--a central action of chlorpromazine on striatal neurones. *Brain Res.* 1972;37:91-9.
300. Shin SY, Kim CG, Kim SH, Kim YS, Lim Y, Lee YH. Chlorpromazine activates p21Waf1/Cip1 gene transcription via early growth response-1 (Egr-1) in C6 glioma cells. *Exp Mol Med.* 2010;42:395-405.
301. Yde CW, Clausen MP, Bennetzen MV, Lykkesfeldt AE, Mouritsen OG, Guerra B. The antipsychotic drug chlorpromazine enhances the cytotoxic effect of tamoxifen in tamoxifen-sensitive and tamoxifen-resistant human breast cancer cells. *Anticancer Drugs.* 2009;20:723-35.

302. Boder GB, Paul DC, Williams DC. Chlorpromazine inhibits mitosis of mammalian cells. *Eur J Cell Biol.* 1983;31:349-53.
303. Hartwell LH, Weinert TA. Checkpoints: controls that ensure the order of cell cycle events. *Science.* 1989;246:629-34.
304. Chen JG, Yang CP, Cammer M, Horwitz SB. Gene expression and mitotic exit induced by microtubule-stabilizing drugs. *Cancer Res.* 2003;63:7891-9.
305. Gabrielli B, Chau YQ, Giles N, Harding A, Stevens F, Beamish H. Caffeine promotes apoptosis in mitotic spindle checkpoint-arrested cells. *J Biol Chem.* 2007;282:6954-64.
306. Ohshima S. Abnormal mitosis in hypertetraploid cells causes aberrant nuclear morphology in association with H<sub>2</sub>O<sub>2</sub>-induced premature senescence. *Cytometry A.* 2008;73:808-15.
307. Chan YW, Ma HT, Wong W, Ho CC, On KF, Poon RY. CDK1 inhibitors antagonize the immediate apoptosis triggered by spindle disruption but promote apoptosis following the subsequent rereplication and abnormal mitosis. *Cell Cycle.* 2008;7:1449-61.
308. Ghiara JB, Richardson HE, Sugimoto K, Henze M, Lew DJ, Wittenberg C, Reed SI. A cyclin B homolog in *S. cerevisiae*: chronic activation of the Cdc28 protein kinase by cyclin prevents exit from mitosis. *Cell.* 1991;65:163-74.
309. Shin HJ, Baek KH, Jeon AH, Park MT, Lee SJ, Kang CM, Lee HS, Yoo SH, Chung DH, Sung YC, McKeon F, Lee CW. Dual roles of human BubR1, a mitotic checkpoint kinase, in the monitoring of chromosomal instability. *Cancer Cell.* 2003;4:483-97.
310. Park SY, Kim S, Cho H, Kwon SH, Chae S, Kang D, Seong YS. Depletion of BubR1 promotes premature centrosomal localization of cyclin B1 and accelerates mitotic entry. *Cell Cycle.* 2009;8:1754-64.
311. Li Y, Gorbea C, Mahaffey D, Rechsteiner M, Benezra R. MAD2 associates with the cyclosome/anaphase-promoting complex and inhibits its activity. *Proc Natl Acad Sci U S A.* 1997;94:12431-6.
312. Yan XX, Najbauer J, Woo CC, Dashtipour K, Ribak CE, Leon M. Expression of active caspase-3 in mitotic and postmitotic cells of the rat forebrain. *J Comp Neurol.* 2001;433:4-22.
313. Hsu SL, Yu CT, Yin SC, Tang MJ, Tien AC, Wu YM, Huang CY. Caspase 3, periodically expressed and activated at G<sub>2</sub>/M transition, is required for nocodazole-induced mitotic checkpoint. *Apoptosis.* 2006;11:765-71.
314. Wang Q, Liu T, Fang Y, Xie S, Huang X, Mahmood R, Ramaswamy G, Sakamoto KM, Darzynkiewicz Z, Xu M, Dai W. BUBR1 deficiency results in abnormal megakaryopoiesis. *Blood.* 2004;103:1278-85.
315. Amaral JD, Xavier JM, Steer CJ, Rodrigues CM. The role of p53 in apoptosis. *Discov Med.* 2010;9:145-52.
316. Yu Y, Little JB. p53 is involved in but not required for ionizing radiation-induced caspase-3 activation and apoptosis in human lymphoblast cell lines. *Cancer Res.* 1998;58:4277-81.
317. Silva A, Wyllie A, Collins MK. p53 is not required for regulation of apoptosis or radioprotection by interleukin-3. *Blood.* 1997;89:2717-22.

318. Yeung TK, Germond C, Chen X, Wang Z. The mode of action of taxol: apoptosis at low concentration and necrosis at high concentration. *Biochem Biophys Res Commun.* 1999;263:398-404.
319. Kops GJ, Foltz DR, Cleveland DW. Lethality to human cancer cells through massive chromosome loss by inhibition of the mitotic checkpoint. *Proc Natl Acad Sci U S A.* 2004;101:8699-704.
320. Gorgun G, Calabrese E, Hideshima T, Ecsedy J, Perrone G, Mani M, Ikeda H, Bianchi G, Hu Y, Cirstea D, Santo L, Tai YT, Nahar S, Zheng M, Bandi M, Carrasco RD, Raje N, Munshi N, Richardson P, Anderson KC. A novel Aurora-A kinase inhibitor MLN8237 induces cytotoxicity and cell-cycle arrest in multiple myeloma. *Blood.* 2010;115:5202-13.
321. Fletcher GC, Brox RD, Denny TA, Hembrough TA, Plum SM, Fogler WE, Sidor CF, Bray MR. ENMD-2076 Is an Orally Active Kinase Inhibitor with Antiangiogenic and Antiproliferative Mechanisms of Action. *Mol Cancer Ther.* 2011;10:126-37.
322. Cohen RB, Jones SF, Aggarwal C, von Mehren M, Cheng J, Spigel DR, Greco FA, Mariani M, Rocchetti M, Ceruti R, Comis S, Laffranchi B, Moll J, Burris HA. A phase I dose-escalation study of danusertib (PHA-739358) administered as a 24-hour infusion with and without granulocyte colony-stimulating factor in a 14-day cycle in patients with advanced solid tumors. *Clin Cancer Res.* 2009;15:6694-701.
323. Noh EJ, Lim DS, Jeong G, Lee JS. An HDAC inhibitor, trichostatin A, induces a delay at G2/M transition, slippage of spindle checkpoint, and cell death in a transcription-dependent manner. *Biochem Biophys Res Commun.* 2009;378:326-31.